Summer 8-2017

Environmentally-Driven Variation in the Population Dynamics of Gulf Menhaden (*Brevoortia patronus*)

Grant D. Adams
University of Southern Mississippi

ENVIRONMENTALLY-DRIVEN VARIATION IN THE POPULATION DYNAMICS OF GULF MENHADEN (BREVOORTIA PATRONUS)

by

Grant D. Adams

A Thesis
Submitted to the Graduate School
and the School of Ocean Science and Technology
at The University of Southern Mississippi
in Partial Fulfillment of the Requirements
for the Degree of Master of Science

August 2017

ENVIRONMENTALLY-DRIVEN VARIATION IN THE POPULATION DYNAMICS

OF GULF MENHADEN (BREVOORTIA PATRONUS)

by Grant D. Adams

August 2017

Approved by:

_____

Dr. Robert Leaf, Major Professor
Assistant Professor, Ocean Science and Technology

_____

Dr. Frank Hernandez, Committee Member
Assistant Professor, Ocean Science and Technology

_____

Dr. Wei Wu, Committee Member
Assistant Professor, Ocean Science and Technology

_____

Dr. Robert J. Griffitt
Department Chair, Ocean Science and Technology, Division of Coastal Sciences

_____

Dr. Karen S. Coats
Dean of the Graduate School

Published by the Graduate School

ABSTRACT

ENVIRONMENTALLY-DRIVEN VARIATION IN THE POPULATION DYNAMICS OF GULF MENHADEN (BREVOORTIA PATRONUS)

by Grant D. Adams

August 2017

Gulf Menhaden (*Brevoortia patronus*) is an abundant forage fish distributed throughout the Northern Gulf of Mexico (NGOM). Gulf Menhaden support the second largest fishery, by weight, in the United States and represent a key linkage between upper and lower trophic levels. Variation in the population dynamics can, therefore, pose consequences for the ecology and economy in the NGOM. Here we aim to understand variation in the individual and population dynamics of Gulf Menhaden throughout ontogeny and how such variation relates to environmental processes. We utilized a suite of fishery-dependent and –independent, remote sensing, modeled, and *in situ* data to explicitly model the relationship between the condition, distribution, and growth of Gulf Menhaden and river discharge, climate, temperature, wind, mesoscale circulation, and hypoxia using a series of regression techniques. Results presented here advance our understanding of the biology and ecology Gulf Menhaden and can be used to inform future ecosystem based fisheries management in the NGOM.

ACKNOWLEDGMENTS

I would like to especially thank my advisor, Robert T. Leaf, and committee members, Wei Wu and Frank Hernandez, for their patient guidance and support in the development of my thesis. I thank David A. Dippold, Trevor Moncrief, and Morgan M. Corey for their helpful comments throughout the research process. I thank David Hanisko and Glenn Zapfe for their helpful comments and advice regarding ichthyoplankton analysis. I thank Joseph W. Smith, David Hanisko, and Glenn Zapfe at the NOAA Southeast Fisheries Science Center for providing data for the analysis. I would like to thank Simon Wood for updating the "mgcv" package to run models included in the current work.

DEDICATION

To my family and friends who supported and encouraged me throughout my graduate experience. Thank you to my parents, John and Anne, for supporting me in my endeavors. Your love and support throughout my journeys means so much to me. Thanks to all my fellow students at the Gulf Coast Research Lab for providing a network of support, fun, and venting. I want to thank Soulmates/Moonshadow for taking me on some wonderful adventures in the Mississippi Sound, Captain Zak will remember. In particular, I dedicate this to Motherclucker for waking me up bright and early every morning.

TABLE OF CONTENTS

ABSTRACT ii

ACKNOWLEDGMENTS iii

DEDICATION iv

LIST OF TABLES viii

LIST OF ILLUSTRATIONS x

LIST OF ABBREVIATIONS xv

CHAPTER I – ENVIRONMENTALLY-DRIVEN FLUCTUATIONS IN CONDITION FACTOR OF ADULT GULF MENHADEN (*BREVOORTIA PATRONUS*) IN THE NORTHERN GULF OF MEXICO 1

1.1 Abstract 1

1.2 Introduction 1

1.3 Methods 4

1.3.1 Study Area and Data Collection. 5

1.3.2 Statistical Analysis. 6

1.4 Results 10

1.5 Discussion 13

CHAPTER II - EVALUATION OF MISSISSIPPI RIVER DISCHARGE, PRODUCTIVITY, AND TEMPERATURE ON THE SPATIO-TEMPORAL

DYNAMICS OF LARVAL GULF MENHADEN (*BREVOORTIA PATRONUS*) IN THE NORTHERN GULF OF MEXICO 37

2.1 Abstract 37

2.2 Introduction 38

2.3 Methods 40

2.3.1 Data 40

2.3.2 Statistical Analysis 43

2.4 Results 46

2.5 Discussion 49

CHAPTER III - SIZE-SELECTIVE MORTALITY AND GROWTH VARIATION OF GULF MENHADEN *BREVOORTIA PATRONUS* IN RELATION TO DENSITY DEPENDENT AND INDEPENDENT CONDITIONS. 70

3.1 Introduction 70

3.2 Methods 73

3.2.1 Data 73

3.2.2 Candidate Drivers of Age and Growth 74

3.2.3 Length-at-Age 76

3.2.4 Scale Increment Width Growth Analysis 78

3.2.5 Size-Selective Mortality 79

3.3 Results 80

3.4 Discussion 82

REFERENCES 100

LIST OF TABLES

Table 1.1 Summary of environmental data used to examine the impacts of bottom-up processes on relative condition of Gulf Menhaden in the northern Gulf of Mexico. 21

Table 1.2 Model selection for generalized additive mixed models relating relative condition of adult Gulf Menhaden in year αy, month m, latitude (φ), and longitude (λ) to environmental predictors (xj). s and g are 1- and 2-dimensional nonparametric smoothing functions and bv is the random effect term of v. Deviance Explained (Dev. expl.), Akaikie information criterion (AIC), delta AIC (ΔAIC), and AIC weights (AICw), and sample size (N) of each candidate model is included. Final model is indicated in bold. 22

Table 1.3 Summary of base and final Generalized Additive Mixed Models that relate Gulf Menhaden relative condition to spatial-temporal and environmental predictors ($\boldsymbol{xj}$). Estimated year-specific coefficients are shown for the first year analyzed (e.g. 1964 or 2003) and estimated degrees of freedom are shown for nonparametric terms. AIC and deviance explained (%; Dev. expl.) are noted. 26

Table 2.1 Model selection of the two-strata variable-coefficient GAMs relating the spatial distribution of larval presence and relative abundance collected by SEAMAP bongo trawls, 1982 to 2012..... 56

Table 2.2 Model selection of the two-strata variable-coefficient GAMs relating the spatial distribution of larval presence and relative abundance collected by SEAMAP neuston trawls, 1982 to 2012..... 57

Table 2.3 Summary of the two-strata variable-coefficient GAMs relating the spatial distribution of larval presence and relative abundance collected by SEAMAP trawls, 1982 to 2012, to high, average, and low winter Mississippi River discharge levels.

Asterisks denote significance of nominal predictors at the following alpha levels: *0.05; **0.01; ***0.001. 58

Table 2.4 Correlation coefficients between standardized estimates of annual larval relative abundance and indices of abundance and biomass estimates from the most recent assessment of Gulf Menhaden (SEDAR, 2013). Asterisks denote significance of nominal predictors at the following alpha levels: *0.05; **0.01; ***0.001. 59

Table 2.5 Estimates and standard errors (SE) of standardized annual relative abundance of larval Gulf Menhaden collected by SEAMAP bongo (larvae under 10 m^2 of sea surface) and neuston (larvae per 10 minute tow) trawls, 1982 to 2013. 60

Table 3.1 Forward model selection for the extended von Bertalannfy growth function (VBGF) with environmental covariates fit to Gulf Menhaden length-at-age data. 90

Table 3.2 Parameter estimates from the extended von Bertalannfy growth function with environmental covariates fit to Gulf Menhaden length-at-age data. 91

Table 3.3 Predicted length-at-age and growth increment from the best fit extended von Bertalanffy growth function assuming a 1 standard deviation increase in each environmental covariate. 92

Table 3.4 Forward model selection for hierarchical linear models fit to Gulf Menhaden scale increment width and data environmental covariates. $\sigma x, j2 \neq 0$ indicates the random age effect for parameters relating environmental covariates to the response. Number of parameters (P) and samples (N) are indicated. 93

Table 3.5 Estimates of the fixed- and mixed-effects for the hierarchical linear models fit to Gulf Menhaden scale increment width and data environmental covariates. 94

LIST OF ILLUSTRATIONS

Figure 1.1 Study area and number of adult Gulf Menhaden (N = 251,712) sampled from the commercial fishery in the northern Gulf of Mexico (1964 to 2011) analyzed in this study. 27

Figure 1.2 Histograms of (a) fork length and (b) weight, (c) fitted weight-at-length curve ($W = 1.77\times10 - 5L3.03$) and (d) histogram of relative condition (*Kn*) of adult Gulf Menhaden sampled from the commercial fishery in the northern Gulf of Mexico (1964 to 2011). 28

Figure 1.3 Annual mean ± S.D. (in grey) for (a) Annual number of adult Gulf Menhaden sampled from the commercial fishery in the northern Gulf of Mexico (1964 to 2011), (b) relative condition (*Kn*), (c) monthly Multivariate ENSO Index, and (d) monthly aggregated daily flow rates (f^3 s^{-1}) of the Mississippi River collected at Talbert Landing, MS. Horizontal lines indicate mean values. 29

Figure 1.4 (a) Partial effect of monthly Mississippi River discharge on relative condition (*Kn*) of adult Gulf Menhaden sampled from the commercial fishery in the northern Gulf of Mexico (1964 to 2011) estimated from the spatially-invariant Generalized Additive Mixed Model. (b) Histogram indicates the number of samples. 30

Figure 1.5 (a) Partial effect of monthly Mississippi River discharge on relative condition (Kn) of adult Gulf Menhaden sampled from the commercial fishery in the northern Gulf of Mexico (1964 to 2011) estimated from the spatially-invariant Generalized Additive Mixed Model. (b) Histogram indicates the number of samples. 31

Figure 1.6 (a) Partial effect of the Multivariate ENSO Index on relative condition (*Kn*) of adult Gulf Menhaden sampled from the commercial fishery in the northern Gulf of

Mexico (1964 to 2011) estimated from the spatially-invariant Generalized Additive Mixed Model. Positive values of the Multivariate ENSO Index indicate El Niño-like conditions and negative values indicate La Niña-like conditions. (b) Histogram indicates the number of samples. 32

Figure 1.7 Spatially-explicit effects of the (a) zonal (East-West) and (b) meridional (North-South) wind vectors (m s^{-1}) on relative condition (*Kn*) of adult Gulf Menhaden sampled from the commercial fishery in northern Gulf of Mexico (1964 to 2011) estimated from the spatially-variant Generalized Additive Mixed Model. Circle size is proportional to the estimated increase in relative condition for one-unit increase (white circle) or decrease (dark grey circle) in the velocity (m s^{-1}) of the zonal or meridional wind vectors. Spatially-explicit wind direction favorable to condition is indicated in each panel. (c) Distribution of (d) *k*-means clustering (n = 3, clusters) of significant spatially-explicit effects of zonal and meridional wind vectors. 33

Figure 1.8 (a) Partial effect of SST on relative condition (*Kn*) of adult Gulf Menhaden sampled from the commercial fishery (2003 to 2011) estimated from the spatially-invariant Generalized Additive Mixed Model. (b) Histogram indicates the number of samples..... 34

Figure 1.9 (a) Year-specific intercepts, (b) partial effect of week, histograms (c, d) of the number of samples, and (e) predicted spatial distribution of relative condition (*Kn*) of adult Gulf Menhaden sampled from the commercial fishery in the northern Gulf of Mexico (2003 to 2011) estimated from the base Generalized Additive Mixed Model. Note: predicted spatial distribution is scaled to July condition. 35

Figure 1.10 Standard model diagnostics of base, spatially- invariant, and spatially-variant generalized additive mixed model (GAMMs), relating relative condition of adult Gulf Menhaden spatial-temporal and environmental predictors (Table 3): (a) histogram of the Pearson residuals, (b) normal QQ-plot of Pearson residuals against theoretical quantiles, (c) density plot of observed against fitted values, and (d) density plot of Pearson residuals against the linear predictor. 36

Figure 2.1 Location of Gulf Menhaden samples collected by SEAMAP bongo and neuston trawls, 1982 to 2012, during average (a, b), high (c, d), and low (e, f) Mississippi River discharge. Presence is indicated as • and absence as ×. 61

Figure 2.2 Kernel density of standard lengths of larval Gulf Menhaden sampled by SEAMAP bongo and neuston trawls, 1982 to 2012. 62

Figure 2.3 GAM predicted spatial distribution of log-transformed larval Gulf Menhaden relative abundance collected by SEAMAP bongo (a; larvae under 10 m^2 of sea surface) and neuston (b; larvae per 10 minute tow) trawls, 1982 to 2012, and distribution during high (c, d) and low (e, f) Mississippi River discharge levels. 63

Figure 2.4 GAM predicted spatial distribution anomaly of larval Gulf Menhaden relative abundance collected by SEAMAP bongo (larvae under 10 m^2 of sea surface) and neuston (larvae per 10 minute tow) trawls, 1982 to 2013, during high (a, b) and low (c, d) Mississippi River discharge levels relative to average discharge level. 64

Figure 2.5 Fits of one-dimensional smoothing functions relating the presence of larval Gulf Menhaden to environmental covariates collected by SEAMAP bongo trawls, 1982 to 2012. Shaded area indicates 95% confidence area. 65

Figure 2.6 Fits of one-dimensional smoothing functions relating the presence of larval Gulf Menhaden to environmental covariates collected by SEAMAP neuston trawls, 1982 to 2012. Shaded area indicates 95% confidence area. 66
Figure 2.7 Estimates of standardized annual relative abundance of larval Gulf Menhaden collected by SEAMAP bongo (larvae under 10 m^2 of sea surface) and neuston (larvae per 10 minute tow) trawls, 1982 to 2012. 67
Figure 2.8 Scatterplots and correlation coefficients between standardized estimates of annual larval relative abundance and indices of abundance and biomass estimates from the most recent assessment of Gulf Menhaden (SEDAR, 2013). 68
Figure 2.9 Standard model diagnostics of GAM second-stratum models relating larval Gulf Menhaden CPUE collected by SEAMAP trawls, 1982 to 2012, to spatial-temporal and environmental predictors. 69
Figure 3.1 Histograms of (a) fork length and (b) scale width, (c) fork length-scale length regression, and (d) histogram of fractional age of Gulf Menhaden sampled from the commercial fishery in the northern Gulf of Mexico (1964 to 2011). 95
Figure 3.2 Time series of annual (a) mesoscale circulation activity, (b) day of spring transition, (c) mean monthly Mississippi River discharge (November to March), and (d) annual extent of the mid-summer hypoxic zone. 96
Figure 3.3 Time series of daily v-wind vectors (North-South) from the NCEP/NCAR Reanalysis Project. Regime series as analyzed by the STARS algorithm is indicated in red, first day of the year is indicated as a black tic mark, and day of spring transition is indicated by the blue circles. 97

Figure 3.4 Predicted scale increment width at age and age-specific parameter estimates (±SE) from the hierarchical linear model fit to Gulf Menhaden scale increment width and data environmental covariates. Population level parameter estimates are indicated by the dotted line and SE by the grey box. 98
Figure 3.5 Posterior probability distribution of age-level estimates of mean size-at-age-one (length to first scale annuli) and differences between age-one estimates. 99

LIST OF ABBREVIATIONS

AIC	Akaike information criterion
BANOVA	Bayesian Analysis of Variance
CPUE	Catch per unit effort
DOC	Day of capture
ENSO	El Niño Southern Oscillation
GAM	Generalized Additive Model
GAMM	Generalized Additive Mixed Model
Kn	Relative condition
MDT	Mean dynamic topography
NGOM	Northern Gulf of Mexico
NMFS	National Marine Fisheries Service
NOAA	National Oceanic and Atmospheric Administration
SEAMAP	Southeast Area Monitoring and Assessment Program
SSH	Sea Surface Height
SSHA	Sea Surface Height Anomaly
SST	Sea Surface Temperature
STARS	Sequential t-test analysis of regime shifts
VBGF	von Bertalanffy growth function

CHAPTER I – ENVIRONMENTALLY-DRIVEN FLUCTUATIONS IN CONDITION FACTOR OF ADULT GULF MENHADEN (*BREVOORTIA PATRONUS*) IN THE NORTHERN GULF OF MEXICO

1.1 Abstract

We evaluated the effects of multiple bottom-up processes on the relative condition (an index of length-specific weight) of adult Gulf Menhaden *Brevoortia patronus* sampled from the U.S. commercial fishery, from 1964 to 2011, in the northern Gulf of Mexico (NGOM). A series of Generalized Additive Mixed Models (GAMMs) were constructed to examine the influence of Mississippi River Discharge, El Niño Southern Oscillation (ENSO), wind vector components, and sea surface temperature (SST°C). Relative condition was positively correlated with Mississippi River discharge throughout the NGOM. The effect of wind vector components was variable across the NGOM. This observation is likely due to geographic differences in wind-related transport of nutrient rich river plume waters. Relative condition was greatest at 24°C and declined when SST was less than 23° and greater than 29°C. Relative condition exhibited intra-annual variability with a small peak during May and increasing condition from August until November, likely caused by seasonal phytoplankton blooms and provisioning by individuals for spawning. We show that multiple bottom-up processes impact the individual dynamics of Gulf Menhaden in the NGOM and these results can be used to inform on their impacts on the fisheries and ecology of the NGOM.

1.2 Introduction

The northern Gulf of Mexico (NGOM) is a river-dominated ecosystem that serves as the terminus of the watershed for much of the continental US (van der Leeden, Troise,

& Todd, 1990). Discharge from the Mississippi, Atchafalaya, and Mobile rivers among others input large quantities of freshwater and nutrients into the NGOM, driving high levels of primary and secondary productivity (Churchill B. Grimes, 2001; S E Lohrenz et al., 1997). Variations in river discharge rates alter nutrient flux as well as the spatial distribution of productive river plume waters (S E Lohrenz et al., 1997; Steven E. Lohrenz, Redalje, Cai, Acker, & Dagg, 2008; N. D. Walker, 1996). Productivity in the NGOM is also influenced by other external bottom-up processes. For example, inter-annual climate regimes such as the El Niño Southern Oscillation (ENSO) are associated with variations in rainfall patterns across the continental US (Enfield, Mestas-Nuñez, & Trimble, 2001), altering subsequent nutrient flux into the NGOM (Goolsby, Battaglin, Aulenbach, & Hooper, 2001). Wind-driven variations in nutrient export pathways from river drainages alter the distribution and rates of primary production (Huang, Cai, Castelao, Wang, & Lohrenz, 2013). Such variations impact fisheries resources, underlying a critical need for research in the NGOM (Churchill B. Grimes, 2001; Karnauskas et al., 2015).

Gulf Menhaden *Brevoortia patronus* is an abundant forage fish distributed throughout coastal waters of the NGOM. In addition to supporting the second largest fishery, by weight, in the United States (Vaughan, Shertzer, & Smith, 2007), Gulf Menhaden is a prey item for commercially and recreationally important fishes, sea birds, and mammals, providing an important link between primary producers and secondary consumers (Ahrenholz, 1991; Bethea, Buckel, & Carlson, 2004; Sagarese et al., 2016; Scharf & Schlight, 2000). Variations in the population dynamics of Gulf Menhaden can

therefore have implications for ecosystem productivity and fisheries in the NGOM (Geers, Pikitch, & Frisk, 2016; Robinson et al., 2015).

Weight-at-length condition indices are used to identify seasonal trends in energy storage strategies (Cubillos & Claramunt, 2009) and the effects of environmental conditions on fish species (Ballón, Wosnitza-Mendo, Guevara-Carrasco, & Bertrand, 2008; Thorson, 2015; Ventresca, 1995). Condition indices are a metric for evaluating the "fatness" of fish (Blackwell et al 2000) such that heavier individuals of the same length have greater condition (Froese, 2006). A greater condition value indicates that the individual has a larger amount of stored energy, which is positively correlated to reproductive investment and survival (Glazier, 2000; Jørgensen, Ernande, Fiksen, & Dieckmann, 2006; Rideout, Rose, & Burton, 2005). Given the correlation between reproduction and individual condition, information on individual condition may also explain the variable relationship between spawning stock biomass and recruitment (Thorson, 2015). Individual condition is influenced by prey availability, environmental conditions, and seasonal reproductive dynamics (Cubillos & Claramunt, 2009; Ventresca, 1995). Decreases in individual condition can have consequences for individual survival, recruitment, and abundance (Lambert & Dutil, 1997; Scott, Marteinsdottir, Begg, Wright, & Kjesbu, 2006). Despite the utility of the condition metric and its relevance to population dynamics, little is known about the intra- and inter-annual variation of condition of Gulf Menhaden or its environmental determinants.

The impacts of bottom-up processes on the individual dynamics of adult Gulf Menhaden are not well understood. Gulf Menhaden are obligate filter feeders (Olsen, Fulford, Dillon, & Graham, 2014) and processes that enhance primary and secondary

productivity in the NGOM may lead to contrasts in condition of adults, similar to that observed for individual growth of age-0 Gulf Menhaden (Zhang et al., 2014). Increases in temperature are associated with increased mean length and lipid content of juvenile Gulf Menhaden (Deegan, 1986) and increased growth rate potential of age-0 fish in normoxic waters (Zhang et al., 2014). While temperature variation likely impacts the growth and lipid content of adult Gulf Menhaden, such effects may vary through ontogeny. A conspicuous feature in the NGOM is the Mississippi River plume front, which is the result of river discharge from the Mississippi and Atchafalaya Rivers. The Mississippi River plume front is the zone of hydrodynamic convergence between nutrient rich freshwater discharge and oxygen rich continental shelf waters. Horizontal mixing across this gradient supports the greatest biomass of plankton, zooplankton and icthyoplankton in the NGOM (Govoni, Hoss, & Colby, 1989; C. B. Grimes & Finucane, 1991). It is unknown how much Gulf Menhaden dynamics are influenced by the spatial distribution and dynamics of the Mississippi River Plume. Growth of Gulf Menhaden is highly variable (SEDAR, 2013) and such variation may be a result of contrasts in ecosystem-level productivity.

To address gaps in our understanding of the impacts of various bottom-up processes on Gulf Menhaden condition, we examined the relationship between the condition of adult Gulf Menhaden and a suite of environmental variables. This study has two objectives: 1.) to examine the spatial-temporal dynamics of relative condition of adult Gulf Menhaden and 2.) the influence of Mississippi River discharge, ENSO, wind vector components, and SST on relative condition of adult Gulf Menhaden.

1.3 Methods

1.3.1 Study Area and Data Collection.

Gulf Menhaden length and weight data were obtained from the National Oceanic and Atmospheric Administration's National Marine Fisheries Service (NMFS). Between 1964 and 2011, NMFS recorded the length (mm fork length; FL), weight (g), age (yrs), and fishing location at a 10-min by 10-min grid resolution of 538,757 Gulf Menhaden sampled from the commercial purse-seine fishery during the fishing season (April to November). The fishery is composed of large purse seine vessels (> 60 m) whose landings are processed in shore-side reduction factories which produce meal, oil, and other fish solubles (Vaughan et al., 2007). The study area included all fishing grounds in the northern Gulf of Mexico, ranging from 28.5 to 31°N and 95 to 84°W (Figure 1). Some individuals were considered questionable and removed from the analysis including: specimens reported as sampled entirely from land-based grid cells (n = 13,708), sampled from outside the study area (n = 35,432), older than ten years (n = 25,568), weighing less than 1 gram (n = 2,004), longer than 500 mm FL (n = 1), and missing either weight or length data (n = 699). Because fishing by the commercial fishery rarely exceeds depths of 100 m, fish sampled from reported locations with depths greater than 100 m were removed from analysis (n = 670). We removed specimens of Gulf Menhaden less than the length at 99% maturity (L99; 162 FL; n removed = 212,336; Brown-Peterson, in Review) and focus our investigation on adult fish. An additional quality control measure was to eliminate, from analysis, all specimens outside of the 99.999% prediction interval of the log-transformed weight-at-length relationship (n = 424). Therefore, the final sample size used in the present analysis was 251,712.

Relative condition factor was the response variable for analysis. Relative condition factor (Kn) was calculated for each fish:

Eq. 1 $$Kn = \frac{W}{\widehat{W}} \times 100,$$

where W is weight (g) and $\widehat{W}$ is the mean predicted weight-at-length derived from $\widehat{W} = aL^b$ (LeCren, 1951). Values of a (1.77×10^{-5}) and b (3.03) were estimated using nonlinear least-squares (Figure 2).

Time series of potential climatological, oceanographic, and environmental variables were identified from measured, remotely sensed, and modelled data (Table 1). Monthly river discharge of the Mississippi River was calculated for each individual fish by summing daily values from Talbert Landing, Louisiana for the first 30 days prior to the date of capture. The transit time of river water from Talbert Landings to the Gulf of Mexico is 2 to 5 days, depending on discharge (Pereira & Hostettler, 1993). Given previous research which has documented seasonal effects of river discharge on Gulf Menhaden (Govoni, 1997), we also constructed indices of spring and winter river discharge for analysis. An index of winter and spring river discharge was created by averaging monthly values from November to March and March to May for each year, respectively. Monthly SST and the zonal and meridional wind vector components (Table 1) were averaged for each 10-min by 10-min fishing grid.

1.3.2 Statistical Analysis.

To examine the effect of environmental predictors on relative condition of adult Gulf Menhaden in the NGOM we constructed a series of Generalized Additive Mixed Models (GAMMs; Hastie & Tibshirani 1986). First, "base" models were constructed for 1964-2011 and 2003-2011:

Eq. 2 $$Kn_{y,m} = \alpha_y + s_1(m) + b_v + \varepsilon_{y,m},$$

where $Kn_{y,m}$ is the relative condition of adult Gulf Menhaden in year y and month m, α_y is the year-specific intercept, s is a 1-dimensional nonparametric smoothing functions (thin-plate regression spline), b_v is the random effect term of vessel v assumed to be independent and identically distributed $N(0, \sigma_v^2)$, and $\varepsilon_{y,m}$ is the random error. Random effects were treated like a smooth for computational efficiency where the identity matrix is the penalty coefficient matrix and the associated smoothing parameter controls for σ_v^2 (Wood, 2008). Second, "spatially-explicit" models were constructed to evaluated changes in relative condition as a function of location:

Eq. 3 $$Kn_{y,m,(\varphi,\lambda)} = \alpha_y + s_1(m) + g_1(\varphi, \lambda) + b_v + \varepsilon_{y,m,(\varphi,\lambda)},$$

where φ and λ are the latitude and longitude, respectively, calculated from the centroid of the fishing grid from which the sample originated and g is a 2-dimensional nonparametric smoothing functions (thin-plate regression splines).

Two different model formulations were then used to examine the effect of environmental predictor variables on relative condition of adult Gulf Menhaden, a "stationary" model that assumes nonlinear stationarity in the predictor-response relationship and a variable coefficient model that accounts for non-stationarity in the predictor-response relationship as a function of location. While environmental predictors and location are correlated to some degree, both location and environmental predictors can be included in the same model to estimate general trends while accounting for localized effects (Winton, Wuenschel, & McBride, 2014). The full "stationary" model was:

Eq. 4 $$Kn_{y,m,(\varphi,\lambda)} = \alpha_y + s_1(m) + g_1(\varphi, \lambda) + \sum_{j=1}^{q} s_{j+1}(x_j) + b_v + \varepsilon_{y,m,(\varphi,\lambda)},$$

where the effect of the j^{th} predictor (x_j) of q predictors on relative condition is assumed to be nonlinear and stationary over the geographic range from which Gulf Menhaden samples were taken. For evaluation non-stationarity in the effect of environmental predictors on relative condition, variable-coefficient GAMMs were constructed (Hastie & Tibshirani, 1993). The full "non-stationary" model was:

Eq. 5 $$Kn_{y,m,(\varphi,\lambda)} = \alpha_y + s_1(m) + g_1(\varphi, \lambda) + \sum_{j=1}^{q} g_{j+1}(\varphi, \lambda) * x_j + b_v + \varepsilon_{y,m,(\varphi,\lambda)},$$

where g_{j+1} is a 2-dimensional smoothing function that describes the spatial variation in the effect of predictor x_j. The model formulation is structured such that the effect of x_j is linear, but variable in magnitude and direction among locations. The spatially-explicit statistical significance of each predictor (locations where the predictor had a significant effect) was based on the estimates of the 95% confidence interval (L. Ciannelli, Bartolino, & Chan, 2012).

To accommodate differences between temporal availability of predictors (Table 1) and reduce large computation times, stationary and non-stationary models were run separately for each predictor. However, the non-stationary model was not considered for the Multivariate ENSO Index and Mississippi River discharge because location-specific information on discharge is not available. Additionally, the zonal and meridional wind vector components were considered together. Separate candidate models were constructed for stationary and non-stationary model formulations with temporal lags of zero to three months for each predictor. Annual lags in the effect of climate regimes on

the oceanographic and biological processes have been previously documented (Black, 2009; Sanchez-Rubio, Perry, Biesiot, Johnson, & Lipcius, 2011) and, therefore, we extended the range of temporal lags explored for the Multivariate ENSO Index to 12 months. Stationary and non-stationary models were constructed with and without the location term, $g_1(\varphi, \lambda)$(Winton et al., 2014). A total of n = 91 model formulations were fit using Maximum Likelihood (ML), and assuming a Gamma distribution and a log link function in the "mgcv" in the R programming language (R Core Team, 2015; Wood, 2006, 2011). Base, spatially-variant, and spatially–invariant candidate models for each predictor were then compared using AIC and associated weights (Bacheler, Bailey, Ciannelli, Bartolino, & Chan, 2009; Burnham & Anderson, 2004; L. Ciannelli et al., 2012). For all models, each smooth term was centered around zero and a constant (α_y) was added to convert back to the original values to maintain model identifiability. Comparison between semivariance of residuals from final models and distance between locations indicated negligible spatial autocorrelation in the residuals (L. Ciannelli et al., 2012). In addition, there was no strong temporal autocorrelation left in the residuals from the final models (Feng et al., 2014; Hollowed, Hare, & Wooster, 2001).

We determined *a priori*, that if the spatially-variant model formulation was selected for the wind vector components, a non-hierarchical *k*-means cluster analysis (Hartigan & Wong, 1979) would be performed on the spatially-variant parameter estimates to assess geographic similarities of wind-driven variation in relative condition. The *k*-means algorithm, using a predetermined number of clusters, serves to group data to the closest cluster center until the within-cluster sum of squares is minimized. To determine the number clusters, we used the "NbClust" package in R (Charrad, Ghazzali,

Boiteau, & Niknafs, 2014), which suggests an optimal clustering scheme using 30 indices developed to determine the number of clusters in a data set.

1.4 Results

We analyzed length and weight data from 251,712 adult Gulf Menhaden sampled between 1964 and 2011 by NMFS from the commercial reduction fishery in the NGOM. An average of 5,356 adult Gulf Menhaden were sampled annually during this time period (Figure 3). There was substantial intra- and inter-annual variability in relative condition, Mississippi River Discharge, and the Multivariate ENSO Index (Figs. 3 & 4). Relative condition was generally lower in the late 1970's and early 2000's and greater during the early 1990's (Figure 3). This was further evidenced by the year specific intercepts estimated from the 1964 to 2011 spatially-explicit GAMM (Eq. 3; Figure 4a). There was a small peak in relative condition in May, while relative condition in July (Figure 4b). Relative condition then from August until the end of the fishing season. However, the number of samples from the commercial fishery was greatest during the summer months (Figure 4d). Spatial predictions of relative condition indicated greater values of relative condition at locations near the Mississippi River Delta, with the greatest values offshore near 90° W (Figure 4e). Results from the 2003 to 2011 spatially-explicit GAMM (Eq. 3) were consistent with the longer term model (Figure 9). AIC weights of all candidate GAMMs indicated that inclusion of environmental predictors improved model support and increased the deviance explained when related to the base models (Table 2). For the remainder of the analysis, only the most supported models are discussed (Table 3). Standard model diagnostics indicated a qualitatively good fit for all models (Figure 10).

For Mississippi River discharge, the stationary model formulation including location (Eq. 4) with a lag of 0 months provided the best model support (Table 2). As Mississippi River discharge increased, relative condition of adult Gulf Menhaden increased throughout the NGOM (Figure 5a). However, the majority of sampled were collected during low discharge scenarios (Figure 5b).

The effect of the Multivariate ENSO Index on relative condition of adult Gulf Menhaden was best supported by the stationary model formulation with location (Eq. 4) and a lag of 10 months (Table 2). Relative condition was greatest at Multivariate ENSO Index values of -1 and 1.5 (Figure 6). Positive values of the Multivariate ENSO Index are associated with El Niño-like conditions while negative values are associated with La Niña-like conditions. Therefore, relative condition of adult Gulf Menhaden was greatest during weak ($|\pm 1| \geq$ Multivariate ENSO Index $\geq |\pm 0.5|$) to moderate ($|\pm 1.5| \geq$ Multivariate ENSO Index $\geq |\pm 1|$) La Niña- and El Niño-like conditions.

Comparison of AIC and AIC weights for all candidate models indicated that the non-stationary model formulation with location (Eq. 5) incorporating a 2-month lag provided the best support for the effect of the zonal and meridional wind vector components on relative condition of adult Gulf Menhaden (Table 2). Collinearity between wind vector components was not detectable (Pearson's $r = 0.28$). We found large areas of both positive and negative correlations between relative condition and the wind vector components, implying that the effect of wind vector components on relative condition differs across the study area (Figure 7). The zonal (East-West) wind vector is positive for a west wind (i.e. eastward in direction), therefore, a positive effect indicates relative condition was elevated 2 months after west winds, while a negative effect

indicates relative condition was elevated 2 months after east winds (i.e. in a westward direction). Relative condition was elevated after west winds at locations near the Mississippi River Delta, in Mobile Bay (30.5°N 88°W), and the eastern Chandeleur Sound (29.5 to 30.5°N 89°W)(Figure 7a). However, relative condition was elevated 2 months after east winds offshore western Atchafalaya Bay (29°N 91.5°W). For the meridional (North-South) wind vector, positive values are south winds (i.e. in a northward direction), therefore, a positive (negative) effect indicates relative condition was elevated 2 months after south (north) winds. Relative condition was enhanced offshore the Louisiana Bight (29°N 90°W) and offshore between Atchafalaya Bay and the Texas-Louisiana Border 2 months after south winds (Figure 7b). However, the opposite occurred in the remainder of the study region, where North winds were associated with enhanced condition 2 months later. The greatest magnitude of this effect occurred in eastern Texas (> 94° W) and near the Mississippi River Delta, while relative condition increased disproportionately less in relation to North winds near Atchafalaya Bay and the eastern Chandeleur Sound. The spatially-variant effect of the zonal and meridional wind vector components were analyzed using a k-means cluster analysis. After exploring a range of numbers of clusters up to 15, a model with 3 clusters was the most parsimonious. We identified regions that were similarly affected by the wind vector components (Figure 7c). Similarities were observed among areas offshore eastern Atchafalaya Bay, the Mississippi River Delta, and eastern Chandeleur Sound, where relative condition was similarly elevated after North and West winds (Figure 7d).

Based on AIC scores, the stationary model formulation including location (Eq. 4) with SST lagged 0 months provided the best model parsimony (Table 2), suggesting that

the effect of SST nonlinear and stationary across study area. Relative condition was greatest at 24°C and declined steeply below 23°C and above 29°C (Figure 8).

1.5 Discussion

In this study we demonstrate that multiple bottom-up processes impact the individual dynamics of adult Gulf Menhaden and highlight the temporal and spatial complexity of these processes in the NGOM. Specifically, we found correlations between relative condition and Mississippi River discharge, ENSO, wind vector components, and SST. Previous research has demonstrated that the processes examined in our study are critical determinants of ecosystem productivity in the region (Churchill B. Grimes, 2001; Hitchcock et al., 1997; Huang, Cai, Castelao, Wang, & Lohrenz, 2013; Karnauskas et al., 2015). Our work complements recent research that demonstrates that population dynamics of forage fishes are correlated with multiple bottom-up processes (Brosset et al., 2015; Brunel & Dickey-Collas, 2010; Humphrey, Wilberg, Houde, & Fabrizio, 2014; Rojbek, Tomkiewicz, Jacobsen, & Stottrup, 2014; Takahashi, Checkley, Litz, Brodeur, & Peterson, 2012).

Throughout the NGOM, relative condition of adult Gulf Menhaden was positively correlated with Mississippi River discharge. Although our study area is much greater than the area directly influenced by Mississippi River plume waters, we excluded discharge estimates from other rivers (e.g. Atchafalaya and Mobile Rivers) because of high collinearity between discharge rates (Atchafalaya River: Pearson's $r = 0.98$) and given that, on average, the Mississippi and Atchafalaya Rivers discharge 10.5 times more water affecting an area 30 times greater than the Mobile River (https://www.usgs.gov/). Additionally, the majority of fishing by the commercial Gulf Menhaden fishery is located

in areas impacted principally by the Mississippi River (Vaughan, Shertzer, & Smith, 2007). Increases in river discharge in the NGOM are associated with elevated nutrient flux and subsequent increases in primary and secondary productivity (S E Lohrenz et al., 1997; Steven E. Lohrenz, Redalje, Cai, Acker, & Dagg, 2008; Zhao & Quigg, 2014). Specifically, enhanced nutrient flux from the Mississippi and Atchafalaya Rivers leads to the dominance of diatoms in planktonic community assemblages (Zhao & Quigg, 2014), which are a major component of adult Gulf Menhaden diets (Olsen, Fulford, Dillon, & Graham, 2014). Increases in river discharge can also enhance the areal distribution of nutrient rich river plumes (N. D. Walker, 1996), promoting primary productivity in regions that are otherwise nutrient limited such as continental shelf and river plume front waters (Eldridge & Roelke, 2010; Huang et al., 2013). For example, high river discharge is associated with the anti-cyclonic curvature of plume waters from the Mississippi River Delta into locations offshore Terrebonne Bay (N. D. Walker, 1996). Therefore, it is likely that increased nutrient loading through freshwater delivery across the NGOM enhances feeding opportunities for Gulf Menhaden, leading to greater condition. However, contrary to Govoni (1997) who found that recruitment dynamics of Gulf Menhaden are correlated to winter discharge, we found that variation in relative condition best supported by immediate (lag 0 months) River Discharge. This is likely due to the immediate impact of Mississippi River discharge on the physical and community structure of the NGOM and subsequent impacts on adult Gulf Menhaden dynamics.

ENSO is associated with shifts in multiple environmental processes in the NGOM. For example, Lau & Nath (2001) found a negative correlation between the Niño-3 SST index and SST in the Gulf of Mexico, indicating that El Niño-like events are

associated with below-normal SST in the region. Rainfall in states along the NGOM coast increases during warm ENSO events (Enfield, 1996; Gershunov & Barnett, 1998; Ropelewski & Halpert, 1986), which enhances discharge and nutrient flux from smaller drainages. ENSO rainfall patterns in the Mississippi–Atchafalaya River basin can also flush nitrogen accumulated in soils, which is eventually discharged into the NGOM (Goolsby, Battaglin, Aulenbach, & Hooper, 2001; Sanchez-Rubio & Perry, 2015; Ward, Beets, Bouwer, Aerts, & Renssen, 2010). Nitrogen inputs in the NGOM promote the growth of phytoplankton (Zhao & Quigg, 2014), which would enhance feeding for adult Gulf Menhaden (Olsen et al., 2014). Temporal lags in the effect of ENSO on adult Gulf Menhaden are consistent with previous work relating the influence of climate regimes to environmental conditions in the NGOM (Enfield, 1996; Lau & Nath, 2001; Sanchez-Rubio et al., 2011). We suggest that moderate positive ENSO anomalies enhance relative condition of adult Gulf Menhaden through increased feeding conditions, primarily through river-driven inputs. Alternatively, in normoxic conditions increases in SST due to moderate La Niña like conditions could possibly promote the growth and condition of Adult Gulf Menhaden, similar to juveniles (Zhang et al., 2014).

We found a complex relationship between relative condition of Gulf Menhaden and the wind vector components. The improvement in the fit of GAMMs due to the inclusion of the wind vector components as non-stationary predictors indicates the presence of regional wind dynamics in relation to adult Gulf Menhaden populations. This was further highlighted by geographic clusters of similar wind-driven variability in relative condition of Gulf Menhaden. Such a spatial effect is likely due to differences in local geography (e.g. locations of freshwater inputs), bathymetry, and upwelling. In the

NGOM, winds influence the extent and distribution of river plume waters (Huang et al., 2013; N. D. Walker, 1996) and can increase productivity by mixing stratified or hypoxic waters (N N Rabalais, Turner, & Wiseman, 2001). Regional clusters that were identified reflect similarities in wind driven across- and alongshore transport of productive plume waters. Comparison of different temporal lags in the effect of zonal and meridional wind vectors on relative condition indicated that a temporal lag of two months best explains variation in relative condition of Gulf Menhaden. In numerous systems biological uptake can lag nutrient loading (Botsford, Lawrence, Dever, Hastings, & Largier, 2003, 2006; S E Lohrenz et al., 1999), therefore, the temporal lag we note in the effect of wind on relative condition is not unexpected. Relative condition of fish caught between Atchafalaya and the Louisiana Bight was improved after west winds two months prior (i.e. positive correlation with the zonal wind vector). West winds can limit the westward movement of productive plume waters out of the Mississippi River Delta and the eastern movement of discharge from the Atchafalaya River, likely leading to the positive correlation between the zonal wind vector and relative condition of Gulf Menhaden in this area. Alternatively, east winds drive the transport of productive plume waters west of Atchafalaya Bay (N. Walker & Hammack, 2000), which would enhance feeding conditions for adult Gulf Menhaden in those locations. In regards to the meridional wind vector, onshore winds can cause the retention of plume waters on the western side of the Mississippi Delta and along the shelf break (R. V. Schiller, Kourafalou, Hogan, & Walker, 2011), which would enhance feeding conditions at these locations (i.e. offshore Louisiana Bight). North winds can promote the offshore displacement of river discharge (N. D. Walker, Wiseman, Rouse, & Babin, 2005), explaining the enhanced condition of

adult Gulf Menhaden offshore Atchafalaya Bay. Thus, the spatially-variant effect of the wind vector components on relative condition of Gulf Menhaden in part reflects wind-driven transport of productive plume waters, likely due to the enhanced feeding opportunities associated with the location of the river plume. Therefore, future research should be directed on the local distribution and location of river plumes and plume fronts and their impacts on the productivity of fisheries in the NGOM.

We note that the influence of SST on relative condition of adult Gulf Menhaden was best supported by the non-linear stationary model, indicating that the effects of the predictor was consistent across the NGOM. We suggest two possible mechanisms underlying the observed trend, but further analyses are required to test these hypotheses. The non-linear trend could indicate an optimal thermal window for individual growth and energy storage, similar to the non-linear effect of SST on the observed survival of blueback herring *Alos aestivalis* (Tommasi et al., 2015). For age-0 Gulf Menhaden, Zhang et al. (2014) suggested 28 to 29°C as the optimal temperature for individual growth and noted restricted individual growth at temperatures above 32°C. Differences between our results are likely due to variations in habitat use and ontogenetic development as adults move offshore to cooler water (Deegan, 1990). The observed non-linear trend may also indicate that energy storage is maximized at the temperatures found at river plume fronts in the NGOM. Plume fronts are associated with high levels of productivity (C. B. Grimes & Finucane, 1991; Hitchcock et al., 1997). Hitchcock et al. (1997) noted that SST along the Mississippi River plume front during the peak of fishing season (summer) was 24 to 26°C, these are the SST values at which we predicted maximum condition. Given the high productivity of frontal regions relative to plume and

oceanic waters, it is likely that Gulf Menhaden caught at the plume front benefit from greater feeding opportunities leading to increased condition.

Seasonal energy storage strategies of small forage fishes are influenced by the spatial-temporal distribution of prey as well as seasonal spawning (Cubillos, Arcos, Bucarey, & Canales, 2001; Rojbek et al., 2014). For example, lipid content of herring *Clupea harengus* and sprat *Sprattus sprattus* is greatest near the end of the annual zooplankton peak (Rojbek et al., 2014). In the NGOM, phytoplankton abundance peaks in the spring (Chakraborty & Lohrenz, 2015; Steven E. Lohrenz et al., 2008). The results presented here indicate that Gulf Menhaden benefit from high food abundance during spring months, leading to greater condition in April and May. Gulf Menhaden also spawn during the winter (Dean W Ahrenholz, 1991) and improved condition in the autumn may be related to a capital-breeding strategy, where Gulf Menhaden depend on energy gained during the autumn for winter spawning. Temporal patterns in relative condition in Gulf Menhaden are likely a result of food availability and reproductive strategy. However, despite the link between relative condition and lipid content (Sutton, Bult, & Haedrich, 2000), a majority of samples from the fishery were taken during the summer months when average condition was relatively low.

The spatial distribution of relative condition measured from adult Gulf Menhaden supports the hypothesis that relative condition is driven by food availability. Productivity of zooplankton and phytoplankton in the NGOM is greatest in locations affected by freshwater inputs (Del Castillo et al., 2001; Hitchcock et al., 1997; S E Lohrenz et al., 1997). Relative condition of Gulf Menhaden follow a similar distribution as primary and secondary production, with peak values occurring west of the Mississippi River Delta in

locations most influenced by river discharge. Prey-driven bottom-up forcing has been found in the Peruvian anchoveta *Engraulis ringens* stock where anchoveta biomass varied with zooplankton biovolume (Ayón, Swartzman, Bertrand, Gutiérrez, & Bertrand, 2008). Spatial variability in the growth and survival of Walleye Pollock *Theragra chalcogramma* has also been shown to be driven by the spatial patterns in prey composition (Siddon et al., 2013). Therefore, future research should be directed towards describing the linkage between zooplankton and phytoplankton abundance and Gulf Menhaden population dynamics.

Multiple factors may potentially be confounding our analysis, contributing to the low percent deviance explained by the GAMMs. Similar efforts to model the dynamics of Gulf Menhaden (Langseth et al., 2014) and Atlantic croaker (Craig & Crowder, 2005) in the NGOM have also exhibited low precision, which may be indicative of the highly dynamic nature of the NGOM. In addition, sex is not recorded by NMFS for each sample and sex-specific differences in energy storage strategies could reduce precision. Mature females likely increase energetic provisioning for late fall or early winter spawning, which may influence their relative condition. Vaughan et al. (1996, 2007) suggested that a change in selectivity occurred in the commercial fishery in 1975 after observing shifts in the age composition of the harvest. Changes in the age structure of the stock may alter habitat use patterns and other ecological dynamics. Similarly, while previous research has indicated that there is minimal gulf wide migration of Gulf Menhaden (Pristas, Levi, & Dryfoos, 1976; SEDAR, 2013), the fine scale movement of schools in relation to the sampling grid is unknown and may have added uncertainty to our results. Therefore, future efforts should be directed towards understanding age-specific habitat use and fine

scale movement of Gulf Menhaden. Our modelling efforts would also benefit from increased spatial resolution of the response and environmental predictor variables.

We have demonstrated that multiple bottom-up processes impact the individual dynamics of adult Gulf Menhaden in the NGOM. The spatially-explicit processes identified in this study are likely linked to primary and secondary productivity and the extent and location of river plumes in the NGOM. Variation in bottom-up processes that impact the distribution and productivity of the Mississippi River plume will lead to contrasts relative condition of Gulf Menhaden and may pose consequences for the commercial fishery and the ecology in the NGOM. For example, given correlations between fat content and condition of Menhaden (Dahlberg, 1969), lower oil yields from the commercial reduction fishery would be expected during years of low river discharge, winds that promote the transport of plume waters away from fishing grounds, and SST values outside the threshold for optimum condition. Gulf menhaden is also an important food fish for recreationally and commercially important species (Bass & Avault, 1975; Scharf & Schlight, 2000) as well as other upper trophic-level species (Barry, Condrey, Driggers, & Jones, 2008; Robinson et al., 2015; Sagarese et al., 2016). Therefore, variations in the relative condition of Gulf Menhaden could alter energy pathways among trophic levels.

Table 1.1

Summary of environmental data used to examine the impacts of bottom-up processes on relative condition of Gulf Menhaden in the northern Gulf of Mexico.

Variables	**Units**	**Spatial resolution**	**Temporal resolution**	**First year available**	**Source**
Mississippi River discharge	$ft^3\ s^{-1}$		Daily	1930	1USACE
Multivariate ENSO Index			Monthly	1950	2ESRL
Zonal and meridional wind vector components	$m\ s^{-1}$	2.5°	Monthly	1948	3ESRL PSD
SST	°C	9 km^2	Monthly	2002	4GSFC

1USACE: US Army Corps of Engineers. River discharge measured at Tarbert Landing, MS. (http://rivergages.mvr.usace.army.mil/).
2ESRL: Earth Systems Research Laboratory (http://www.esrl.noaa.gov/).
3NOAA/OAR/ESRL PSD: Earth Systems Research Laboratory Physical Sciences Division. NCEP Reanalysis data (Kalnay et al., 1996) (http://www.esrl.noaa.gov/psd/).
4GSFC: Goddard Space Flight Center. MODIS Aqua Sensor. (http://modis.gsfc.nasa.gov/)

Table 1.2

Model selection for generalized additive mixed models relating relative condition of adult Gulf Menhaden in year α_y, month m, latitude (φ), and longitude (λ) to environmental predictors (x_j). s and g are 1- and 2-dimensional nonparametric smoothing functions and b_v is the random effect term of v. Deviance Explained (Dev. expl.), Akaikie information criterion (AIC), delta AIC (ΔAIC), and AIC weights (AICw), and sample size (N) of each candidate model is included. Final model is indicated in bold.

Model formulation	Lag (months)	Dev. expl.	AIC	ΔAIC	AIC*w*	N
Mississippi River Discharge (1964 to 2011)						
$\sim \boldsymbol{\alpha_y + s_1(m) + b_v + \varepsilon_{y,m}}$		19.11%	1,764,862	4842	0.0	251,712
$+\boldsymbol{g_1(\varphi, \lambda)}$		19.98%	1,762,187	2166	0.0	251,712
$+\boldsymbol{g_1(\varphi, \lambda) + s_2(x_j)}$	**0**	**20.67%**	**1,760,021**	**0**	**1.0**	**251,712**
$+\boldsymbol{g_1(\varphi, \lambda) + s_2(x_j)}$	1	20.24%	1,761,374	1353	0.0	251,712
$+\boldsymbol{g_1(\varphi, \lambda) + s_2(x_j)}$	2	20.22%	1,761,449	1428	0.0	251,712
$+\boldsymbol{g_1(\varphi, \lambda) + s_2(x_j)}$	3	20.23%	1,761,403	1382	0.0	251,712
$+\boldsymbol{g_1(\varphi, \lambda) + s_2(x_j)}$	Spring index	19.99%	1,761,687	1666	0.0	251,712
$+\boldsymbol{g_1(\varphi, \lambda) + s_2(x_j)}$	Winter index	20.05%	1,761,757	1737	0.0	251,712
$+\boldsymbol{s_2(x_j)}$	0	19.81%	1,762,693	2672	0.0	251,712
$+\boldsymbol{s_2(x_j)}$	1	19.37%	1,764,051	4031	0.0	251,712
$+\boldsymbol{s_2(x_j)}$	2	19.35%	1,764,113	4093	0.0	251,712
$+\boldsymbol{s_2(x_j)}$	3	19.36%	1,764,096	4075	0.0	251,712
$+\boldsymbol{s_2(x_j)}$	Spring index	19.11%	1,764,770	4750	0.0	251,712
$+\boldsymbol{s_2(x_j)}$	Winter index	19.18%	1,764,526	4505	0.0	251,712
Multivariate ENSO Index (1964 to 2011)						

$\sim \alpha_y + s_1(m) + b_v + \varepsilon_{y,m}$		19.11%	1,764,862	5309	0.0	251,712
$+g_1(\varphi, \lambda)$		19.98%	1,762,187	2633	0.0	251,712
$+g_1(\varphi, \lambda) + s_2(x_j)$	0	20.46%	1,760,692	1139	0.0	251,712
$+g_1(\varphi, \lambda) + s_2(x_j)$	1	20.18%	1,761,562	2009	0.0	251,712
$+g_1(\varphi, \lambda) + s_2(x_j)$	2	20.11%	1,761,781	2228	0.0	251,712
$+g_1(\varphi, \lambda) + s_2(x_j)$	3	20.19%	1,761,539	1986	0.0	251,712
$+g_1(\varphi, \lambda) + s_2(x_j)$	4	20.28%	1,761,251	1698	0.0	251,712
$+g_1(\varphi, \lambda) + s_2(x_j)$	5	20.35%	1,761,025	1472	0.0	251,712
$+g_1(\varphi, \lambda) + s_2(x_j)$	6	20.27%	1,761,287	1734	0.0	251,712
$+g_1(\varphi, \lambda) + s_2(x_j)$	7	20.29%	1,761,208	1655	0.0	251,712
$+g_1(\varphi, \lambda) + s_2(x_j)$	8	20.43%	1,760,761	1208	0.0	251,712
$+g_1(\varphi, \lambda) + s_2(x_j)$	9	20.47%	1,760,655	1102	0.0	251,712
$+g_1(\varphi, \lambda) + s_2(x_j)$	**10**	**20.82%**	**1,759,553**	**0**	**1.0**	**251,712**
$+g_1(\varphi, \lambda) + s_2(x_j)$	11	20.51%	1,760,526	973	0.0	251,712
$+g_1(\varphi, \lambda) + s_2(x_j)$	12	20.30%	1,761,179	1626	0.0	251,712
$+s_2(x_j)$	0	19.62%	1,763,281	3728	0.0	251,712
$+s_2(x_j)$	1	19.30%	1,764,261	4708	0.0	251,712
$+s_2(x_j)$	2	19.25%	1,764,426	4873	0.0	251,712
$+s_2(x_j)$	3	19.32%	1,764,204	4651	0.0	251,712
$+s_2(x_j)$	4	19.42%	1,763,890	4337	0.0	251,712
$+s_2(x_j)$	5	19.50%	1,763,659	4106	0.0	251,712
$+s_2(x_j)$	6	19.42%	1,763,889	4336	0.0	251,712
$+s_2(x_j)$	7	19.46%	1,763,777	4224	0.0	251,712
$+s_2(x_j)$	8	19.60%	1,763,350	3797	0.0	251,712
$+s_2(x_j)$	9	19.64%	1,763,203	3650	0.0	251,712

$+s_2(x_j)$	10	20.02%	1,762,025	2472	0.0	251,712
$+s_2(x_j)$	11	19.66%	1,763,137	3584	0.0	251,712
$+s_2(x_j)$	12	19.44%	1,763,846	4292	0.0	251,712
Wind vector components (1964 to 2011)						
$\sim \alpha_y + s_1(m) + b_v + \varepsilon_{y,m}$		19.11%	1,764,862	5862	0.0	251,712
$+g_1(\varphi, \lambda)$		19.98%	1,762,187	3186	0.0	251,712
$+g_1(\varphi, \lambda) + s_2(x_j)$	0	20.30%	1,761,219	2218	0.0	251,712
$+g_1(\varphi, \lambda) + s_2(x_j)$	1	20.62%	1,760,182	1181	0.0	251,712
$+g_1(\varphi, \lambda) + s_2(x_j)$	2	20.30%	1,761,191	2190	0.0	251,712
$+g_1(\varphi, \lambda) + s_2(x_j)$	3	20.23%	1,761,430	2429	0.0	251,712
$+g_1(\varphi, \lambda) + g_2(\varphi, \lambda) * x_j$	0	20.71%	1,759,973	972	0.0	251,712
$+g_1(\varphi, \lambda) + g_2(\varphi, \lambda) * x_j$	1	21.00%	1,759,046	46	0.0	251,712
$+g_1(\varphi, \lambda) + g_2(\varphi, \lambda) * x_j$	**2**	**21.02%**	**1,759,001**	**0**	**1.0**	**251,712**
$+g_1(\varphi, \lambda) + g_2(\varphi, \lambda) * x_j$	3	20.80%	1,759,697	696	0.0	251,712
$+s_2(x_j)$	0	19.42%	1,763,905	4905	0.0	251,712
$+s_2(x_j)$	1	19.74%	1,762,925	3924	0.0	251,712
$+s_2(x_j)$	2	19.46%	1,763,803	4802	0.0	251,712
$+s_2(x_j)$	3	19.36%	1,764,096	5096	0.0	251,712
$+g_1(\varphi, \lambda) * x_j$	0	20.08%	1,761,930	2930	0.0	251,712
$+g_1(\varphi, \lambda) * x_j$	1	20.29%	1,761,274	2274	0.0	251,712
$+g_1(\varphi, \lambda) * x_j$	2	20.39%	1,760,964	1964	0.0	251,712
$+g_1(\varphi, \lambda) * x_j$	3	20.16%	1,761,663	2663	0.0	251,712
Sea surface temperature (SST) (2003-2011)						
$\sim \alpha_y + s_1(m) + b_v + \varepsilon_{y,m}$		15.25%	170,949	530	0.0	25,365
$+g_1(\varphi, \lambda)$		16.27%	170,668	249	0.0	25,365
$+g_1(\varphi, \lambda) + s_2(x_j)$	**0**	**17.15%**	**170,419**	**0**	**1.0**	**25,365**

$+\boldsymbol{g_1(\varphi, \lambda) + s_2(x_j)}$	1	16.43%	170,634	215	0.0	25,365
$+\boldsymbol{g_1(\varphi, \lambda) + s_2(x_j)}$	2	17.10%	170,431	12	0.0	25,365
$+\boldsymbol{g_1(\varphi, \lambda) + s_2(x_j)}$	3	16.97%	170,469	50	0.0	25,365
$+\boldsymbol{g_1(\varphi, \lambda) + g_2(\varphi, \lambda) * x_j}$	0	16.70%	170,557	138	0.0	25,365
$+\boldsymbol{g_1(\varphi, \lambda) + g_2(\varphi, \lambda) * x_j}$	1	16.51%	170,618	199	0.0	25,365
$+\boldsymbol{g_1(\varphi, \lambda) + g_2(\varphi, \lambda) * x_j}$	2	16.94%	170,486	66	0.0	25,365
$+\boldsymbol{g_1(\varphi, \lambda) + g_2(\varphi, \lambda) * x_j}$	3	16.76%	170,539	119	0.0	25,365
$+\boldsymbol{s_2(x_j)}$	0	16.26%	170,666	247	0.0	25,365
$+\boldsymbol{s_2(x_j)}$	1	15.44%	170,909	489	0.0	25,365
$+\boldsymbol{s_2(x_j)}$	2	16.23%	170,672	253	0.0	25,365
$+\boldsymbol{s_2(x_j)}$	3	16.10%	170,712	293	0.0	25,365
$+\boldsymbol{g_1(\varphi, \lambda) * x_j}$	0	16.52%	170,598	179	0.0	25,365
$+\boldsymbol{g_1(\varphi, \lambda) * x_j}$	1	16.29%	170,666	246	0.0	25,365
$+\boldsymbol{g_1(\varphi, \lambda) * x_j}$	2	16.52%	170,597	178	0.0	25,365
$+\boldsymbol{g_1(\varphi, \lambda) * x_j}$	3	16.33%	170,656	237	0.0	25,365

Table 1.3

Summary of base and final Generalized Additive Mixed Models that relate Gulf Menhaden relative condition to spatial-temporal and environmental predictors ($\boldsymbol{x_j}$). Estimated year-specific coefficients are shown for the first year analyzed (e.g. 1964 or 2003) and estimated degrees of freedom are shown for nonparametric terms. AIC and deviance explained (%; Dev. expl.) are noted.

Predictor	**Model**	**Years included**	**Coef**	**Estimated Degrees of Freedom**			**% Dev. expl.**
			$\boldsymbol{\alpha_y}$	$\boldsymbol{g_1(\varphi, \lambda)}$	$\boldsymbol{s_1(m)}$	$\boldsymbol{x_j}$	
	$\sim \alpha_y + s_1(m) + g_1(\varphi, \lambda) + b_v$	1964 to 2011	4.6	28.2	5		1,765,625
	$\sim \alpha_y + s_1(m) + g_1(\varphi, \lambda) + b_v$	2003-2011	4.6	21.5	5		170,735
Mississippi River discharge	$+g_1(\varphi, \lambda) + s_2(x_j)$	1964 to 2011	4.6	28.3	5	8.9	1,763,434
Multivariate ENSO Index	$+g_1(\varphi, \lambda) + s_2(x_j)$	1964 to 2011	4.6	28.2	5	9	1,762,930
Wind vector components	$+g_1(\varphi, \lambda) + g_2(\varphi, \lambda) * x_j$	1964 to 2011	4.6	27.6	5	Zonal: 27.4 Meridional: 28.9	1,759,001
SST	$+g_1(\varphi, \lambda) + s_2(x_j)$	2003-2011	4.6	21	4.9	8.4	170,493

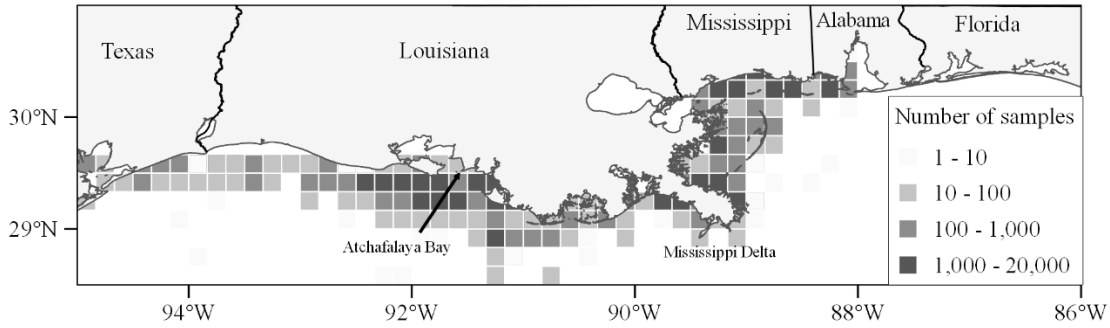

Figure 1.1 Study area and number of adult Gulf Menhaden (N = 251,712) sampled from the commercial fishery in the northern Gulf of Mexico (1964 to 2011) analyzed in this study.

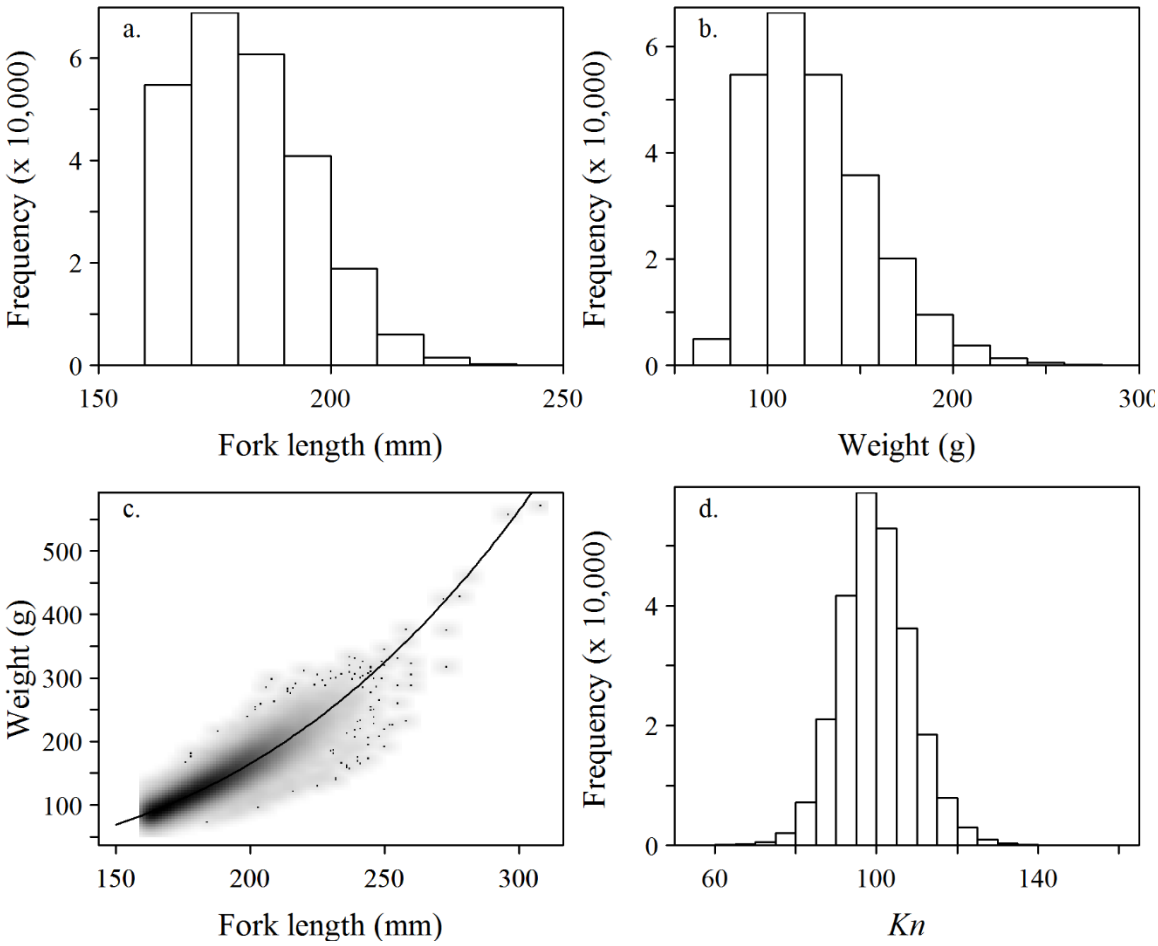

Figure 1.2 Histograms of (a) fork length and (b) weight, (c) fitted weight-at-length curve ($\widehat{W} = 1.77\times10^{-5}L^{3.03}$) and (d) histogram of relative condition (*Kn*) of adult Gulf Menhaden sampled from the commercial fishery in the northern Gulf of Mexico (1964 to 2011).

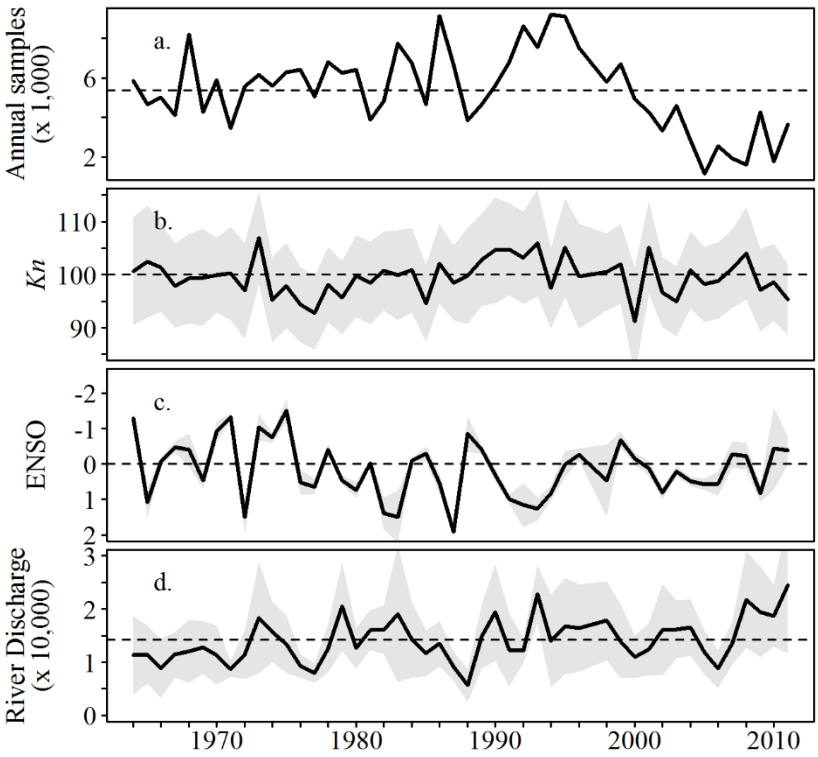

Figure 1.3 Annual mean ± S.D. (in grey) for (a) Annual number of adult Gulf Menhaden sampled from the commercial fishery in the northern Gulf of Mexico (1964 to 2011), (b) relative condition (*Kn*), (c) monthly Multivariate ENSO Index, and (d) monthly aggregated daily flow rates (f^3 s^{-1}) of the Mississippi River collected at Talbert Landing, MS. Horizontal lines indicate mean values.

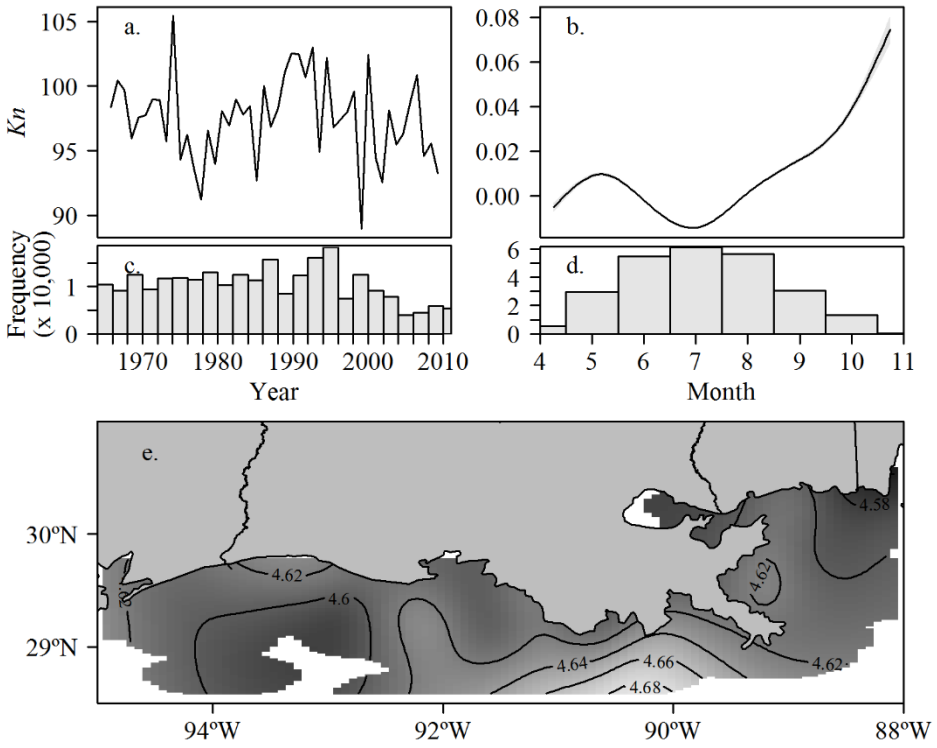

Figure 1.4 (a) Partial effect of monthly Mississippi River discharge on relative condition (*Kn*) of adult Gulf Menhaden sampled from the commercial fishery in the northern Gulf of Mexico (1964 to 2011) estimated from the spatially-invariant Generalized Additive Mixed Model. (b) Histogram indicates the number of samples.

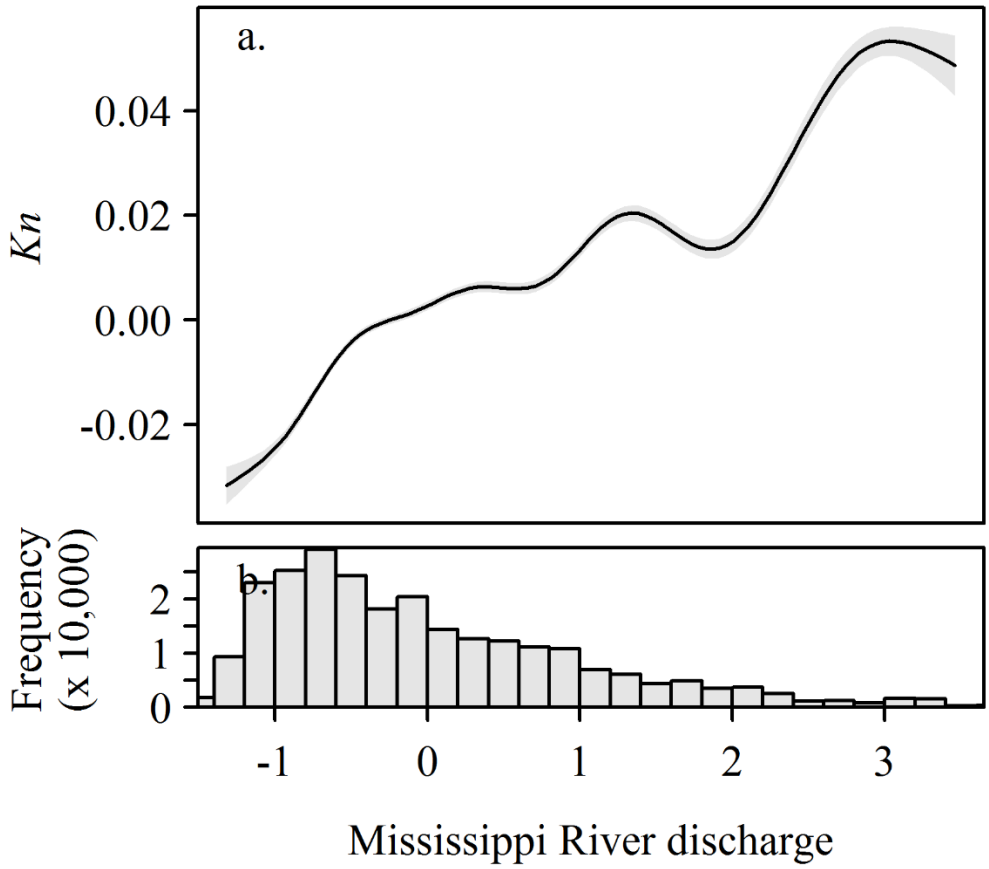

Figure 1.5 (a) Partial effect of monthly Mississippi River discharge on relative condition (Kn) of adult Gulf Menhaden sampled from the commercial fishery in the northern Gulf of Mexico (1964 to 2011) estimated from the spatially-invariant Generalized Additive Mixed Model. (b) Histogram indicates the number of samples.

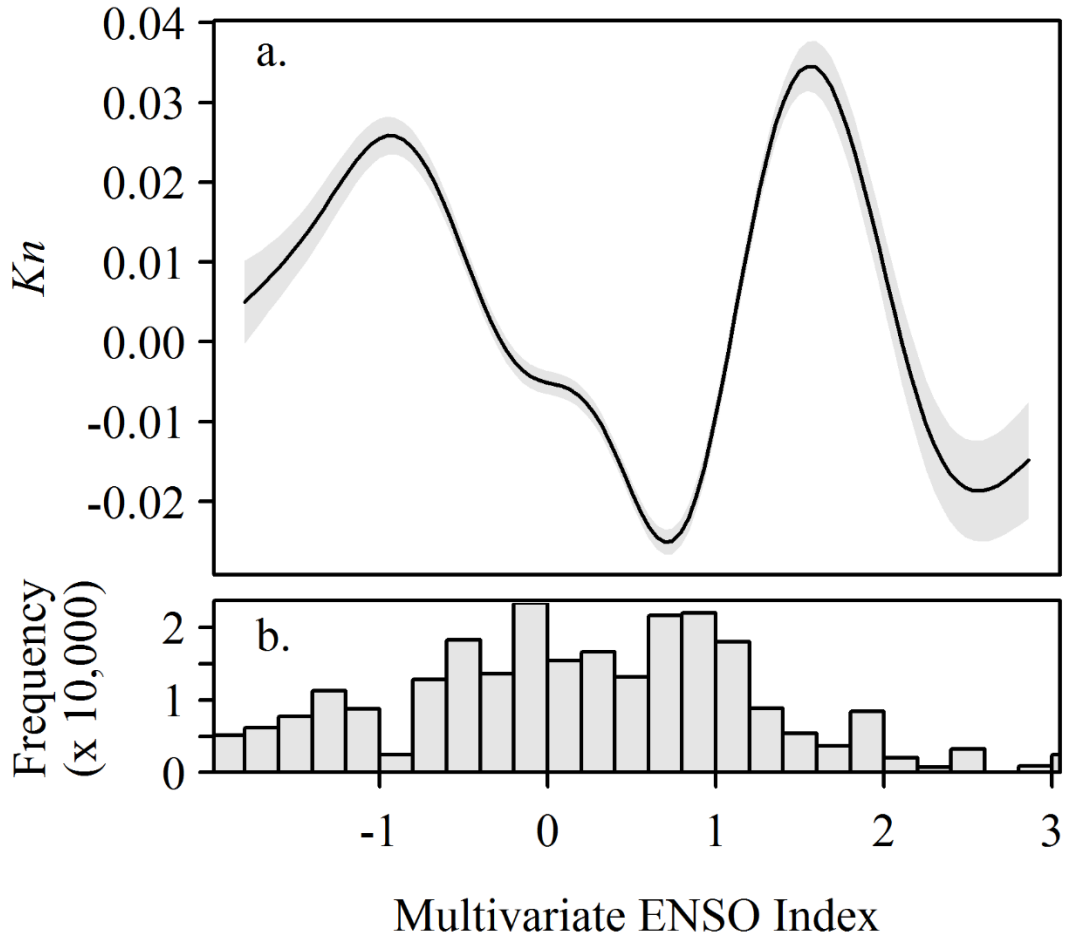

Figure 1.6 (a) Partial effect of the Multivariate ENSO Index on relative condition (*Kn*) of adult Gulf Menhaden sampled from the commercial fishery in the northern Gulf of Mexico (1964 to 2011) estimated from the spatially-invariant Generalized Additive Mixed Model. Positive values of the Multivariate ENSO Index indicate El Niño-like conditions and negative values indicate La Niña-like conditions. (b) Histogram indicates the number of samples.

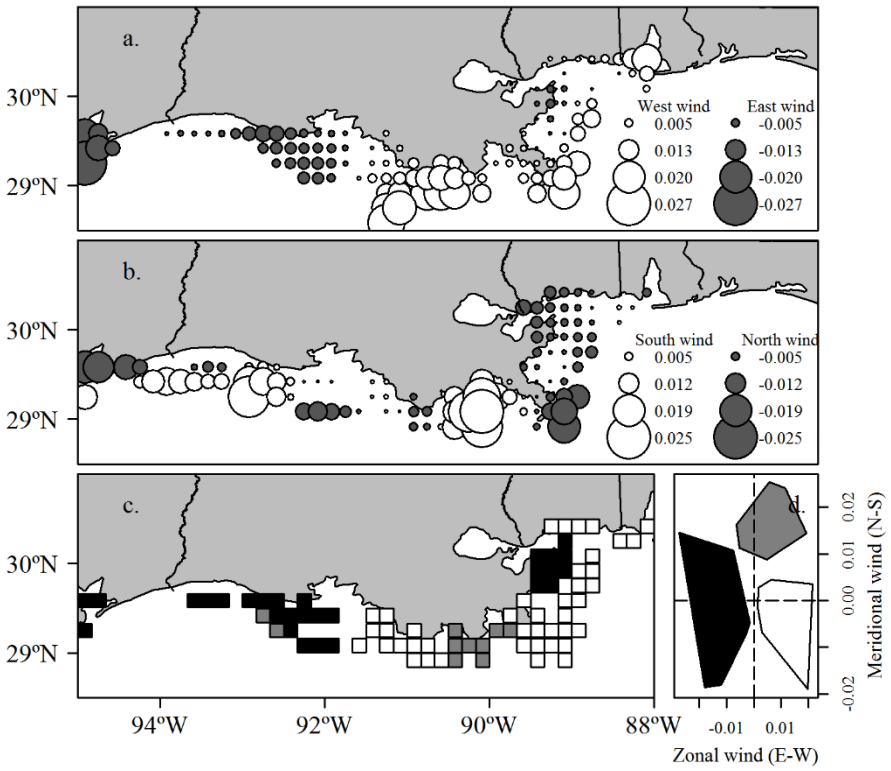

Figure 1.7 Spatially-explicit effects of the (a) zonal (East-West) and (b) meridional (North-South) wind vectors (m s^{-1}) on relative condition (*Kn*) of adult Gulf Menhaden sampled from the commercial fishery in northern Gulf of Mexico (1964 to 2011) estimated from the spatially-variant Generalized Additive Mixed Model. Circle size is proportional to the estimated increase in relative condition for one-unit increase (white circle) or decrease (dark grey circle) in the velocity (m s^{-1}) of the zonal or meridional wind vectors. Spatially-explicit wind direction favorable to condition is indicated in each panel. (c) Distribution of (d) *k*-means clustering (n = 3, clusters) of significant spatially-explicit effects of zonal and meridional wind vectors.

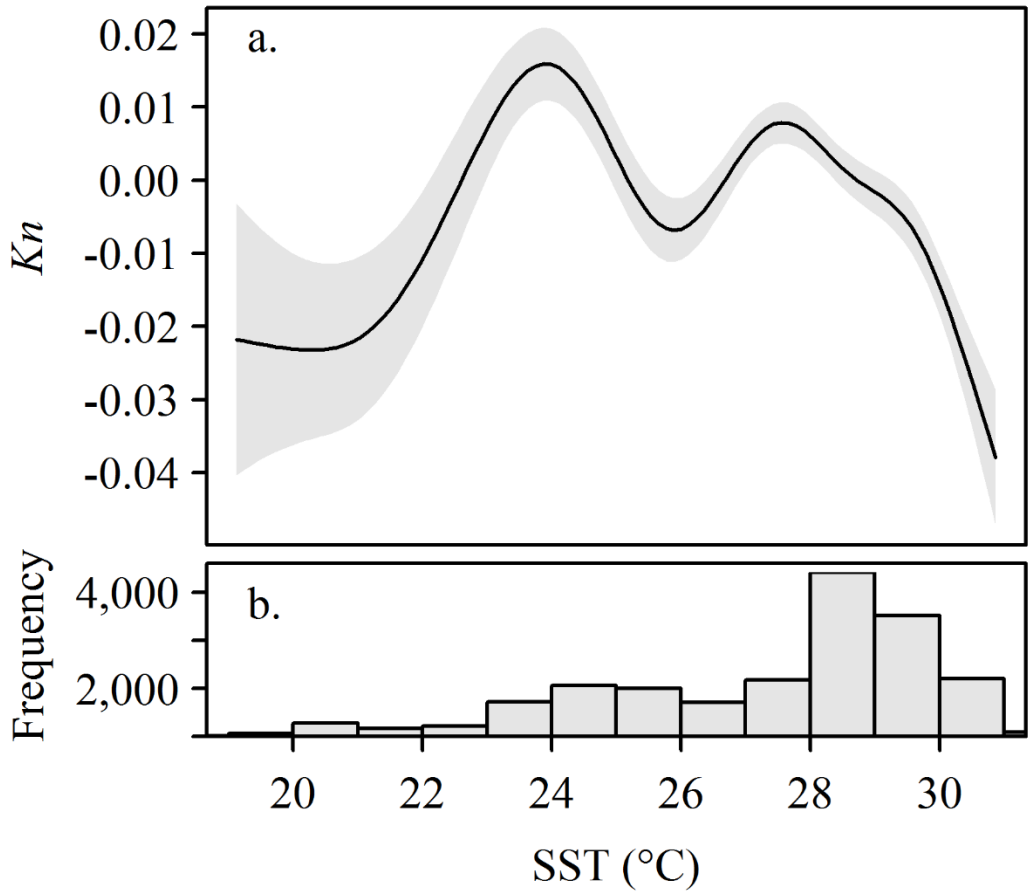

Figure 1.8 (a) Partial effect of SST on relative condition (*Kn*) of adult Gulf Menhaden sampled from the commercial fishery (2003 to 2011) estimated from the spatially-invariant Generalized Additive Mixed Model. (b) Histogram indicates the number of samples.

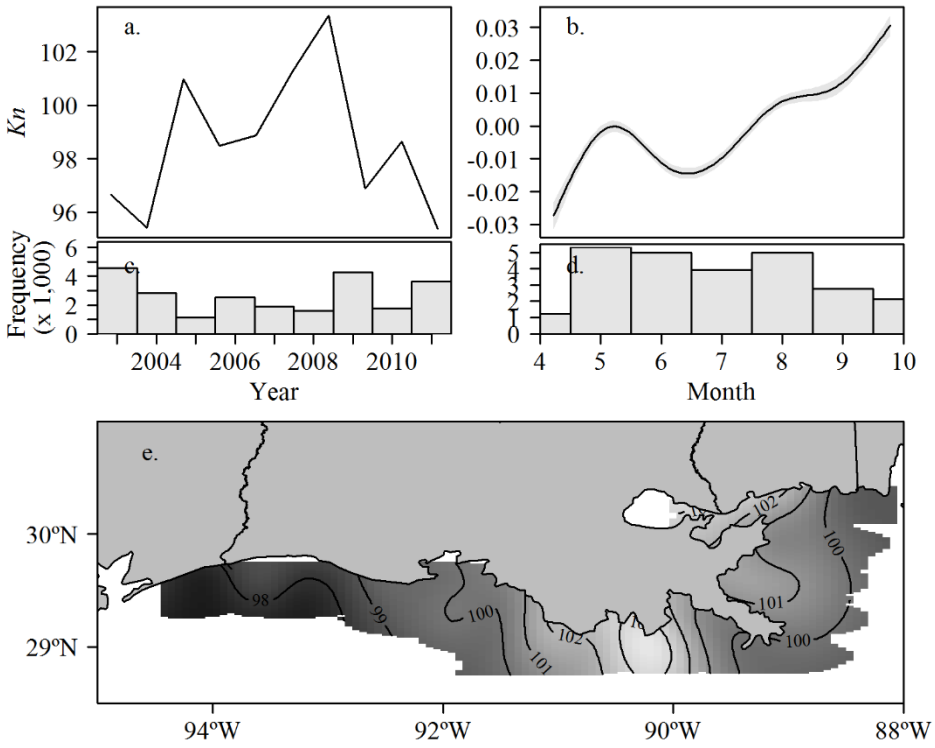

Figure 1.9 (a) Year-specific intercepts, (b) partial effect of week, histograms (c, d) of the number of samples, and (e) predicted spatial distribution of relative condition (*Kn*) of adult Gulf Menhaden sampled from the commercial fishery in the northern Gulf of Mexico (2003 to 2011) estimated from the base Generalized Additive Mixed Model. Note: predicted spatial distribution is scaled to July condition.

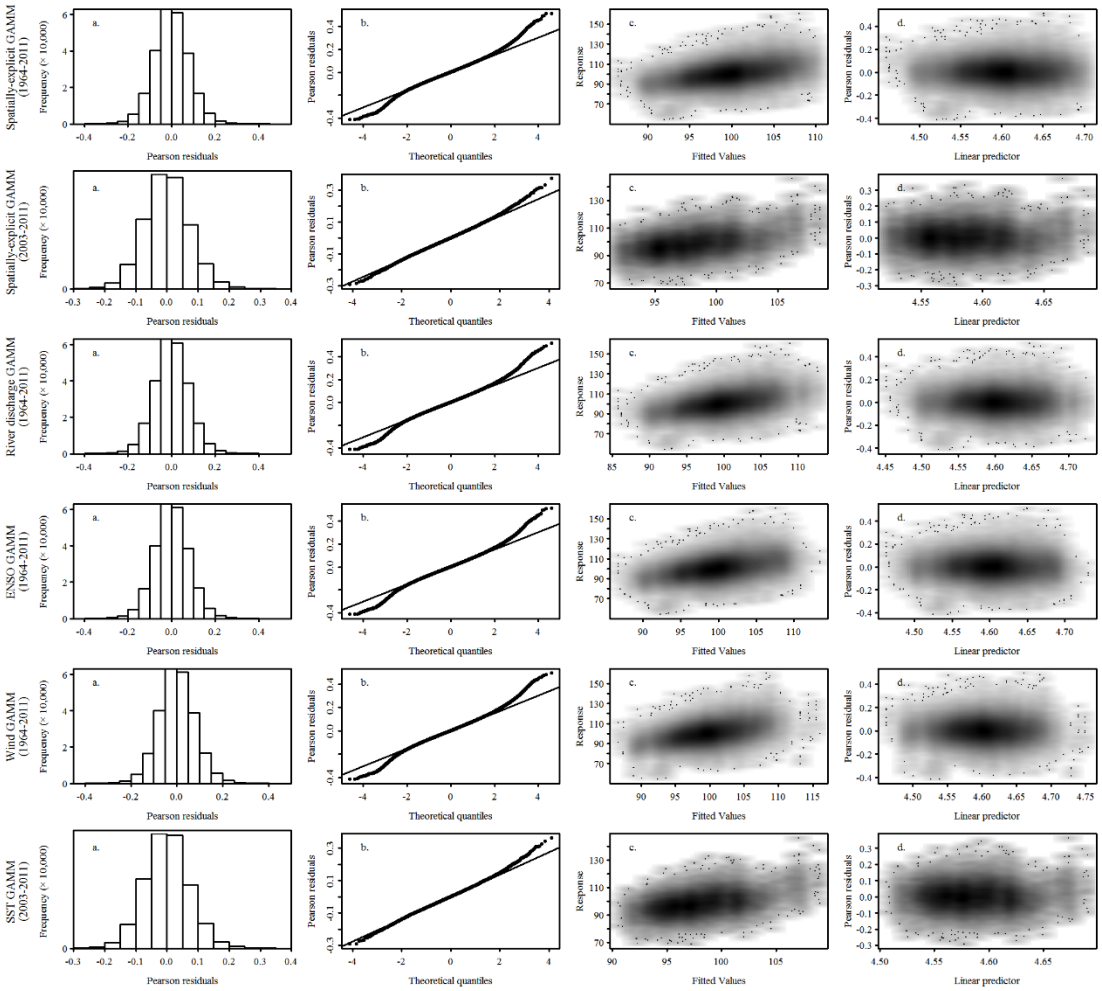

Figure 1.10 Standard model diagnostics of base, spatially- invariant, and spatially-variant generalized additive mixed model (GAMMs), relating relative condition of adult Gulf Menhaden spatial-temporal and environmental predictors (Table 3): (a) histogram of the Pearson residuals, (b) normal QQ-plot of Pearson residuals against theoretical quantiles, (c) density plot of observed against fitted values, and (d) density plot of Pearson residuals against the linear predictor.

CHAPTER II - EVALUATION OF MISSISSIPPI RIVER DISCHARGE, PRODUCTIVITY, AND TEMPERATURE ON THE SPATIO-TEMPORAL DYNAMICS OF LARVAL GULF MENHADEN (*BREVOORTIA PATRONUS*) IN THE NORTHERN GULF OF MEXICO

2.1 Abstract

The recruitment dynamics of Gulf Menhaden *Brevoortia patronus* correlate to annual contrasts in Mississippi River discharge. Explanations for the observed correlation include the impacts of river discharge on the distribution and feeding conditions of larvae. In this work we investigate, using a series of two-stage regression models, plankton survey data obtained from the Southeast Area Monitoring and Assessment Program (SEAMAP) ichthyoplankton surveys (1982 – 2013). We evaluated the effect of Mississippi River discharge levels, chlorophyll *a* concentration, plankton displacement volume, and sea surface temperature (SST) on the relative abundance of larval Gulf Menhaden based on combining the probability of presence and non-zero catch per unit effort (CPUE). We found that river discharge significantly altered the spatial distribution of larvae: greater levels of river discharge served to reduce and enhance their relative abundance to the east and west of the Mississippi River delta, respectively. We hypothesize that such patterns are due to forcing from the anticyclonic curvature of the Mississippi River plume during periods of enhanced discharge. Similarly, the CPUE of larval Gulf Menhaden decreased during high river discharge conditions. We found a significant correlations between the probability of presence of larvae and chlorophyll *a* concentration and SST. We note that the standardized trends of annual relative abundance do not correlate well to estimates of year class strength from stock assessment models or

fishery independent survey indices of recruitment. The identified relationships suggest that the location of spawning and environmental factors that influence the distribution of larvae may limit recruitment strength of Gulf Menhaden.

2.2 Introduction

The early life stages of marine fish (i.e., eggs, yolk-sac larvae, larvae) experience relatively large mortality rates and are considered the most vulnerable ontogenetic stage in the life history of fish (E D Houde & Zastrow, 1993; Edward D. Houde, 2008). Variation in survivorship and growth of early life stages is thought to be one of the forces that influence the recruitment strength of fish populations (John J. Govoni, 1997; Edward D. Houde, 2008). These variations are simultaneously controlled by both bottom-up and top-down forcing mechanisms including food availability, predation, and a variety of oceanographic processes (Edward D. Houde, 2008).

Gulf Menhaden *Brevoortia patronus* is an abundant forage fish distributed throughout the northern Gulf of Mexico (NGOM) and supports the second largest fishery, by weight, in the United States (Vaughan et al., 2007). Based on the presence of eggs in plankton surveys and reproductive studies, adults are thought to spawn in the coastal NGOM between October and February (Dean W Ahrenholz, 1991; Fore, 1970; Lewis & Roithmayr, 1980; Shaw, Cowan, & Tillman, 1985). After hatching, previous research suggests that larvae are found in the greatest abundance south of the Mississippi River Delta along the freshwater river plume front where they are entrained as a result of frontal convergence (John J. Govoni & Grimes, 1992; John J. Govoni, Hoss, & Colby, 1989; S. M. Sogard, Hoss, & Govoni, 1988). Peak ingress into inshore estuaries and bays from offshore frontal zones occurs in February and March, where larvae develop until

recruiting to the offshore adult population in the following summer and early fall (Deegan, 1990; Fore, 1970; J. J. Govoni, 1993; Shaw & Drullinger, 1990).

Multiple hypotheses describing the relationship between freshwater inputs in the NGOM and the dynamics of offshore larval stage of Gulf Menhaden have been proposed to describe the variability in recruitment (John J. Govoni, 1997; Sanchez-Rubio & Perry, 2015; Vaughan, Govoni, & Shertzer, 2011). Govoni (1997) and Vaughan et al. (2011) found a negative correlation between recruitment estimated by virtual population analysis and Mississippi River discharge and speculated that observed recruitment variability is controlled by river plume driven transport and mortality. Increased Mississippi River discharge is associated with the enhanced areal extent of the coastal river plume (N. D. Walker, 1996), which could prolong inshore transport and offshore predation of larval Gulf Menhaden. Alternatively, Sanchez-Rubio and Perry (2015) proposed that recruitment is influenced by river discharge driven variability in feeding conditions after finding positive correlations between wet winter conditions and postlarval abundance of Gulf Menhaden. Increases in river discharge in the NGOM can lead to increased nutrient inputs and primary and secondary productivity (S E Lohrenz et al., 1997; Steven E. Lohrenz et al., 2008; Zhao & Quigg, 2014), which could improve feeding conditions for larval Gulf Menhaden that feed on phytoplankton and zooplankton (Stoecker & Govoni, 1984). However, neither of these hypotheses have been tested and previous investigations on the impact of environmental processes on the dynamics of larval menhaden have been limited. Previous work has evaluated the environmental gradients in which larvae are found (Shaw, Cowan, et al., 1985), but because of the low densities of observed larvae, large number of sets with zero catch, and limited spatial coverage of sampling, it is

difficult to make inferences about regional scales of environmental forcing (Christmas & Waller, 1975; Fore, 1970; Edward D. Houde, 2008; Shaw, Cowan, et al., 1985).

In this work we make use of data collected by the Southeast Area Monitoring and Assessment Program (SEAMAP), a joint Federal-State program coordinated through the Gulf States Marine Fisheries Commission (GSMFC). The annual SEAMAP ichthyoplankton survey has been conducted in the NGOM since 1982. This program collects data on the occurrence, abundance and geographical distribution of fish eggs and larvae, as well as selected physical properties of the oceanographic conditions. This comprehensive dataset provides the means to address the limited spatial coverage of previous efforts. We address two explanatory mechanisms regarding river-driven spatial and temporal dynamics of larval Gulf Menhaden. First, we test the hypothesis that increased river discharge results in offshore and alongshore transport of larvae prior to estuarine ingress. Next, we test the hypothesis that the predicted relative abundance of larvae is positively correlated with food availability. Finally, we evaluate the strength of correlation between indices of adult and juvenile abundance and model-derived abundance for age-0 and age-1 to the predicted relative abundance of larval Gulf Menhaden.

2.3 Methods

2.3.1 Data

Data on the presence and catch per unit effort (CPUE) of larval Gulf Menhaden were obtained from SEAMAP ichthyoplankton surveys conducted cooperatively by the National Oceanic and Atmospheric Administration's National Marine Fisheries Service (NMFS) and the states of Louisiana, Mississippi, Alabama, and Florida. Since 1986,

SEAMAP has continuously conducted fishery-independent plankton surveys in the fall to sample the early-life stages of zooplankton on the continental shelf and shelf edge of the NGOM (Rester, 2012). Several winter surveys were conducted periodically throughout the time series in order to sample larvae spawned during the months December through March. While we recognize that the number of winter cruises was limited compared to fall cruises, we included that data in the analysis in order to examine the entirety of spatial-temporal variation throughout the spawning period when available.. Sampling is conducted using two gears: a 61 cm bongo nets fitted with 0.335 mm mesh netting and a single or double 2 x 1 m neuston net fitted with 0.950 mm mesh netting. The bongo net is towed obliquely at approximately 1.5 knots to a maximum depth of 200 m or between two and five meters off the bottom at station depths less than 200 m, and the neuston net is towed at the surface with the frame half submerged for a target tow time of 10 minutes. The volume of water filtered is measured for bongo net tows using mechanical flowmeters positioned inside each net. The estimated CPUE of larvae from bongo nets is standardized to account for volume of water filtered and depth of the sampled water column and expressed as the number of larvae under 10 m^2 of sea surface:

$$CPUE = total\ fish \times (depth \div volume\ filtered \times 10).$$

CPUE of larvae from neuston nets is standardized to account for net tow duration and expresses as number of larvae per 10 minute tow:

$$CPUE = total\ fish \times (tow\ duration \div 10)$$

Clupeid larvae collected from SEAMAP samples were sorted and identified to the lowest possible taxonomic level at the Sea Fisheries Institute, Plankton Sorting and Identification Center (MIR ZSIOP), in Gdynia and Szczecin, Poland under a Joint Studies

Agreement between the NMFS and the Sea Fisheries Institute. However, the lack of morphological development or pigmentation on small and damaged larvae can preclude identification to lower taxonomic levels for Clupeiformes (Richardson, Vanwye, Exum, Cowen, & Crawford, 2007; Teletchea, 2009). Due to the large number of specimens in the SEAMAP collection identified only to Clupeiformes (118,955) or Clupeidae (83,404), it would be an extremely time consuming effort and include the need for molecular techniques to identify these specimens to a genus level. Therefore, many small specimens in the SEAMAP collection remain at an order or family level resolution even though some of the larvae may be *Brevoortia* spp. For this study we utilized the specimens identified to genus in the understanding that they are a representative portion of the entire *Brevoortia* spp. population, including those left at the order and family taxonomic level. We assumed that all *Brevoortia* spp. collected between 94° and 86° W, north of 28° N, and between October and March were Gulf Menhaden, although we recognize that individuals from the two congeneric species in the region (*B. smithi*, *B. gunteri*) may be present. For each station, the presence and CPUE (larvae under 10 m2 of sea surface) were quantified. We examined the size distributions of Gulf Menhaden larvae sampled by SEAMAP. For each tow, a maximum of 10 individuals we measured to the nearest 0.1 mm SL. If more than 20 individuals were caught, either a subsample of 10 or the smallest and largest individuals were measured. Given the differences in sampling methodologies between cruises and years, only the size distributions of larvae with lengths that were subsampled were compared between bongo and neuston nets. We compared the difference between the lengths of larvae sampled from bongo and neuston nets using a Student's *t*-test.

Environmental variables examined include Mississippi River discharge, sea surface temperature (SST °C), chlorophyll *a* concentration (mg m^{-3}), and plankton displacement volume as an index of zooplankton abundance. An index of monthly Mississippi River discharge level (MRD_m) was created from daily Mississippi River flow rates (ft^3 s^{-1}) measured at Tarbert Landing, Mississippi between 1961 and 2012 provided by the US Army Corps of Engineers (http://rivergages.mvr.usace.army.mil/). For month *i* in each year, daily flow rates were summed from month *i* + (*i*-1) to account for the lag in river discharge structuring of the NGOM. The monthly sum was then scaled to the mean and standard deviation (SD) of months *i* + (*i* - 1) across all years. Annual periods of the index were then categorized into levels of discharge; high (> 0.5 SD), average (-0.5 to 0.5 SD), and low (< -0.5 SD). Temperature and chlorophyll *a* concentration are sampled *in situ* at each station at the surface, mid-water depth, and maximum depth following standardized methods. We selected surface values for all further analysis because Gulf Menhaden larvae are generally found in the upper water column (S. M. Sogard et al., 1988). Plankton displacement volume from bongo tows at each station, an index of station-specific plankton abundance and ecosystem productivity, was estimated by multiplying the observed volume of total plankton by the amount of water sampled at the station:

$$Total\ Volume = biovolume\ (mL) \times (depth \div volume\ filtered\ (mL) \times 10).$$

SEAMAP plankton displacement volume was available for majority of the time series and stations sampled.

2.3.2 Statistical Analysis

To assess the impact of the Mississippi River discharge and ecosystem productivity on variations in the spatial-distribution of larval Gulf Menhaden, a variable-coefficient Generalized Additive Model (GAM) with two strata (Hastie & Tibshirani, 1986; Murase, Nagashima, Yonezaki, Matsukura, & Kitakado, 2009) was developed for each gear. GAMs are semi-parametric regression models that can fit nonlinear relationships between response variables and covariates. The first stratum consisted of the probability of presence (or presence) of larvae modelled assuming a logit-link function and binomial error distribution. The second stratum consisted of the log-transformed larval non-zero CPUE with an added constant of one modelled assuming a Tweedie distribution and identity-link function. A feature of variable-coefficient GAMs is that interactions between spline functions and categorical variables indicate that separate spline functions are created for each categorical level (Wood, 2006). Using this modeling approach, we compared the spatial distribution of larval Gulf Menhaden as a function of average, high, and low Mississippi River discharge. We fit GAMs following the "double penalty" shrinkage approach (Marra and Wood 2011), which reduces error inherent in stepwise selection procedures. We fit models using maximum likelihood:

$$\text{Response} \sim \text{year} + \text{month} + \text{DN} + g_1(\emptyset, \lambda) + g_2(\emptyset, \lambda) \times \text{MRD}_\text{s} + \text{MRD}_\text{s} + s_1(\text{CHL}) + s_2(\text{ZOO}) + s_3(\text{SST}),$$

where year is the year class included as a factor, month is included as a factor, DN indicates either day or night, $\emptyset$ is the latitude and λ the longitude, g and s are two- and one-dimensional nonparametric smoothing functions (thin plate regression splines), respectively, MRD_m is the monthly categorical Mississippi River discharge level (i.e. high, average, and low, described above), CHL is the chlorophyll *a* concentration, ZOO

is the plankton displacement volume, and SST is the sea surface temperature (S. M. Sogard et al., 1988). ZOO was not included in the neuston net models because of the differences in sampling using this gear. To minimize overfitting, the degrees of freedom for all one-dimensional smoothing functions were restricted to 5 (i.e. $k = 6$). For some locations, CHL ($n = 772$), ZOO ($n = 40$), and SST ($n = 418$) were not sampled by SEAMAP. Therefore, we constructed a random effects model in which $s(\mathrm{x})$ is set to zero for any missing value of predictor x by using the variable coefficient mechanism. A Gaussian random effect was then substituted for the missing values of $s(\mathrm{x})$.

The best fit model for each gear and strata was selected following a forward stepwise approach (Su, Sun, Punt, Yeh, & Dinardo, 2011). Predictors were retained in the model if Akaike's Information Criteria (AIC) decreased. The distribution for each strata during different Mississippi River discharge levels (average, high, and low) was predicted for December 2012 using the best fit model and the mean of included environmental predictors. The distribution of relative abundance of larval Gulf Menhaden was then estimated as the product of the predictions from the two strata (Murase et al., 2009). All models were fit using the "mgcv" package in the R Programming Language (R Core Team, 2016; Wood, 2006, 2011). Standard diagnostic plots (distribution of the residuals and quantile-quantile plots) were used to evaluate model fits and select the best error distribution for CPUE using the "gam.check" function in the "mgcv" package (Wood, 2006).

Standardized annual trends in the relative abundance of larval Gulf Menhaden sampled from bongo and neuston nets were estimated following two methodologies: using the estimated year effect (i.e. year class coefficients) obtained from the two-strata

GAMs (Simpson et al., 2016) and using the method of partial dependence (Aires-da-Silva, Lennert-cody, Maunder, & Román-Verdesoto, 2013; Minami, Lennert-Cody, Gao, & Román-Verdesoto, 2007). Partial dependence summarizes the effect of a predictor on the response while accounting for the average effects of all other predictors using the values occurring in the data set of *n* observations used to fit the model (Minami et al., 2007). The annual estimate of relative abundance for each gear type and methodology was determined by taking the product of the year effect or partial dependence from the two strata. We used a jackknife routine to obtain estimates of the mean and standard error for each index (Simpson et al., 2016).

To evaluate the strength of correlation between juvenile/adult abundance and relative abundance of larval Gulf Menhaden, standardized annual estimates of relative abundance were correlated to indices of abundance and biomass estimates from the most recent assessment of Gulf Menhaden (SEDAR, 2013). Five time series were evaluated using Pearson product-moment correlations: 1) a recruitment index based on seine survey data from Louisiana, Mississippi, and Alabama; 2) an adult index lagged 1 year based on the Louisiana gillnet survey; 3) the estimated annual recruitment of age-0 menhaden; 4) the estimated biomass of age-1 menhaden lagged 1 year; and 5) spawning stock biomass (SSB) derived from the estimated biomass of age-1+ menhaden.

2.4 Results

Between 1982 and 2012, SEAMAP bongo (neuston) tows collected 1,835 (1,534) ichthyoplankton samples with 812 (593) non-zero catches for larval Gulf Menhaden and the spatial coverage of the sampling effort in the northern Gulf of Mexico was extensive (Figure 1). The majority of larvae (99.23%) sampled by SEAMAP were less than 20 mm

in length (Figure 2). However, mean length of larvae sampled using bongo nets (7.31 ± 3.84 mm) was significantly smaller than larvae sampled from neuston nets (10.97 ± 3.92; Student's *t*-test: $p < 0.001$). Model selection indicated that the relative abundance of larval Gulf Menhaden was spatially dynamic and that variable-coefficient terms (i.e. river-driven distributional shifts) improved model fit for the presence from both gears and the CPUE from neuston nets (Table 1 & Table 2). The best fit model for the presence of larvae sampled from bongo nets excluded DN and $\mathrm{MRD_s}$ and for CPUE excluded $g_2(\emptyset, \lambda) \times \mathrm{MRD_s}$, ZOO, and SST (Table 1). In addition, we removed CHL from the CPUE bongo model because the estimated degrees of freedom was essentially 0 (Marra & Wood, 2011). The best fit model for the presence of larvae from neuston nets excluded DN and $\mathrm{MRD_s}$, while for CPUE, the best fit model excluded $\mathrm{MRD_s}$, CHL, and SST (Table 2). The interaction between latitude and longitude explained the most variance in the presence and CPUE of larvae (Table 1 & 2), except for CPUE from bongo nets where the year explained the most variance (Table 1). The best fit models explained between 30% and 50% of the variance in the presence and CPUE of larvae (Table 3). During average Mississippi River discharge conditions, the predicted relative abundance of Gulf Menhaden larvae from bongo nets was greatest in the Louisiana Bight (89.5º W 29° N) and off Mobile Bay (87º W), but were encountered to Texas (94º W; Figs 3 & 4). During high discharge conditions, the distribution of larval relative abundance from bongo nets was reduced east of the Mississippi River delta and peak relative abundance shifted west to locations offshore of Atchafalaya Bay (90º to 91.5º W 29° N). Alternatively, during low river discharge, larval relative abundance from bongo nets was greater east of the Mississippi River delta when compared to average and high discharge (Figure 4).

Relative abundance of larvae sampled from neuston nets was much greater inshore compared to relative abundance from bongo nets (Figure 3). The eastern and offshore distribution of larvae from neueston nets was limited and enhanced, respectively, during high discharge (Figure 4). Relative abundance of larvae sampled from neuston nets was also much greater inshore during low discharge when compared to average and high discharge.

The response of the presence and CPUE of larvae to environmental covariates was variable. Despite the wide confidence intervals for some terms, they were retained in the model formulation because inclusion led to a reduction in AIC (Table 1 & 2) and the shrinkage penalization did not remove the term completely from the models (estimated degrees of freedom > 0; Table 3; Marra and Wood 2011). Environmental covariates did not improve model fit of CPUE for both gears (Tables 1-3). However, the presence of larvae samples from both bongo and neuston nets was positively correlated with CHL (Figs 5 & 6). For bongo net samples, the presence of Gulf Menhaden was lowest at reduced ZOO and increased to a plateau with increasing ZOO (Figure 5). The presence of larvae from both bongo and neuston nets had a non-linear response to SST with peak presence at 18 to 19° C (Figure 6).

Results of categorical predictors indicated that there was some intra-annual variation in the presence and CPUE of Gulf Menhaden larvae from both neuston and bongo nets (Table 1; Table 2). The probability of the presence and the CPUE was generally lowest in January relative to other months (Table 3). CPUE of larvae from bongo nets was reduced during high Mississippi River discharge and enhanced during

low discharge (Table 3). Larval CPUE increased and decreased at night for bongo nets and neuston nets, respectively.

Correlations between standardized annual trends of larval relative abundance (year effect and partial dependence) and indices or estimates of juvenile/adult abundance were limited (Table 4; Figure 8). We detected no significant correlations between the standardized estimates of relative abundance of larvae from both gears and the juvenile seine index, estimated recruitment, estimated number of age-1 individuals lagged 1 year, and SSB from the most recent assessment of Gulf Menhaden (SEDAR 32A)(Table 4). However, there was a significant positive correlation between the year effect derived relative abundance of larvae sampled from bongo nets and the adult index lagged 1 year based on the Louisiana gillnet survey (Table 4; Figure 8).

2.5 Discussion

Within the NGOM, Gulf Menhaden larvae were most abundant between the Atchafalaya Mobile Bays, with a center of distribution in the Louisiana Bight. However, larvae were distributed over a large spatial range, from east of Mobile Bay to East Texas. Previous studies have inferred from the distribution and abundance of eggs that Gulf Menhaden spawn mainly over the continental shelf between Sabine Pass and Alabama, but can be found as far as Corpus Christi, Texas (Fore, 1970). The extensive distribution of larvae, therefore, represents the interactions between transport, mortality, and the spawning distribution of Gulf Menhaden. While almost all larvae were smaller than the length at metamorphosis, 20-21 mm SL, reported by Deegan (1986), larvae sampled from bongo nets were significantly smaller than larvae from neuston nets. In addition, the

distribution of larvae sampled from neuston nets was more coastal than that of larvae from bongo nets. From November to March, larvae between 19 and 23 mm SL enter coastal estuaries and bays (Deegan, 1990) and such differences in the latitudinal distribution of larvae between gears is indicative of the shoreward movement of larvae through ontogeny.

Predictions from variable-coefficient GAMs indicate that longshore (longitudinal) distribution of larvae was influenced by Mississippi River discharge. Relative abundance was enhanced in the western NGOM and reduced in the eastern NGOM during high river discharge conditions. To a lesser extent, the offshore distribution of larvae was enhanced during high discharge conditions, directly supporting Govoni (1997). Additionally, in support of Govoni (1997), our models indicated the CPUE of larvae from bongo nets was reduced during high river discharge. These trends are likely driven by the interactive effects of river plume driven transport and spatially-dynamic mortality. Walker (1996) noted that variability in the areal extent of the Mississippi River plume corresponds with variation in river discharge, with the plume front expanding in an anticyclonic manner further south and outward during high river discharge conditions. Given that larval Gulf Menhaden are most abundant along the Mississippi River plume front (John J. Govoni & Grimes, 1992; John J. Govoni et al., 1989), such plume movement is expected to transport larvae. Average densities of copepods, a primary food of larval Gulf Menhaden (W. Chen, Govoni, & Warlen, 1992), are also one to two orders of magnitude greater in the Mississippi River plume than in outside Gulf waters (Churchill B. Grimes, 2001). Feeding conditions are positively correlated with larval growth and survival in many marine fishes (Pepin et al., 2015). Therefore, reduced feeding success of larval Gulf

Menhaden outside the river plume likely translates to higher mortality in these locations. Previous authors have hypothesized that west-northwest longshore advection is the primary mechanism of transport of larval Gulf Menhaden into coastal estuaries (Shaw, Wiseman, et al., 1985). The river-driven variations in the longshore distribution of larvae illustrated in the present study may consequently have implications for recruitment into estuarine nursery grounds if recruitment is dependent on the longitudinal distribution of larvae and if nursery habitat quality is spatially-variable. The average length of larvae sampled from neuston nets (10.97 ± 3.92) is greater than that from bongo nets (7.31 ± 3.84 mm) and represents the size class of individuals beginning to migrate inshore to coastal estuaries (Deegan 1990).Given that longitudinal variation in the relative abundance of larvae was greater for neuston nets, our work supports the idea that longshore transport was influenced by discharge. Shaw et al. (1985b) also hypothesized that larvae found further offshore during elevated discharge conditions may be transported away from key nursery grounds by the persistent offshore eastward countercurrent (Morey, Zavala-Hidalgo, & O'Brien, 2005). However, the lack of larvae in the eastern NGOM during high river discharge conditions does not support this hypothesis.

Gulf Menhaden larvae experience dietary shifts during ontogeny, transitioning from being primarily zooplanktivores to obligate forage feeders as a function of size (Y. Chen, Ye, & Dennis, 2009; Olsen et al., 2014; Stoecker & Govoni, 1984). Given that prey abundance is positively correlated with the survival, growth, and abundance of larval fishes (Garrido et al., 2015; Siddon et al., 2013), we tested whether phytoplankton and zooplankton abundance (i.e. plankton displacement volume) was positively

correlated with the relative abundance of larval Gulf Menhaden. We found that presence of larvae was positively correlated with chlorophyll *a* concentration. The presence-absence stratum of the delta-GAM can be thought of as an index of habitat suitability, indicating that chlorophyll *a* concentration is positively correlated with habitat suitability of larvae. Recent bioenergetics-based growth rate potential modelling of age-0 Gulf Menhaden suggests that chlorophyll *a* concentration is the dominant controlling factor of habitat quality in normoxic waters (Zhang et al., 2014). However, the relationship between plankton displacement volume and the presence of larvae was variable. Larval Gulf Menhaden feed on zooplankton that ranges from 40 to 280 μm in width (W. Chen et al., 1992), which may not be adequately sampled by bongo nets and extruded through the 0.335 mm mesh netting (Pillar, 1984). Future work should utilize a paired net with mesh targeted to adequately sample the size range of larval Gulf Menhaden prey items.

Temperatures associated with productive river plume fronts in the NGOM are generally colder than those of oceanic waters and warmer than river discharge (Hitchcock et al., 1997). The presence of Gulf Menhaden is likely greatest at intermediate temperatures associated with river plume fronts due to frontal convergence (John J. Govoni & Grimes, 1992). Although increased temperatures may enhance growth of larval fishes (Humphrey et al., 2014), over some range, mortality is also positively correlated with temperature (E. D. Houde, 1989). Survival of larval Gulf Menhaden in shelf waters is likely much lower due to absence of prey items despite the potential for increased growth (J. J. Govoni, 1993) as indicated by the negative response of larval presence to low chlorophyll *a* concentrations. These results are consistent with previous work that found the growth rate potential of Gulf Menhaden was nonlinearly related to temperature,

with growth rate potential reduced at temperatures above 32° C (Zhang et al., 2014). Similarly, survival of Atlantic Menhaden eggs is nonlinearly related to temperature (Tsoukali, Visser, & MacKenzie, 2016), suggesting that future variations in temperature may impact recruitment dynamics of Gulf Menhaden.

We found that the indices of juvenile and lagged (1-year) adult abundance from fishery independent data collection efforts and recruitment, lagged (1-year) age-1 abundance and SSB estimates from the most recent stock assessment (SEDAR, 2013) were not correlated to standardized estimates of annual larval abundance in the study region. Differences between the use of annual regression coefficients and partial dependence are likely due to the impact of year-specific variation in the environmental parameters on relative abundance. Future work should be directed towards understanding the potential biases between estimating annual relative abundance using partial dependence and regression coefficients. These results suggest that predicted larval abundance was not strongly related to recruitment strength and that "bottlenecks" for the recruitment of Gulf Menhaden occur after the pelagic larval stage. Alternatively, SEAMAP ichthyoplankton surveys may not be adequate for understanding intra-annual variation in the relative abundance of Gulf Menhaden larvae.

Fall and winter SEAMAP ichthyoplankton surveys were designed for estimating the abundance and distribution of eggs and larvae of fall and winter spawning fishes in the Gulf of Mexico, particularly mackerels, lutjanids, and sciaenids, in the case of the fall survey. Therefore, the utility of using the available SEAMAP data to estimate the abundance and distribution of larval Gulf Menhaden is tempered by some of the characteristics of the gear, sampling, and process error. Inter-annual variation in the

sampling distribution (temporal and spatial) of SEAMAP surveys may have impacted estimates of standardized annual relative abundance (SEDAR, 2013). However, trends in the spatial distribution of larvae was likely accounted for in our modelling efforts because they were informed by multiple years of data and the spawning distribution of fishes is generally spatially constrained and consistent between years (Lorenzo Ciannelli, Bailey, & Olsen, 2015). While we have addressed river-driven variation in the distribution of larvae, other factors such as wind-driven plume dynamics may affect the distribution of larvae as well (R. V. Schiller et al., 2011). We also assumed that, all *Brevoortia* spp. sampled within the study area were Gulf Menhaden. This is reasonable because in the region *B. patronus* compromise over 99% of the catch in the commercial fishery in the northern Gulf of Mexico (D. W. Ahrenholz, 1981), although we recognize that the distributions of *B. smithi* and *B. gunteri* overlap that of Gulf Menhaden (Dean W Ahrenholz, 1991). Spawning of *B. gunteri* is reported to occur in estuarine waters and spawning of both *B. gunteri* and *B. smithi* occurs during late winter until spring (Dean W Ahrenholz, 1991). Therefore, inclusion of *B. gunteri* and *B. smithi* in the present analysis was likely minor. Alternatively, our classification of *B. patronus* may have underestimated the relative abundance of Gulf Menhaden because of the large number of clupeiforme and clupeid larvae collected by SEAMAP trawls can only be identified to the order and/or family. Future studies aimed at identifying larval specimens classified at a lower taxonomic level will prove useful in providing valuable data to discern the effects environmental processes have on the distribution and abundance of early life stages of Gulf Menhaden.

Given their short life-cycle, abundance of small pelagic forage fish like Gulf Menhaden is dependent on year class strength (Edward D. Houde, Annis, Harding, Mallonee, & Wilberg, 2016; Pauly & Tsukayama, 1987). However, recruitment success is strongly influenced by environmental processes (Szuwalski, Vert-Pre, Punt, Branch, & Hilborn, 2015), highlighting the need for understanding how such processes influence the early life history of Gulf Menhaden. Together these results demonstrate that, in the NGOM, the level of Mississippi River discharge impacts the spatial distribution and abundance of larval Gulf Menhaden. During high Mississippi river discharge the distribution of larval Gulf Menhaden is enhanced in the western NGOM and CPUE is reduced. Variation in the spatial distribution of larvae likely poses consequences for the location and timing of estuarine ingress and this may impact subsequent recruitment strength. Evaluation of location-specific patterns in indices of juvenile abundance may provide further information on the recruitment of Gulf Menhaden.

Table 2.1

Model selection of the two-strata variable-coefficient GAMs relating the spatial distribution of larval presence and relative abundance collected by SEAMAP bongo trawls, 1982 to 2012.

	Percent of deviance explained (%)	**AIC**	**Log Likelihood**	**Number of parameters (total)**	**Included (y/n)**
Presence model					
NULL		2,523	-1,261	1	y
+ year	9.89	2,336	-1,136	32	y
+ month	8.71	2,126	-1,026	37	y
+ DN	0.06	2,127	-1,025	38	n
+ $g_1(\emptyset, \lambda)$	21.15	1,638	-759	60	y
+ $g_2(\emptyset, \lambda) \times \mathrm{MRD_s}$	2.58	1,605	-726	76	y
+ $\mathrm{MRD_s}$	-0.02	1,608	-727	77	n
+ $s_1(\mathrm{CHL})$	4.16	1,584	-674	118	y
+ $s_2(\mathrm{ZOO})$	1.75	1,570	-652	133	y
+ $s_3(\mathrm{SST})$	2.65	1,525	-619	144	y
CPUE model					
NULL		3,252	-1,623	1	y
+ year	16.42	3,161	-1,547	31	y
+ month	6.53	3,102	-1,513	36	y
+ DN	0.96	3,093	-1,508	37	y
+ $g_1(\emptyset, \lambda)$	9.07	3,025	-1,454	55	y
+ $g_2(\emptyset, \lambda) \times \mathrm{MRD_s}$	4.65	3,029	-1,424	88	n
+ $\mathrm{MRD_s}$	-4.60	3,028	-1,454	57	y
+ $s_1(\mathrm{CHL})$	13.61	3,004	-1,359	134	n
+ $s_2(\mathrm{ZOO})$	-10.37	3,005	-1,433	67	n
+ $s_3(\mathrm{SST})$	14.87	3,129	-1,323	240	n

Table 2.2

Model selection of the two-strata variable-coefficient GAMs relating the spatial distribution of larval presence and relative abundance collected by SEAMAP neuston trawls, 1982 to 2012.

Neuston net	**Percent of deviance explained (%)**	**AIC**	**Log Likelihood**	**Estimated degrees of freedom (total)**	**Included (y/n)**
Presence model					
NULL		2,050	-1,024	1	y
+ year	11.66	1,871	-905	31	y
+ month	6.60	1,746	-837	36	y
+ DN	0.01	1,748	-837	37	n
+ $g_1(\emptyset, \lambda)$	20.57	1,366	-626	57	y
+ $g_2(\emptyset, \lambda) \times \mathrm{MRD_s}$	2.72	1,344	-598	73	y
+ $\mathrm{MRD_s}$	-0.03	1,346	-599	74	n
+ $s_1(\mathrm{CHL})$	6.52	1,302	-532	119	y
+ $s_3(\mathrm{SST})$	0.48	1,256	-527	101	y
CPUE model					
NULL		2,480	-1,237	1	y
+ year	9.41	2,470	-1,206	27	y
+ month	4.60	2,448	-1,190	32	y
+ DN	2.27	2,433	-1,182	33	y
+ $g_1(\emptyset, \lambda)$	11.85	2,367	-1,135	44	y
+ $g_2(\emptyset, \lambda) \times \mathrm{MRD_s}$	1.86	2,361	-1,127	48	y
+ $\mathrm{MRD_s}$	-0.05	2,365	-1,127	50	n
+ $s_1(\mathrm{CHL})$	5.35	2,367	-1,103	70	n
+ $s_3(\mathrm{SST})$	-2.08	2,366	-1,113	61	n

Table 2.3

Summary of the two-strata variable-coefficient GAMs relating the spatial distribution of larval presence and relative abundance collected by SEAMAP trawls, 1982 to 2012, to high, average, and low winter Mississippi River discharge levels. Asterisks denote significance of nominal predictors at the following alpha levels: *0.05; **0.01; ***0.001.

	Bongo net		**Neuston net**	
Response	Presence	Abundance	Presence	Abundance
Family	Binomial	Tweedie	Binomial	Tweedie
Link function	Logit	Log	Logit	Log
Deviance explained	50.92%	33.03%	48.52%	30.00%
N	1,835	812	1,534	593
	Estimated degrees of freedom			
$g(\emptyset, \lambda)$	25.05	17.97	11.60	12.01
×average discharge	0.00		11.48	0
×high discharge	4.85		4.45	3.24
×low discharge	0.88		25.23	0
CHL	0.97		1.00	
ZOO	3.26			
SST	4.00		3.85	N
	Estimate ± standard error			
Intercept	2.78 ± 0.83***	5.55 ± 0.47***	-1.41 ± 0.99	3.83 ± 0.76***
November	-0.29 ± 0.5	-1.11 ± 0.41**	-0.08 ± 0.46	-0.51 ± 0.42
December	-0.67 ± 0.56	-0.54 ± 0.4	0.24 ± 0.65	0.09 ± 0.53
January	-2.36 ± 0.51***	-2.08 ± 0.38***	-1.27 ± 0.5*	-1.28 ± 0.43**
February	-1.25 ± 0.48**	-1.24 ± 0.37***	-0.05 ± 0.48	-1.02 ± 0.41*
March	-0.08 ± 0.53	-1.02 ± 0.39**	0.44 ± 0.56	-0.39 ± 0.48
Night		0.29 ± 0.12*		-0.19 ± 0.16
High discharge		-0.26 ± 0.26		
Low discharge		0.09 ± 0.24		

Table 2.4

Correlation coefficients between standardized estimates of annual larval relative abundance and indices of abundance and biomass estimates from the most recent assessment of Gulf Menhaden (SEDAR, 2013). Asterisks denote significance of nominal predictors at the following alpha levels: *0.05; **0.01; ***0.001.

	Bongo nets		**Neuston nets**	
	Year effect	Partial dependence	Year effect	Partial dependence
Seine index	-0.02	-0.01	-0.15	0.15
Gillnet index	0.69***	0.58**	0.30	-0.35
Recruitment	-0.15	-0.05	-0.10	0.02
Age-1 abundance	-0.15	-0.05	-0.10	0.02
SSB	-0.05	0.05	-0.18	-0.41*

Table 2.5

Estimates and standard errors (SE) of standardized annual relative abundance of larval Gulf Menhaden collected by SEAMAP bongo (larvae under 10 m^2 of sea surface) and neuston (larvae per 10 minute tow) trawls, 1982 to 2013.

	Bongo nets				**Neuston net**			
	Year effect		Partial dependence		Year effect		Partial dependence	
Year	Estimate	SE	Estimate	SE	Estimate	SE	Estimate	SE
1982	240.5	128.52	211.8	47.08				
1983	55.28	34.82	13.83	5.27	9.82	49.53	2.35	13.37
1984	78.63	43.09	24.54	7.12				
1985	97.5	70	36.39	15.49				
1986	37.78	30.31	22.68	7.28				
1987	56.93	38.78	11.71	2.56	27.88	24.88	17.06	6.2
1988	3.7	3.51	3.85	1.99	10.72	21.47	18.78	9.03
1989	89.87	85.6	39.88	24.2	3.07	8.63	67.85	36.78
1990	20.93	13.19	9.52	3.74	6.59	9.39	3.78	1.84
1991	68.58	39.33	16.27	5.89	31.47	73.54	24.61	28.23
1992	29.6	20.79	11.39	4.39	46.44	42.82	62.56	68.37
1993	40.92	23.65	10.06	3.12	41.75	45.09	15.74	19.72
1994	257.9	191.5	51.46	22.45	11.83	23.24	17.32	13.85
1995	92.53	54.76	23.45	8.87	41.99	39.95	31.46	52.53
1996	285.86	231.06	75.04	56.81	64.9	82.97	26.15	49.68
1997	179.96	117.33	22.2	7.9	34.79	55.28	9.41	22.04
1998	176.19	124.53	53.79	28.56	33.63	50.46	26.85	17.26
1999	88.22	58.96	7.93	6	24.39	22.77	6	6.65
2000	186.58	120.89	36.51	15.33	1.74	2.4	3.37	2.95
2001	54.34	34.48	10.42	3.5	32.24	38.39	13.3	5.5
2002	134.91	86.82	30.48	13.05	11.58	14.23	6.12	2.89
2003	227.3	115.81	38.85	11.76	65.68	48.12	18.44	26.15
2004	81.11	46.3	30.39	10.45	13.54	12.84	15.03	8.31
2005	298.88	200.58	37.04	16.98	32.83	44.01	14.33	8.14
2006	204.56	125.59	31.2	9.83	69	42.28	12.74	4.02
2007								
2008	463.89	244.22	92.23	22.57	73.17	79.66	18.73	25.38
2009	227.76	120.13	60.63	16.33	51.31	40.7	25.41	18.96
2010	152.12	137.54	27.99	12.85	9.86	13.82	9.37	7.77
2011	84.12	71.51	1.59	0.83	15.25	25.94	2.24	4.9
2012	132.07	69.45	15.4	4.36	32.82	21.4	4.04	2.2
2013	174.24	108.18	15.31	5.68	24.14	21.76	4.83	4.35

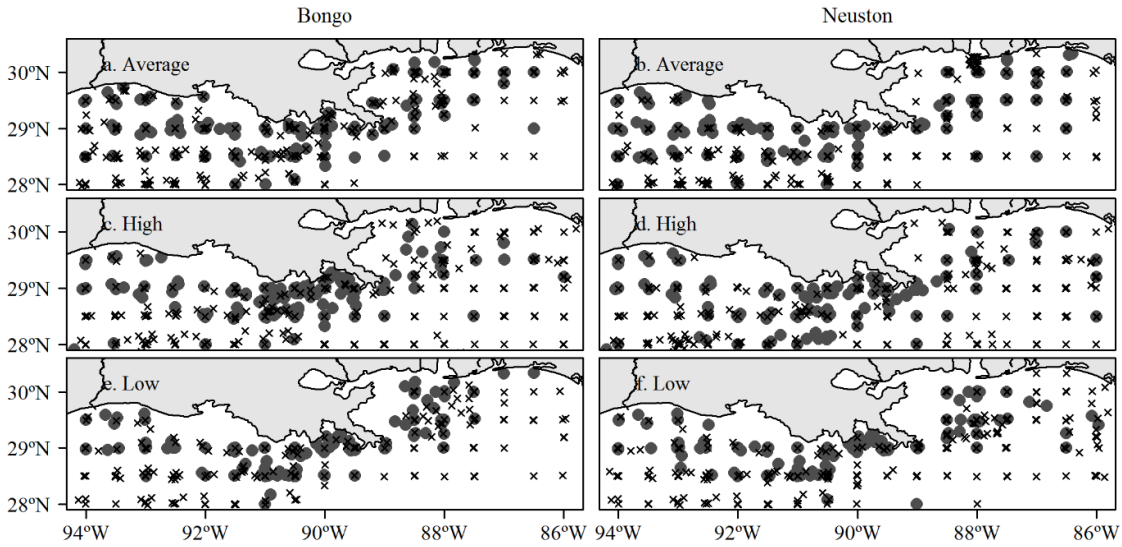

Location of Gulf Menhaden samples collected by SEAMAP bongo and neuston trawls, 1982 to 2012, during average (a, b), high (c, d), and low (e, f) Mississippi River discharge. Presence is indicated as • and absence as ×.

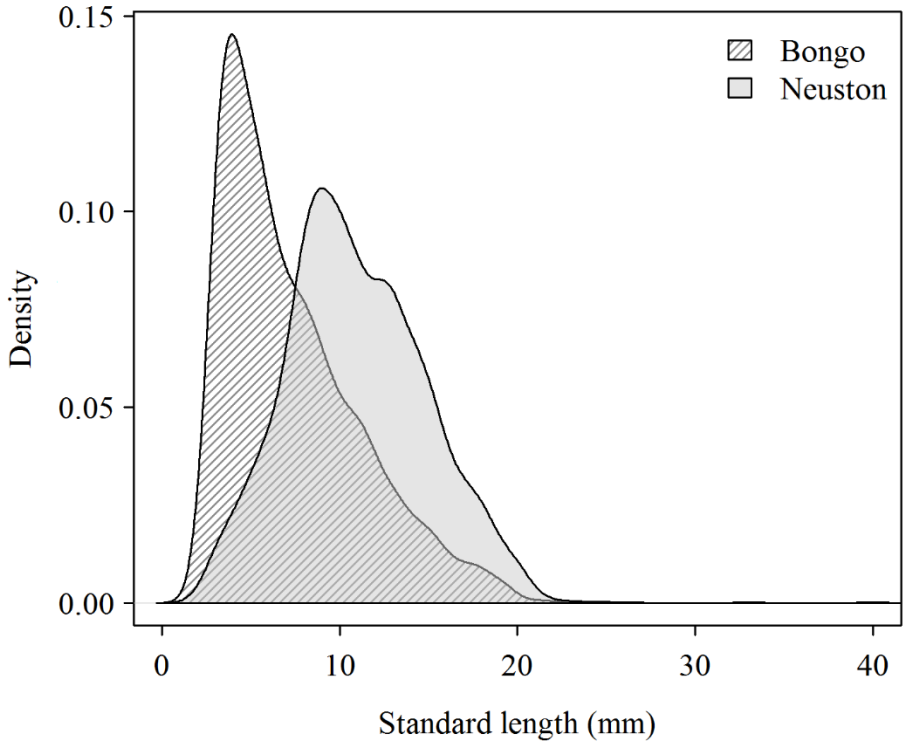

Kernel density of standard lengths of larval Gulf Menhaden sampled by SEAMAP bongo and neuston trawls, 1982 to 2012.

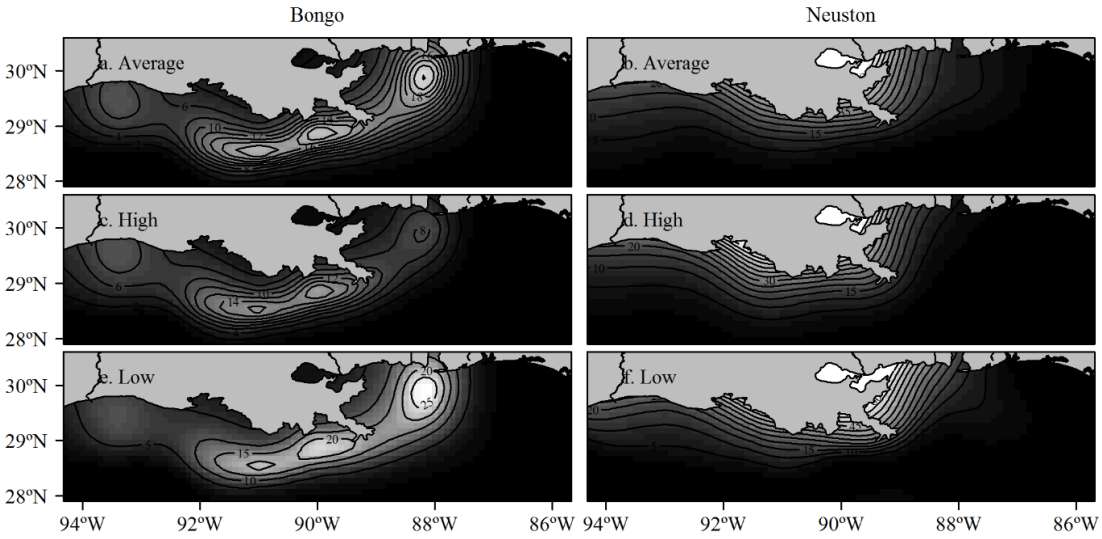

GAM predicted spatial distribution of log-transformed larval Gulf Menhaden relative abundance collected by SEAMAP bongo (a; larvae under 10 m^2 of sea surface) and neuston (b; larvae per 10 minute tow) trawls, 1982 to 2012, and distribution during high (c, d) and low (e, f) Mississippi River discharge levels.

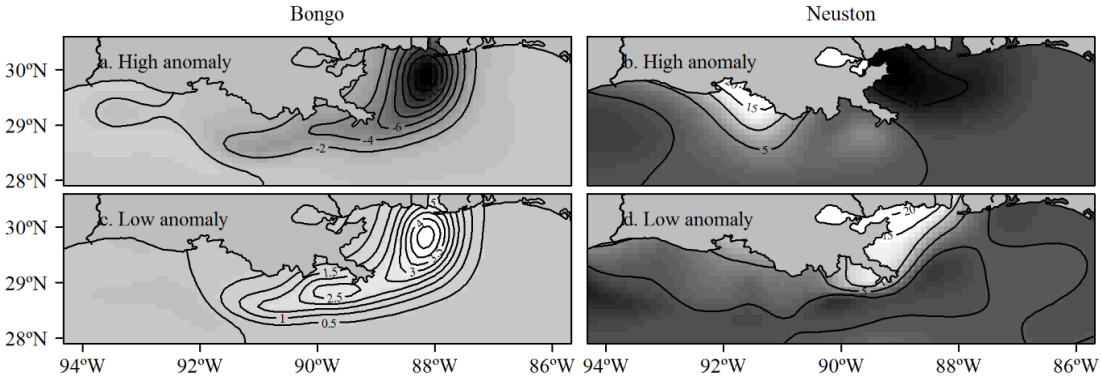

GAM predicted spatial distribution anomaly of larval Gulf Menhaden relative abundance collected by SEAMAP bongo (larvae under 10 m^2 of sea surface) and neuston (larvae per 10 minute tow) trawls, 1982 to 2013, during high (a, b) and low (c, d) Mississippi River discharge levels relative to average discharge level.

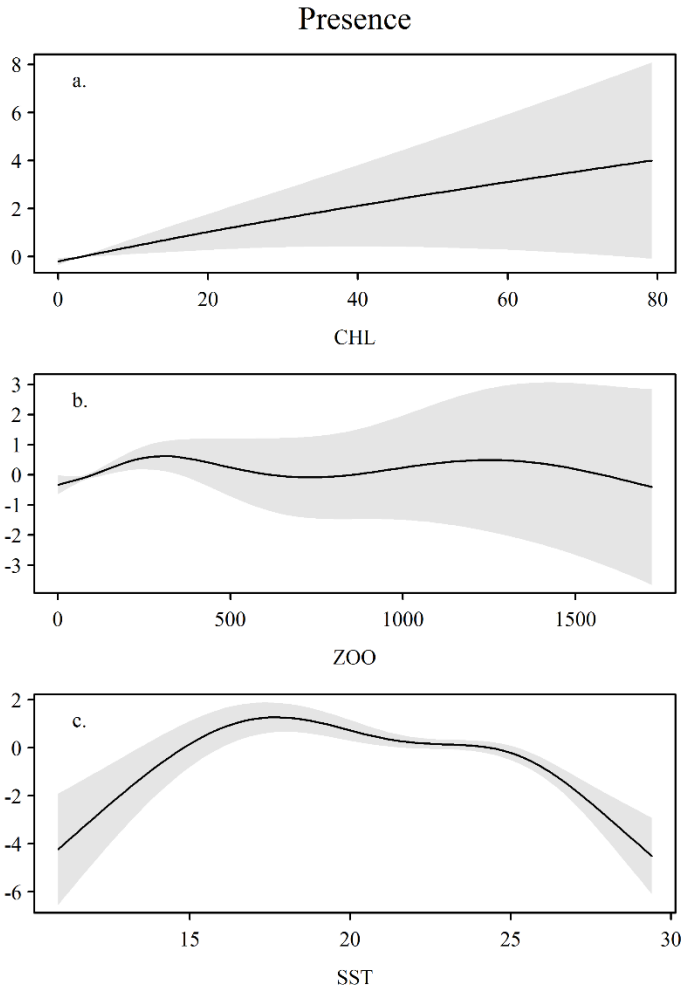

Fits of one-dimensional smoothing functions relating the presence of larval Gulf Menhaden to environmental covariates collected by SEAMAP bongo trawls, 1982 to 2012. Shaded area indicates 95% confidence area.

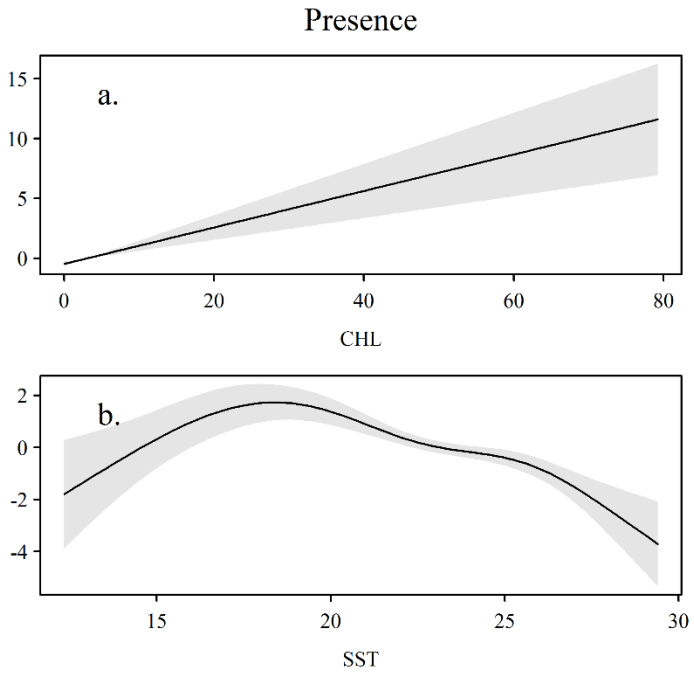

Fits of one-dimensional smoothing functions relating the presence of larval Gulf Menhaden to environmental covariates collected by SEAMAP neuston trawls, 1982 to 2012. Shaded area indicates 95% confidence area.

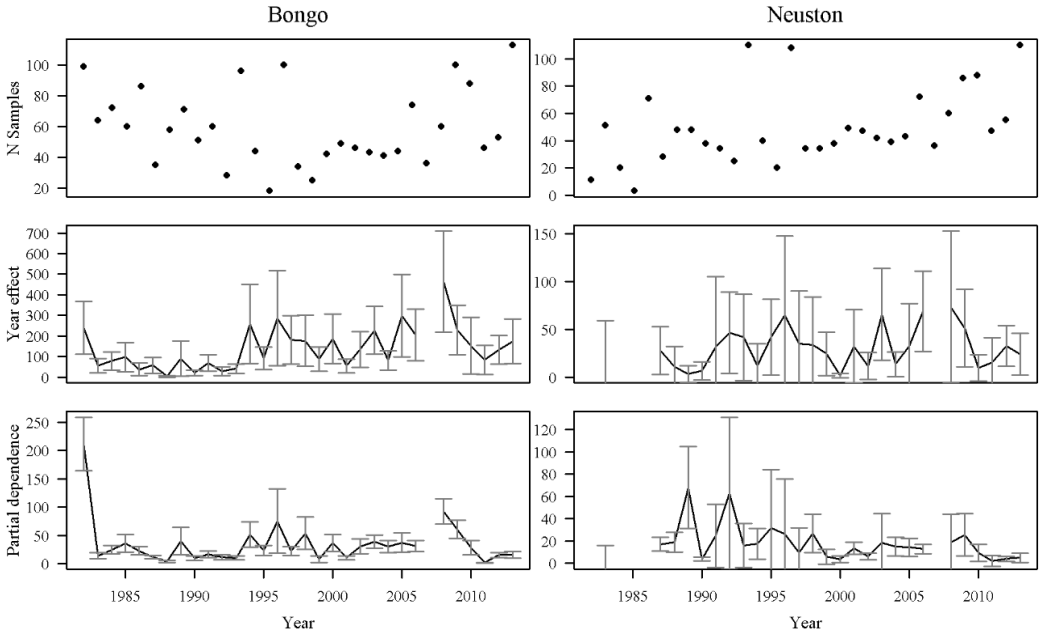

Estimates of standardized annual relative abundance of larval Gulf Menhaden collected by SEAMAP bongo (larvae under 10 m^2 of sea surface) and neuston (larvae per 10 minute tow) trawls, 1982 to 2012.

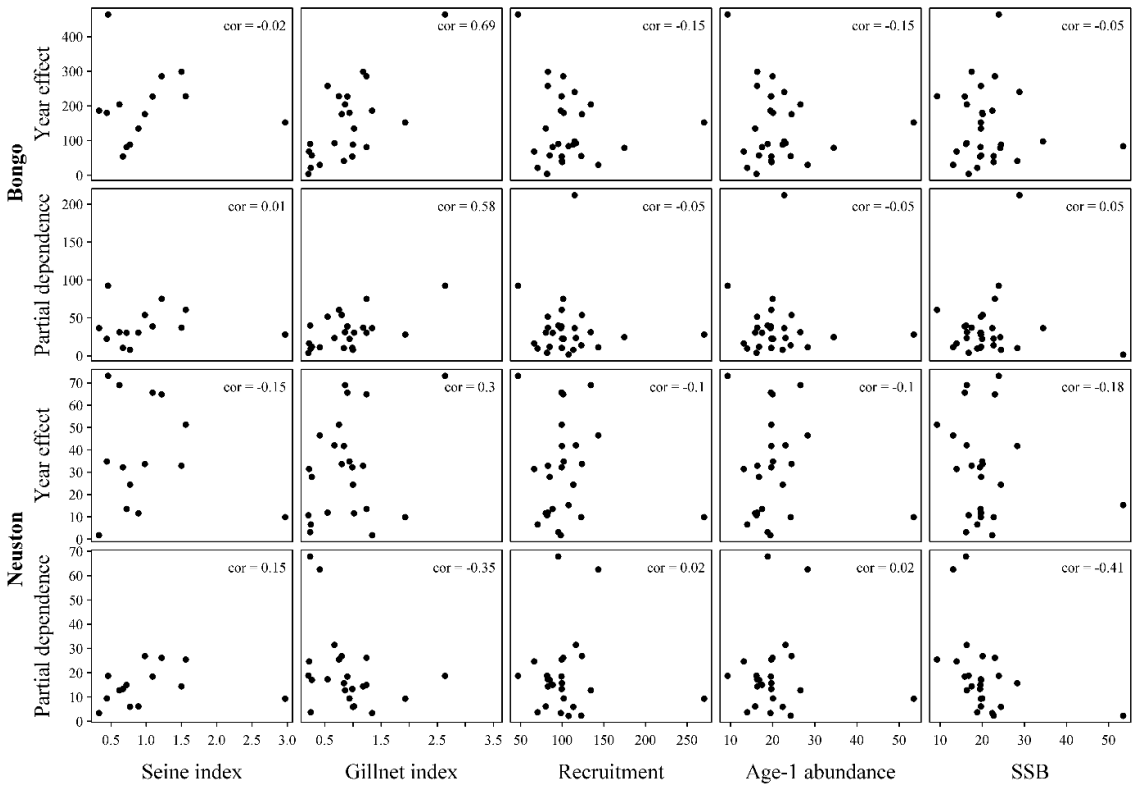

Scatterplots and correlation coefficients between standardized estimates of annual larval relative abundance and indices of abundance and biomass estimates from the most recent assessment of Gulf Menhaden (SEDAR, 2013).

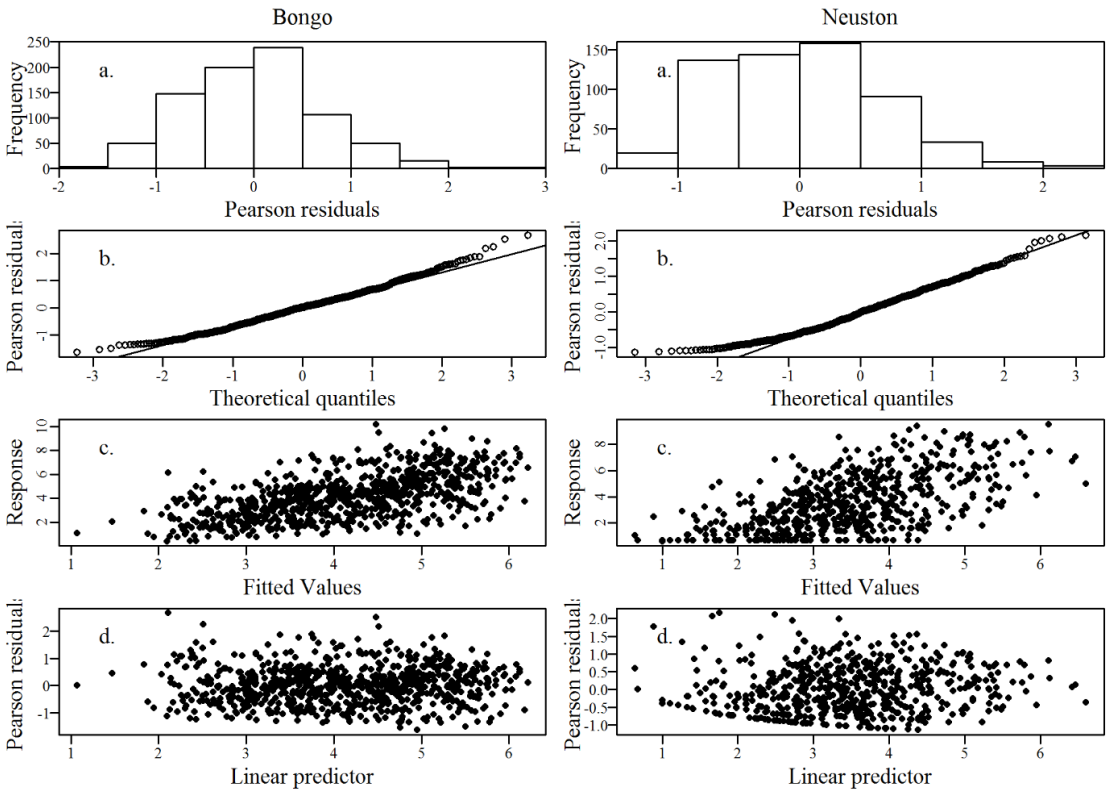

Standard model diagnostics of GAM second-stratum models relating larval Gulf Menhaden CPUE collected by SEAMAP trawls, 1982 to 2012, to spatial-temporal and environmental predictors.

CHAPTER III - SIZE-SELECTIVE MORTALITY AND GROWTH VARIATION OF GULF MENHADEN *BREVOORTIA PATRONUS* IN RELATION TO DENSITY DEPENDENT AND INDEPENDENT CONDITIONS.

3.1 Introduction

An understanding of age and growth and their subsequent impacts on mortality is essential for effective fisheries management. However, age and growth can be temporally dynamic (Van Beveren et al., 2014; Xu, Chai, Rose, Ñiquen, & Chavez, 2013), which has implications for the estimated biological reference points used to manage fisheries (Thorson, Monnahan, & Cope, 2015). Examination of such variation can provide insights into the underlying density-independent and -dependent factors that impact the population dynamics of fishes. For example, temporal variation in the growth of small pelagic forage fish has been found to be correlated to sea surface temperature (SST), food availability, climate variation, and biomass (Brunel & Dickey-Collas, 2010; Cahuin, Cubillos, Ñiquen, & Escribano, 2009; Takahashi et al., 2012). The identification of biologically meaningful drivers of age and growth among multiple candidate factors can be informative of ecosystem processes and can improve assessments and projections of stock status (Holsman, Ianelli, & Aydin, 2016; Lorenzen, 2016).

Temporal variations in growth can have implications for stock status if mortality is in part dependent on size (e.g. size-selective morality) (S. E. Campana, 1996; Rice et al., 1993; Sirois & Dodson, 2000). For some populations, larger individuals are generally thought to experience enhanced survival through improved avoidance of predation and the ability to outcompete smaller individuals for food resources (Susan M. Sogard, 1997; Takasuka, Aoki, & Mitani, 2004). For example, Campana (1996) found that both otolith

increment width and mean length-at-age of juvenile Atlantic Cod (*Gadus morhua*) were positively correlated with survival. The presence of such size-selective morality during the early life-stages of fish can have substantial effects on recruitment variability (Johnson, Grorud-Colvert, Sponaugle, & Semmens, 2014). Therefore, an understanding of size-selective mortality in the context of individual growth variability can improve our understanding of the mechanisms that affect fish populations.

Fish growth and size-selective mortality can be examined by analyzing the calcified structures found in fishes (Pilling, Millner, Easey, Maxwell, & Tidd, 2007; Stocks, Stewart, Gray, & West, 2011). Calcified structures such as otoliths and scales are composed of opaque and translucent zones, termed annuli or circuli, that can be used to determine the age and growth history of individuals. Age estimates from the number of annuli can be used with length data to estimate the mean individual growth trajectory of a population (i.e. length-at-age models). For example, von Bertanlanffy growth functions (VBGFs) are two or three parameter asymptotic length-at-age models that are used to estimate the mean asymptotic length and growth rate of individuals in a population (S. Campana, 2001; von Bertalanffy, 1957). Apart from length-at-age models, the width of the opaque zone (the increment width) can be used to evaluate the growth history of an individual and has been used as a proxy for somatic growth (Fossen, Albert, & Nilssen, 1999) because increment width has been shown to have a strong linear relationship with fish length (Thresher, Koslow, Morison, & Smith, 2007). Therefore, comparison of larval and juvenile otolith increment width among year classes can be used to identify the presence size-selective mortality (D'Alessandro, Sponaugle, & Cowen, 2013). However, validation of increment width as a proxy of somatic growth is required because this

relationship may be taxon-specific (Beckman & Wilson, 1995). Growth models describing both length-at-age and increment width can be parametrized to incorporate indices of forcing factors (Dycus, Wisniewski, & Peterson, 2015; Holsman et al., 2016; Kimura, 2008; Morrongiello & Thresher, 2014) to evaluate the possible impacts of such density-independent and -dependent factors on age and growth and the implications for the dynamics of exploited fishes via size-selective mortality.

In the northern Gulf of Mexico, annual variation of VBGF parameter estimates has been documented for the abundant forage fish Gulf Menhaden (*Brevoortia patronus*) (SEDAR 2013). Despite the economic and ecologic role of Gulf Menhaden in the northern Gulf of Mexico (Vaughan et al., 2007), little is known about the drivers of individual growth variation, the presence of size-selective mortality, or how such growth variability impacts mortality. The Gulf Menhaden fishery is the second largest fishery by weight in the United States and represents an important trophic link between primary production and higher trophic levels (Dean W Ahrenholz, 1991). Thus, information regarding variation in individual growth and size-selective mortality can provide an understanding of the role of Gulf Menhaden in the northern Gulf of Mexico ecosystem and the drivers of stock dynamics.

Variability in river discharge (John J. Govoni, 1997), climate variation (Sanchez-Rubio & Perry, 2015), density-dependence (Edward D. Houde et al., 2016), and mesoscale circulation features (N. D. Walker et al., 2005) in the Northern Gulf of Mexico are probable drivers of interannual variability of growth of Gulf Menhaden. Gulf Menhaden are obligate forage feeders, preying on a range of zooplankton and phytoplankton throughout ontogeny (W. Chen et al., 1992; Olsen et al., 2014; Stoecker &

Govoni, 1984). Growth can be food limited (Bjornsson, 2001; Lorenzen, 2016) and factors that alter nutrient flux in the Gulf of Mexico such as river discharge and climate likely impact growth of Gulf Menhaden (S E Lohrenz et al., 1997; Steven E. Lohrenz et al., 2008; Sanchez-Rubio & Perry, 2015; Sanchez-Rubio et al., 2011). Similarly, increases in abundance can result in increased intra-specific competition and subsequent density dependent growth, as found for age-0 Atlantic Menhaden (*B. tyrannus*) in the Chesapeake Bay (Edward D. Houde et al., 2016). Temperature is also correlated with the growth of Atlantic Menhaden (Humphrey et al., 2014), likely because of processes such as metabolism and consumption (Bjornsson, 2001; Krohn, Reidy, & Kerr, 1997; Takasuka, Oozeki, & Aoki, 2007). Thus, climate and river discharge, which drive temperature gradients in the Gulf of Mexico (Hitchcock et al., 1997; Sanchez-Rubio & Perry, 2015), may have consequences for the growth of Gulf Menhaden.

This study will address gaps regarding our understanding of the temporal variability of Gulf Menhaden growth and size-selective mortality by evaluating variation in length-at-age and increment width measurements. Using these data, the present study aims to examine (1) inter-annual growth variation in relation to multiple drivers (river discharge, circulation, hypoxia, abundance, and climate variability) and (2) the impact of size on the survival of Gulf Menhaden (e.g. size-selective mortality).

3.2 Methods

3.2.1 Data

Fishery-dependent data taken from port collection of the commercial reduction fishery in the Gulf of Mexico from 1964 to 2011 were provided by NOAA Fisheries, formerly the National Marine Fisheries Service (NMFS). The data included

measurements of fork length (mm FL), scale increment width (µm), scale width (µm), and age (yr) that were recorded for each individual. Data of estimated age was supplied from processing scales that were taken along the flank below the insertion of the dorsal fin and adjacent to the lateral line following NMFS protocol (SEDAR, 2013). Age was estimated for each individual using information on the number of rings counted on an individual scale (e.g. circuli) and assuming a January 1st birthdate. Fractional age was calculated as following:

Eq. 1 $$Fractional\ Age = Circuli + \frac{DOC}{365}$$

where DOC is the ordinal number (1 to 365) of the day of the year of capture. Therefore, fractional age are in years. Regression analyses of fork length (FL) and scale width were used to verify scale growth as a predictor of somatic growth and scale radius-at-age was used as a proxy for size-at-age (Figure 1). Prior to analysis we removed questionable records including individuals with recorded age greater than 10, scale increment width greater than the entire scale width, FL less than 1 mm, FL more than 500 mm, and that lacked scale width data.

3.2.2 Candidate Drivers of Age and Growth

Candidate drivers of age and growth considered in the present analysis include: an index of mesoscale circulation features associated with the Loop Current, the day of annual spring transition, magnitude of winter Mississippi River Discharge, areal extent of the annual hypoxic zone, and estimated adult population size. To quantify the distribution of mesoscale circulation features associated with the Loop Current in the NGOM we expanded the methodology outlined in Domingues et al. (2016). Weekly fields of gridded sea surface height anomaly (SSHA) at a 0.5° resolution were derived from sea level

reconstruction data (CCAR, of Colorado, & Boulder, 2013). SSHA data was derived from cyclostationary empirical orthogonal functions fit to satellite altimetry data combined with historical sea level data from tide gages and spans from 1950 to 2009 (Hamlington, Leben, & Kim, 2012; Hamlington, Leben, Strassburg, & Kim, 2014). Mean dynamic topography (MDT, 0.25° resolution) for the 1993 to 2012 period were obtained from AVISO (http://www.aviso.altimetry.fr/) and were converted to a 0.5° grid resolution by using the weighted cell mean. MDT and SSHA fields were combined to create weekly sea surface height (SSH) fields. We assumed that the regional distribution of sea-level trends in the NGOM over the past two decades is consistent since 1963. Weekly SSH fields were then classified into anti-cyclonic, cyclonic, common water, and their respective boundary regions following Domingues et al. (2016). A spatially-independent time series of mesoscale circulation activity in the Gulf of Mexico was then created by taking the annual mean of the first principal component calculated from the weekly area of each categorized mesoscale feature.

The day of spring transition, the transition from wintertime North winds to summer South winds, was estimated using a sequential t-test analysis of regime shifts (STARS ; Rodionov 2004) fit to the daily meridional (North-South) surface wind from the NCEP/NCAR Reanalysis project provided by NOAA's Earth System Research Laboratory (http://www.esrl.noaa.gov/). For each day, meridional wind vector measurements were averaged between 95° and 87.5°W and 28° and 33°N to create a time series of meridional wind vector in the NGOM. The STARS algorithm was fit using a moving window of 90 days, Huber weight value of 20, and alpha at 0.05. Day of spring

transition was defined as the first day of the maximum South wind regime before the 300th day of the year (Figure 3).

Govoni (1997) demonstrated that Mississippi River discharge during the winter months impacts the population dynamics of Gulf Menhaden. We therefore used an index of winter river discharge estimated following Govoni (1997). Briefly, daily flow values (ft^3/s) of the Mississippi River from Tarbert Landing, Louisiana obtained from the Army Corps of Engineers (http://rivergages.mvr.usace.army.mil/) were summed by month and averaged from November to March for each year. Mid-summer estimates of the area (km^2) of bottom water hypoxia (< 2 mg/l of dissolved oxygen) between 1985 and 2011 were provided by the Hypoxia Research Team at the Louisiana Universities Marine Consortium (http://www.gulfhypoxia.net/). Given that these estimates were from the Texas-Louisiana Shelf and Gulf Menhaden are sampled from Texas to Alabama, we assumed that variability in hypoxia was consistent across the northern Gulf of Mexico. Adult population size was estimated as the sum of the estimated numbers of age-1, 2, and 3 Gulf Menhaden at the start of the year in the most recent stock assessment (SEDAR, 2013). The length-at-age data largely consisted of age-1+ individuals, therefore, we assumed that competition between adults and recruits was negligible and exclude estimated number of recruits from this index.

3.2.3 Length-at-Age

The VBGF equates growth rate to the difference between catabolism and anabolism (Essington, Kitchell, & Walters, 2001; Lorenzen, 2016; von Bertalanffy, 1957):

Eq. 2 $$\frac{dW_t}{dt} = HW_t^d - kW_t^n$$

where W_t is the weight (g) at age (t), k is the catabolic rate (g $g^{-n} \cdot y^{-1}$), n is the unitless allometric slope of catabolism, H is the anabolism rate ($g \cdot g^{-d} \cdot y^{-1}$), and d is the unitless allometric slope of anabolism. To simplify, we assume that d = 2/3 and n = 1. Given a linear decrease in growth rate with increasing weight, dW_t/dt will equal 0 at an asymptotic weight (W_∞), which $= \left(H/k\right)^3$. Therefore, W_∞ is dependent on both anabolism and catabolism and W_t will approach W_∞ at:

Eq. 3 $$W_t = W_\infty\left(1 - \exp(-K(t - t_0))\right)^3$$

where the Brody growth rate (K: y^{-1}) = $k/3$ and t_0 is the age (y) when weight is 0 g. The VBGF can then be converted to length through the length-weight power equation $W = aL^b$ assuming that weight scales as the cube of length:

Eq. 4 $$L_t = L_\infty\left(1 - \exp\left(-K(t - t_0)\right)\right)$$

where L_∞ is the asymptotic length (mm).

To model the impact of environmental processes on individual growth, an extended growth model based on the 3-parameter VBGF (Eq. 4) following Kimura (2008) was used. Specifically, we are interested in understanding time-varying growth and assumed variability in both L_∞ and K:

Eq. 5 $$log\left(L_{\infty,t}\right) = \left(\beta_{L_\infty,0} + \sum_{j=1}^{q} \beta_{L_\infty,j} \times X_{t,j}\right)$$

Eq. 6 $$log(K_t) = \left(\beta_{K,0} + \sum_{j=1}^{q} \beta_{K,j} \times X_{t,j}\right)$$

where $L_{\infty,t}$ is the is the asymptotic length for year *t* and K_t is the Brody growth rate for year *t*. Both $L_{\infty,t}$ and K_t are a linear function of q covariates X_j and associated parameters: $\beta_{L_\infty,j}\ and\ \beta_{K,j}$. The inputs in the model are length L_t (mm FL) and age t (y).

For the extended VBGF, annual time-series of mesoscale activity, the day of annual spring transition, Mississippi River Discharge, areal extent of the annual hypoxic zone, and adult abundance were included as covariates. Covariates were scaled to the mean and standard deviation, which allows $\beta_{L_\infty,0}$ and $\beta_{K,0}$ to be interpreted as the average values for L_∞ and K when log transformed, respectively. We assumed that t_0 is constant to improve biological interpretation of the other parameters and improve model fitting (Vincenzi, Crivelli, Munch, Skaug, & Mangel, 2016). To account for years of missing environmental data (n = 22 yrs), models were only fit to years with complete cases (n = 23 yrs). The best fit model was selected following a forward stepwise approach starting with the 3-parameter VBGF. Environmental covariates were included in the model if Akaike's Information Criterion (AIC) was reduced upon inclusion. To account for the impacts of size-selectivity in fishery-dependent samples, we assumed a truncated lognormal error structure for all candidate models that accounts for the minimum (73 mm) and maximum (260 mm) lengths in the sample (Schueller, Williams, & Cheshire, 2014) Nonlinear optimization was accomplished in the R statistical platform (R Core Team, 2016) using Template Model Builder (Kristensen et al. 2015; Appendix 1).

3.2.4 Scale Increment Width Growth Analysis

To further investigate the contrast in growth as a result of environmental processes we fit a linear mixed effects model to scale increment width data following Weisberg et al. (2010):

Eq. 7 $$IW_{i,a} = t_a + f_i + \sum_{j=1}^{q} \beta_{a,j} \times X_{i,a,j} + \varepsilon_{i,a}$$

where $IW_{i,a}$ is a^{th} annual increment width for individual i, t_a is the annual increment width for fish in the a^{th} year of life, f_i is the random effect of individual i which is drawn

from a normal distribution with a variance σ_f^2, and $\varepsilon_{i,a}$ is the random error assumed to be normally distributed around a mean of zero and variance σ^2. $\sum_{j=1}^{q} \beta_{a,j} \times X_{a,j}$ is the linear function of q continuous environmental covariates $X_{i,a,j}$ and respective parameters $\beta_{a,j}$. For $\beta_{a,j}$, we assumed a random age effect (e.g. random slope) drawn from a normal distribution with variance $\sigma_{X,j}^2$ to account for variation in the effect of environmental covariates through ontogeny. For the hierarchical linear model, annual time-series of mesoscale activity, the day of annual spring transition, Mississippi River Discharge, and areal extent of the annual hypoxic zone were all evaluated as potential covariates. To account for years of missing environmental data (n = 22 yrs), models were only fit to years with complete cases (n = 23 yrs). The best fit model was selected following a forward stepwise approach in maximum likelihood, where, beginning with a model that only included t_a, environmental covariates were included in the model if AIC was reduced upon inclusion. The best fit model was then fit using restricted maximum likelihood and linear mixed effects models were constructed using the "lme4" package in the R statistical platform (Bates, Mächler, Bolker, & Walker, 2015; R Core Team, 2016).

3.2.5 Size-Selective Mortality

To examine possible size-selective mortality a comparison of mean scale-width at age-1 between age classes was performed with a Bayesian Analysis of Variance (BANOVA). Results are expressed as a probability distribution, with the smaller the overlap between the confidence intervals, indicating a greater probability of size-selective mortality. For all models, we assumed a normally distributed error structure after preliminary data analysis. All models were fit using Markov Chain Monte Carlo

(MCMC) implemented in JAGS software, version 4.1.0 in the R package "runjags" with 100,000 iterations, 20,000 burn in, thinning at 10, and diffuse priors (Denwood, 2016; R Core Team, 2016).

3.3 Results

We analyzed 511,817 Gulf Menhaden sampled by NOAA Fisheries between 1964 and 2011. Fork length of Gulf Menhaden ranged between 57 and 308 mm with a mean of 166.29 ± 21.08 mm (Figure 1). Gulf Menhaden ranged in age from 0 to 7 yrs, however, the majority of samples were from age-1 and age-2 fish (Figure 1). Scale width was positively correlated with FL ($r^2 = 0.583$, $p < 0.001$), indicating that scale size can be used as proxy for fish length throughout the age range sampled (Figure 1). Time series of mesoscale circulation activity indicated elevated values in the 1970's and early 1980's (Figure 2). Positive values of the mesoscale circulation activity index are associated with increased anti-cyclonic gyres (e.g. Loop Current) in the northern Gulf of Mexico. The mean day of spring transition between 1964 and 2011 was the 67^{th} day of the year and was annually dynamic (Figure 2). Time series of mean monthly winter Mississippi River discharge was temporally dynamic as well with a mean of 464 $m^3 s^{-1}$ (Figure 2). The mean annual extent of the mid-summer hypoxic zone was 13,851 km^2, however, data prior to 1985 were absent from the time series (Figure 2).

Comparison of AIC values indicated that inclusion of all environmental covariates improved fit of the extended VBGF (Table 1). The northern intrusion of the Loop Current index was positively correlated with L_∞ and negatively correlated with K (Table 2). Similarly, the day of annual spring transition was positively correlated with L_∞ and negatively correlated with K, indicating that a later spring transition is associated with

increased asymptotic lengths and reduced growth rates in Gulf Menhaden. Compared to all environmental covariates, Mississippi River discharge had the greatest effect size on VBGF parameters as indicated by the values of $\beta_{a,j}$ (Table 2). Mississippi River discharge and the areal extent of the annual hypoxic zone were negatively correlated with L_∞ and positively correlated with K. To assist in the comparison of growth curves given the correlation structure between VBGF parameters (Pilling, Kirkwood, & Walker, 2002), length-at-age was predicted across the range of available ages (1 to 7 ys) assuming a 1 standard deviation increase in each scaled environment covariate, holding all other covariates constant. Enhanced northern intrusion of the Loop Current and a later day of spring transition was associated with reduced length-at-age for age 1, 2, 3, and 4 individuals (Table 3). However, given the enhanced L_∞, after age 5, enhanced Loop Current intrusion and a later spring transition was associated with greater length-at-age relative to no environmental forcing. Alternatively, enhanced Mississippi River discharge and areal hypoxic extent was associated with enhanced length-at-age for ages 1, 2, and 3 and reduced length-at-age for individuals at age 5, 6, and 7 (Table 3).

Scale increment width was analyzed using hierarchical linear models. Evaluation of AIC indicated that a random effect for individual fish did not improve model fit (Table 4). However, inclusion of all environmental covariates and associated age-specific random effects did improve model fit (Table 4). Scale increment width decreased with age (Table 5). Population-level fixed effects indicated that the index of mesoscale circulation activity and day of spring transition were positively correlated with scale increment width (Table 5) while Mississippi River discharge and the areal extent of the hypoxic zone were negatively correlated with scale increment width. However, age-

specific random effects associated with parameter estimates indicated that correlations between scale increment width and environmental covariates were variable through ontogeny (Table 5). Such differences in parameter estimates through ontogeny were most evident for age-1 individuals (Figure 4). For example, mesoscale circulation activity and day of spring transition were negatively correlated with scale increment width for age-1 Gulf Menhaden in contrast to the positive population level effect. For Mississippi River discharge, negative correlations were greatest for age 1 fish, while there was a positive correlation between increment width and discharge for age 3 fish. Alternatively, the areal extent of the hypoxic zone was positively correlated with scale increment width for age 1 fish, but negatively correlated for all other age classes included in the analysis.

Analysis of mean scale width at age-1 for each age class from 470,308 Gulf Menhaden indicated size-selective mortality (Figure 5). Given the limited data of age 6 (N = 8) and age 7 (N = 1) individuals, we excluded these age classes from analysis. The lack of overlap between posterior probability distributions of mean scale increment width at age-1 indicated that Gulf Menhaden that older individuals were significantly smaller at age-1 (Figure 5). However, scale increment width at age-1 for age-3 individuals was slightly larger than age-2 fish (Figure 5).

3.4 Discussion

Understanding variation in individual growth and size-selective mortality can provide insight into the factors that influence the population dynamics of exploited fish species and subsequent ecosystem dynamics (He, Bence, Roseman, Fielder, & Ebener, 2015; Takasuka et al., 2004; Whitten, Klaer, Tuck, & Day, 2013). Despite the commercial importance and ecosystem role of the Gulf Menhaden stock in the NGOM

(Sagarese et al., 2016; Vaughan et al., 2007), little is known about the biological factors that influence individual growth and the implications of selective mortality. Previous assessment efforts have documented inter-annual variation in individual growth of Gulf Menhaden (SEDAR, 2013) and here we describe correlations between possible environmental and biological drivers in the northern Gulf of Mexico and length-at-age and scale increment width sampled from the commercial fishery. By comparing scale-based size-at-age-1 across year classes of Gulf Menhaden, we demonstrate that size-selective mortality in part determines the survival of individuals during the early-life history stages. Results of the present study suggest that growth of Gulf Menhaden is significantly altered by environmental and biological factors that likely poses consequences for stock dynamics.

The VBGF can be understood at the result of anabolic and catabolic processes, where asymptotic size is related to the ratio of both processes and growth rate coefficient is dependent only of catabolism (Lorenzen 2016). Therefore, variation in growth due to processes that impact basal metabolism (a catabolic process) should be reflected in both parameters. However, processes related to anabolism such as food availability and density dependence will only impact asymptotic size. However, by allowing both parameters to vary we removed assumptions of independence that are inconsistent with the statistical and physiological properties of the von Bertalanffy growth equation (Pilling et al., 2002; Shelton & Mangel, 2012). In addition, Gulf Menhaden reach maturity before being harvested by the commercial reduction fishery (SEDAR, 2013) and, therefore, the VBGF presented in this study may reflect reality when accounting for reproduction (Essington et al., 2001; Lester, Shuter, & Abrams, 2004).

The effects of environmental covariates on individual growth when estimated from length-at-age and scale increment data was largely consistent at the population level. For example, asymptotic length and scale increment width across age classes were positively correlated with mesoscale circulation activity and the day of spring transition and negatively correlated with Mississippi River discharge and the areal extent of the recurring hypoxic zone. Variation in growth through ontogeny was consistent for both methodologies in most instances. Predicted length-at-age and scale increment width for age-1 individuals was reduced with elevated values of the index of circulation activity and a later spring transition. Similarly, increased areal extent of the hypoxic zone was associated with enhanced length-at-age-1 and scale increment width for age-1 individuals. However, comparison of predicted length-at-age and age-specific random effects on scale increment width indicated that in some instances the effects of environmental covariates on individual growth was variable between methodologies. For example, enhanced Mississippi River discharge was associated with enhanced length-at-age-1, but reduced scale increment width at age-1. Such differences are likely a result of differences in model structure and the correlation structure between VBGF parameter estimates (Millar, 1992; Pilling et al., 2002). Therefore, for the remainder of the study we refer to the otolith increment analysis when discussing variation in individual growth for specific age classes. Future efforts would benefit from incorporating age-specific random effects when modelling the impact of environmental covariates on VBGF parameters.

Variation in individual growth was correlated to mesoscale circulation activity in the Gulf of Mexico. We found a positive correlation between mesoscale circulation activity related to the northern intrusion of the Loop Current and individual growth of

Gulf Menhaden estimated from length-at-age and scale increment width data. However, reduced growth for age-1 fish was associated with increased circulation activity. Although the specific mechanism responsible for this is unclear, several hypotheses may explain such variation in individual growth. The northern intrusion of the Loop Current and mesoscale eddies can alter circulation patterns in the northern Gulf of Mexico, directly and indirectly driving the physiological, biological, and chemical properties in the region (Karnauskas et al., 2015; Morey, 2003; R. V. Schiller & Kourafalou, 2014; N. D. Walker, 1996). Such variations in circulation patterns can alter planktonic communities, salinity gradients, and sea surface temperatures. Such factors can impact individual growth of fishes (Drinkwater, 2005; E. D. Houde, 1989). In addition, the Loop Current can entrain Mississippi River discharge into the continental shelf east of the delta, which results in a ~11% offshore transport of freshwater (Morey, 2003). This may poses consequences for growth of juvenile Gulf Menhaden, which are highly dependent on river plume dynamics (John J. Govoni et al., 1989).

Gulf Menhaden growth was also related to the timing of the spring transition, which we defined as the first day of the regime shift from winter North winds to summer South winds. A later spring transition was associated with enhanced asymptotic size and increased scale increment width. Such trends are presumably because growth is related to food availability and water temperature. Gulf Menhaden are obligate filter feeders (Olsen et al., 2014) and enhanced primary productivity is correlated with growth in forage fish (Brosset et al., 2015). North winds enhance the areal extent of the highly productive Mississippi River plume (Huang et al., 2013), which can elevate primary productivity in locations that were previously nutrient limited (Hitchcock et al., 1997). A later spring

transition may lead to prolonged nutrient uptake across a larger area of the northern Gulf of Mexico, enhancing feeding opportunities for Gulf Menhaden leading to elevated L_{∞}. Alternatively, a later spring transition will also have consequences for the growth of juvenile Gulf Menhaden. Prolonged North winds and associated offshore movement of the Mississippi River plume, which likely prolongs ingress of larval and juvenile Gulf Menhaden into coastal estuarine nursery grounds (Deegan, 1990; John J. Govoni, 1997). North winds can also flush nutrients and detritus from coastal estuaries, leading to reduced feeding opportunities for juvenile Gulf Menhaden. Deegan (1990) found that cooler spring temperatures, which are associated with a later spring transition, led to reduced growth of juvenile Gulf Menhaden, similar to our study.

Similar to the timing of the spring transition, Mississippi River discharge and scale increment width of age-1 Gulf Menhaden were negatively correlated. Elevated Mississippi River discharge prolongs inshore ingress of larval and juvenile Gulf Menhaden and serves to reduce temperatures throughout the northern Gulf of Mexico. Previous research has demonstrated that high river discharge and low water temperature are correlated with decreased growth of juvenile Gulf Menhaden (Deegan, 1990). Reduced growth-degree-days has also indicated a strong effect of temperature on growth of juvenile Atlantic Menhaden, *B. tyrannus* (Humphrey et al., 2014). The impacts of Mississippi River discharge on the growth of age-1 Gulf Menhaden may pose consequences for growth through ontogeny. For example, for all age classes, asymptotic length and scale increment width of Gulf Menhaden were negatively correlated to Mississippi River discharge. Negative correlations between temperature and asymptotic size have been previous documented in numerous fish species (Baudron, Needle, &

Marshall, 2011; Van Beveren et al., 2014). Our results indicating that asymptotic size is negatively correlated with river discharge may also be a result of density-dependent forcing (Bacheler, Buckel, Paramore, & Rochet, 2012) because previous work has indicated that recruitment variability is in part driven by river discharge (John J. Govoni, 1997). Therefore, future research would benefit from understanding the impacts of Gulf Menhaden abundance on individual growth.

The improved fit of growth models due to the inclusion of the areal extent of the annual hypoxic zone may reflect the impact of hypoxia on the foraging behavior and habitat availability. Both scale increment width and asymptotic size were negative correlated with the areal extent of the hypoxic zone. Recent research has indicated that increased hypoxia can lead to reduced biomass (de Mutsert et al., 2016) and alter the spatial distribution of the Gulf Menhaden fishery (Langseth et al., 2014). Hypoxia limits primary productivity and habitable space in the water column (Nancy N. Rabalais, Turner, & Wiseman, 2002; Zhang et al., 2014), likely leading to density dependence and food limitation as the drivers of growth. For example, Zhang et al. (2014) found that hypoxia and associated reductions in chlorophyll and increased temperatures led to reduced growth rate potential for Gulf Menhaden. In addition, shifts in the spatial distribution of Gulf Menhaden linked to hypoxia (Langseth et al., 2014) may displace fish to locations outside the optimal growth window (Craig & Crowder, 2005). However, the areal extent of the hypoxic zone was positively correlated to the scale increment width of age-1 fish. Juvenile Gulf Menhaden inhabit inshore estuaries and would likely be unaffected by hypoxia on the continental shelf. Hypoxia is also positively correlated with Mississippi River discharge among other factors (N N Rabalais et al., 2001). While

there was no correlation between the indices of Mississippi River discharge and areal extent of the hypoxic zone used in the present analysis (Pearson's $r = 0.04$), we cannot rule out the positive feedback of reduced density-dependent growth as a result of possible reductions in recruitment due to elevated discharge (John J. Govoni, 1997).

Variation in the individual growth of Gulf Menhaden as indicated by the present study may pose consequences for survival via size-selective mortality. Comparison of scale increment widths at age-1 indicated that size-selective mortality occurs in Gulf Menhaden, with smaller individuals surviving to later year classes. Houde et al. (2016) also noted that growth anomaly is negatively correlated with relative abundance of age-0 Atlantic Menhaden. An earlier spring transition and reduced Mississippi River discharge may serve to reduce survival through size-selective mechanisms. However, we cannot rule out that such trends are due to the impact of strong recruitment years on growth as a result of density dependence because enhanced abundance of age-1 fish may lead to a greater number of individuals surviving to later age classes while reducing growth. In addition, given that the samples analyzed in the present analysis were from fishery-dependent sources, such variation in scale increment width at age-1 across age classes may be a result of size-selective fishing. Larger, faster-growing individuals would be more likely to be harvested by the commercial fishery skewing our results. The present study would benefit from the analysis of scale increment widths sampled from fishery-independent sources.

Variability in growth has been documented in most commercially targeted fish species (Lorenzen, 2016), however, assessment models, including the Gulf Menhaden stock assessment (SEDAR, 2013), often treat growth as static through time. This can lead

to underrepresentation of the biological response to variation in extrinsic environmental conditions (Neill 2004). In addition, the inclusion of such variation has been shown to lead to increased model fit for assessment models and improve the accuracy of scientific advice (Whitten et al., 2013). However, assessment models that assume variation in growth are limited in their ability to forecast responses to fishing growth variation may be difficult to estimate for recent years. Therefore, an understanding of the underlying environmental drivers of individual growth variability can improve the accuracy of forecasting (Lorenzen, 2016). Furthermore, the use of extrinsic factors in growth modelling can improve predictions of future climate scenarios on marine systems (Morrongiello, Thresher, & Smith, 2012).

Table 3.1

Forward model selection for the extended von Bertalannfy growth function (VBGF) with environmental covariates fit to Gulf Menhaden length-at-age data.

Model	**AIC**	**Log Likelihood**	**Number of Parameters**	**N**	**Included (y/n)**
VBGF	-515,268	-257,638	4	223,605	
+Mesoscale circulation activity	-517,553	-258,782	6	223,605	Y
+ Day of annual spring transition	-517,579	-258,797	8	223,605	Y
+Mississippi River discharge	-525,525	-262,773	10	223,605	Y
+Areal extent of the annual hypoxic zone	-534,633	-267,328	12	223,605	Y

Table 3.2

Parameter estimates from the extended von Bertalannfy growth function with environmental covariates fit to Gulf Menhaden length-at-age data.

Type	**Parameter**	**Estimate**	**SE**	***t* value**	***p* value**
Constant	L_∞	273.36721	2.07482	131.75444	$\ll 0.001$
	K	0.26825	0.00533	50.32956	$\ll 0.001$
	t_0	-1.45902	0.02542	-57.39242	$\ll 0.001$
	$\beta_{L_\infty,0}$	5.61082	0.00759	739.24990	$\ll 0.001$
	$\beta_{k,0}$	-1.31585	0.01987	-66.22617	$\ll 0.001$
Mesoscale circulation activity	$\beta_{L_\infty,1}$	0.03057	0.00156	19.56207	$\ll 0.001$
	$\beta_{k,1}$	-0.06914	0.00250	-27.67445	$\ll 0.001$
Day of annual spring transition	$\beta_{L_\infty,2}$	0.01536	0.00117	13.11173	$\ll 0.001$
	$\beta_{k,2}$	-0.04129	0.00209	-19.79983	$\ll 0.001$
Mississippi River Discharge	$\beta_{L_\infty,3}$	-0.04201	0.00262	-16.06322	$\ll 0.001$
	$\beta_{k,3}$	0.09704	0.00437	22.19548	$\ll 0.001$
Areal extent of the annual hypoxic zone	$\beta_{L_\infty,4}$	-0.03814	0.00164	-23.32708	$\ll 0.001$
	$\beta_{k,4}$	0.09331	0.00248	37.60655	$\ll 0.001$

Table 3.3

Predicted length-at-age and growth increment from the best fit extended von Bertalanffy growth function assuming a 1 standard deviation increase in each environmental covariate.

	No effect	**Mesoscale circulation activity**	**Day of annual spring transition**	**Mississippi River Discharge (m^3 s^{-1})**	**Areal extent of the annual hypoxic zone (km^2)**
Mean		-0.14035	67.29	464.5	13,752.4
SD		1.05357	25.42	126.12	5,450.9
Predicted length-at-age					
Age 1	132.0	-2.4	-1.8	3.4	3.6
Age 2	165.3	-2	-1.7	2.5	2.8
Age 3	190.7	-1.2	-1.2	1.3	1.7
Age 4	210.2	-0.2	-0.7	-0.3	0.2
Age 5	225.0	0.9	-0.1	-1.7	-1.1
Age 6	236.4	1.9	0.5	-3.2	-2.5
Age 7	245.1	2.8	1	-4.5	-3.8
Predicted growth increment					
Age 1	36.7	0.4	0.1	-0.7	-0.4
Age 2	28.5	0.8	0.3	-1.4	-1
Age 3	22.1	1	0.4	-1.8	-1.3
Age 4	17.1	1.2	0.6	-1.8	-1.4
Age 5	13.3	1.1	0.5	-1.8	-1.4
Age 6	10.3	1.1	0.5	-1.7	-1.3
Age 7	8.0	1	0.5	-1.5	-1.2

Table 3.4

Forward model selection for hierarchical linear models fit to Gulf Menhaden scale increment width and data environmental covariates. $\sigma^2_{x,j} \neq 0$ indicates the random age effect for parameters relating environmental covariates to the response. Number of parameters (P) and samples (N) are indicated.

Model	**AIC**	**Log Likelihood**	**P**	**N**	**Included (y/n)**
$IW_{i,a,c} \sim t_a$	2,307,578	-1,153,782	7	272,576	
+ f_i	2,307,580	-1,153,782	8	272,576	N
+ Mesoscale circulation activity	2,307,442	-1,153,713	8	272,576	Y
+ $\sigma^2_1 \neq 0$	2,306,209	-1,153,095	9	272,576	Y
+ Day of annual spring transition	2,306,171	-1,153,075	10	272,576	Y
+ $\sigma^2_2 \neq 0$	2,306,022	-1,153,000	11	272,576	Y
+ Mississippi River discharge	2,305,804	-1,152,890	12	272,576	Y
+ $\sigma^2_3 \neq 0$	2,305,774	-1,152,874	13	272,576	Y
+ Areal extent of the annual hypoxic zone	2,305,507	-1,152,740	14	272,576	Y
+ $\sigma^2_4 \neq 0$	2,303,814	-1,151,892	15	272,576	Y

Table 3.5

Estimates of the fixed- and mixed-effects for the hierarchical linear models fit to Gulf Menhaden scale increment width and data environmental covariates.

	Fixed Effects		**Random Effects**					
Coefficient	Estimate	SE	Age 1	Age 2	Age 3	Age 4	Age 5	Age 6
Age 1	83.067	0.053						
Age 2	58.753	0.069						
Age 3	23.959	0.191						
Age 4	14.123	0.616						
Age 5	10.769	2.231						
Age 6	8.021	9.578						
Mesoscale circulation activity	0.477	0.489	-1.366	0.568	0.496	0.318	-0.008	-0.009
Day of annual spring transition	0.274	0.255	-0.502	0.538	0.018	-0.062	-0.001	0.008
Mississippi River discharge	-0.211	0.421	-0.989	-0.052	0.861	0.163	0.020	-0.003
Areal extent of the annual hypoxic zone	-0.296	0.661	2.036	-0.823	-0.608	-0.462	-0.121	-0.021

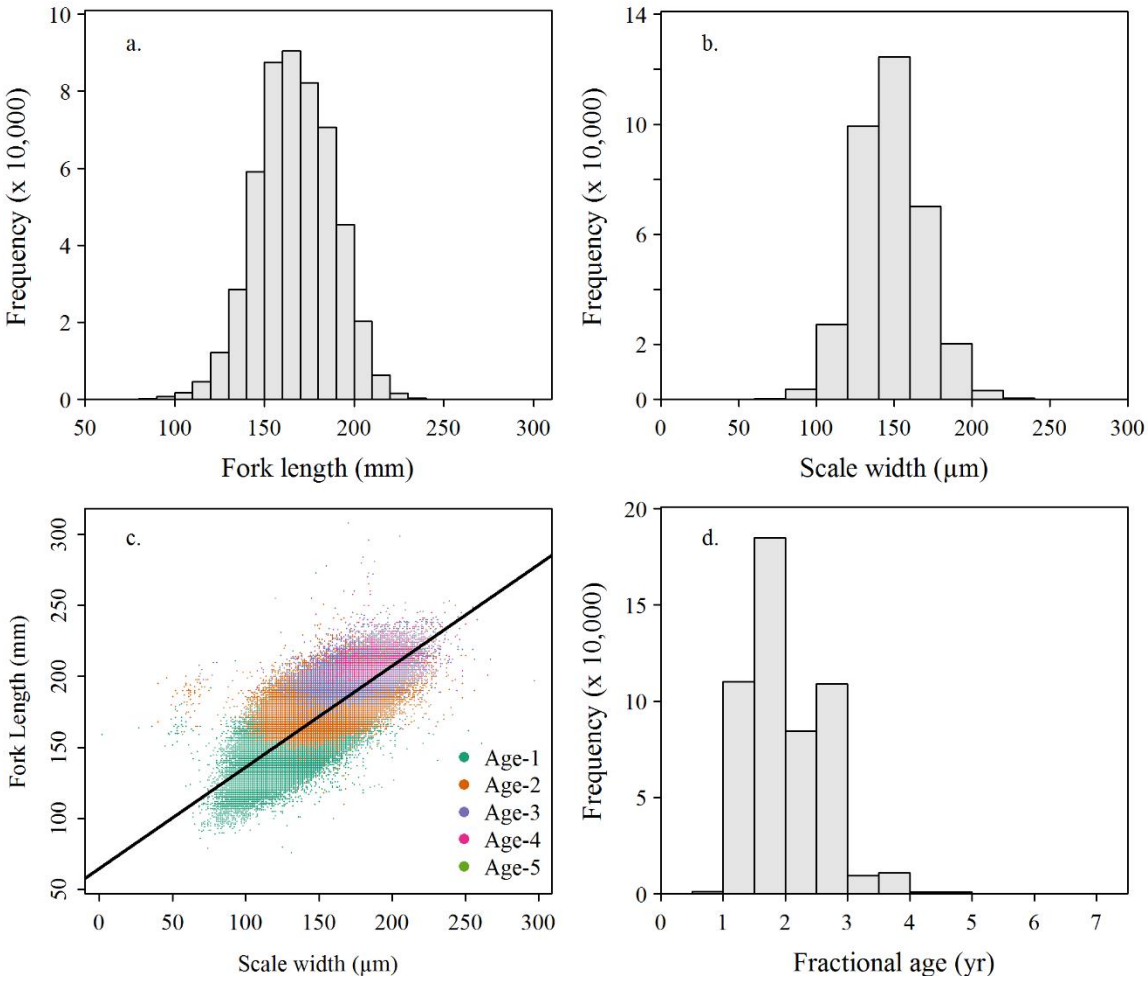

Histograms of (a) fork length and (b) scale width, (c) fork length-scale length regression, and (d) histogram of fractional age of Gulf Menhaden sampled from the commercial fishery in the northern Gulf of Mexico (1964 to 2011).

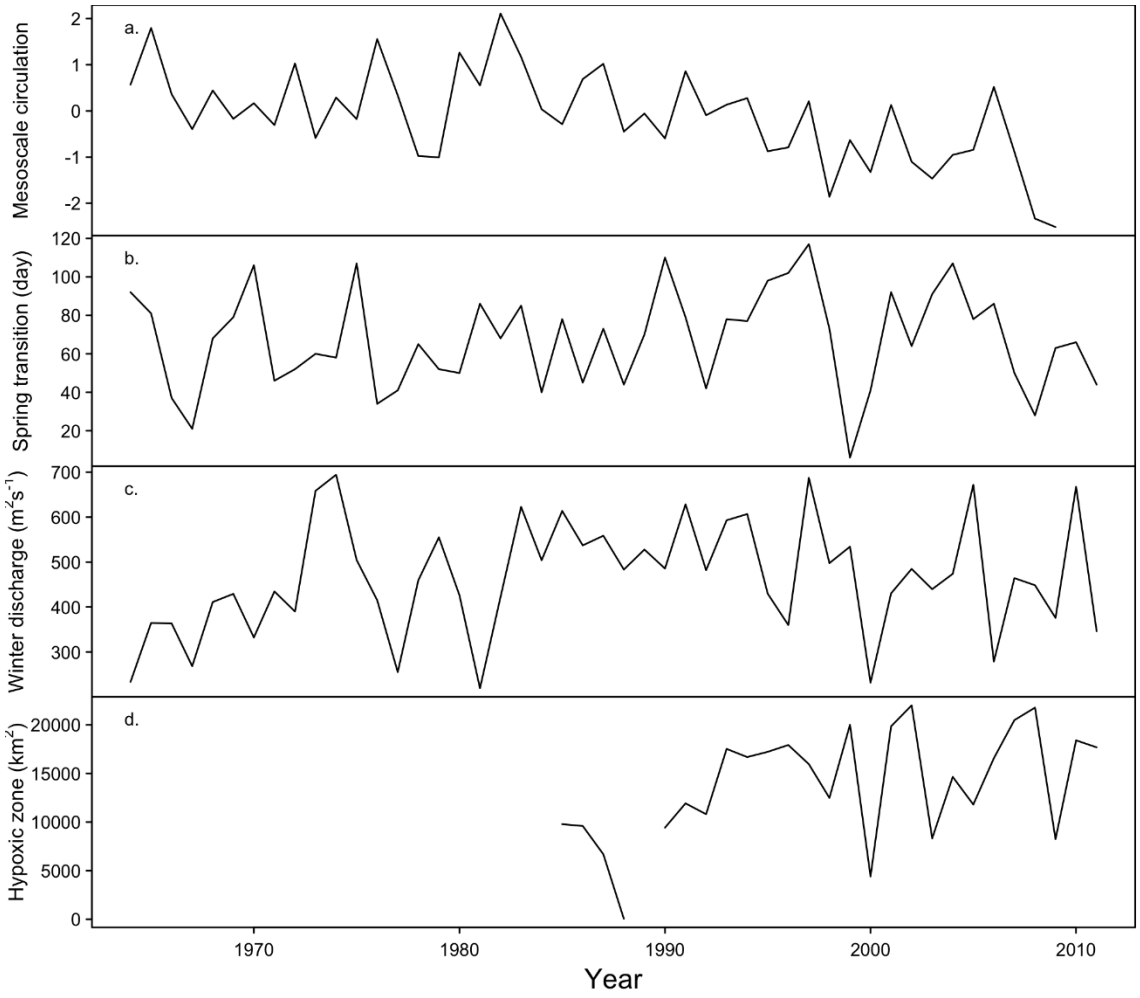

Time series of annual (a) mesoscale circulation activity, (b) day of spring transition, (c) mean monthly Mississippi River discharge (November to March), and (d) annual extent of the mid-summer hypoxic zone.

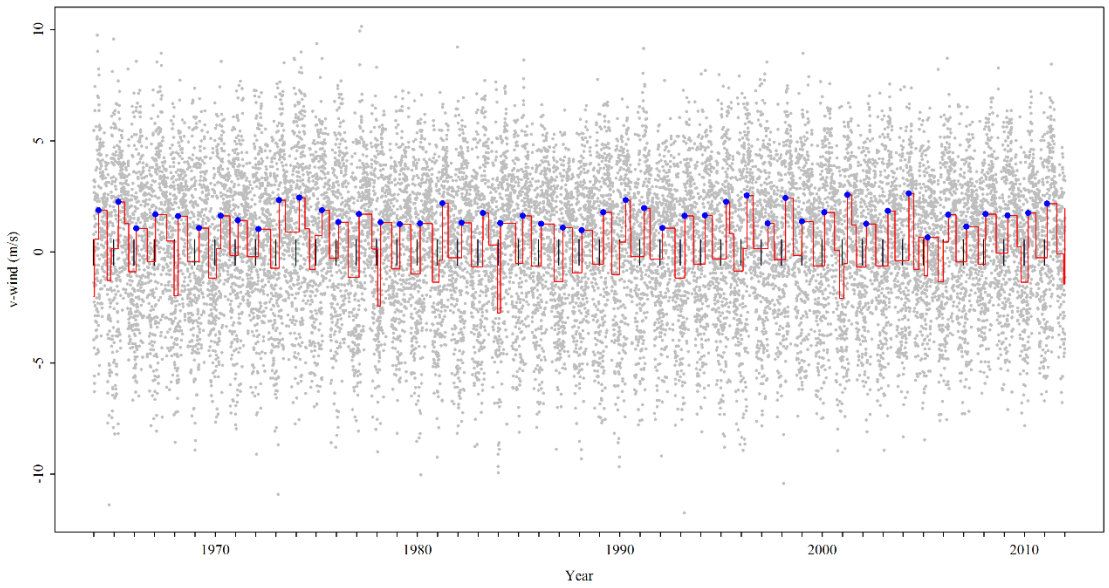

Time series of daily v-wind vectors (North-South) from the NCEP/NCAR Reanalysis Project. Regime series as analyzed by the STARS algorithm is indicated in red, first day of the year is indicated as a black tic mark, and day of spring transition is indicated by the blue circles.

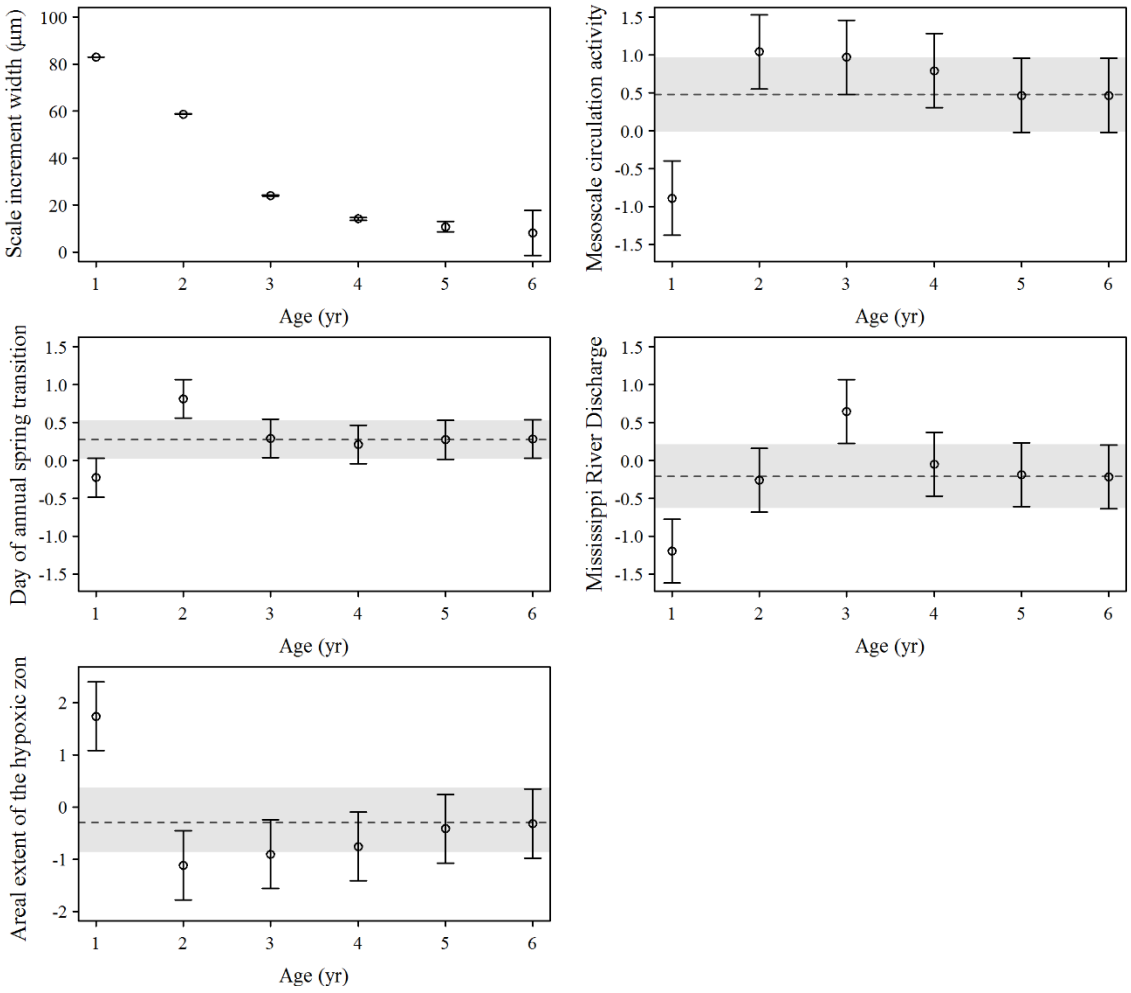

Predicted scale increment width at age and age-specific parameter estimates (±SE) from the hierarchical linear model fit to Gulf Menhaden scale increment width and data environmental covariates. Population level parameter estimates are indicated by the dotted line and SE by the grey box.

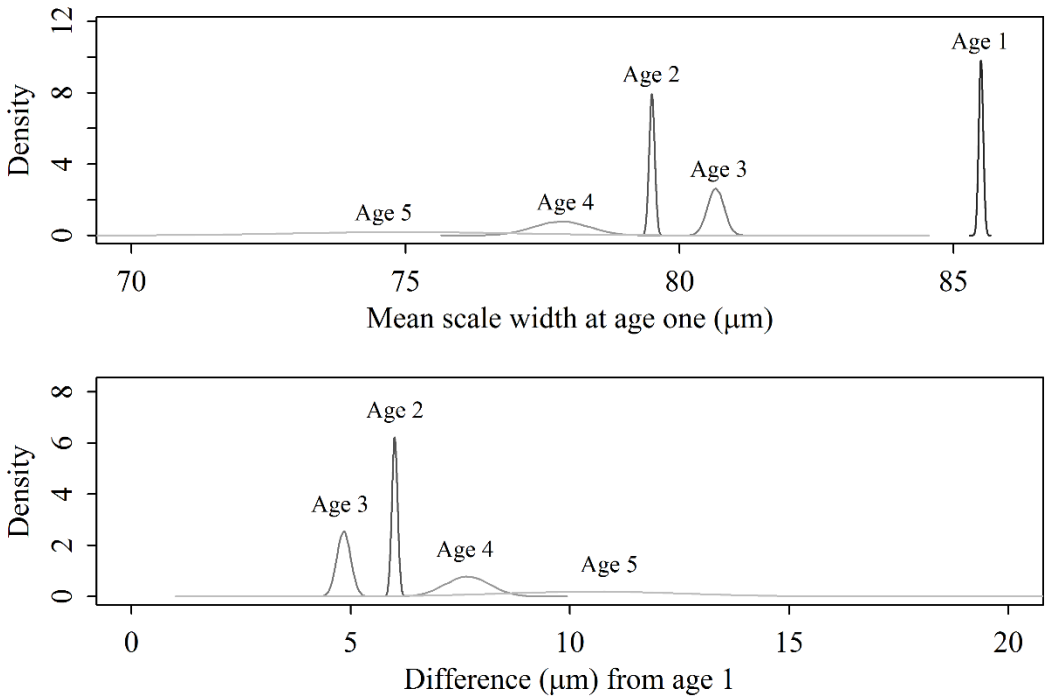

Posterior probability distribution of age-level estimates of mean size-at-age-one (length to first scale annuli) and differences between age-one estimates.

REFERENCES

Ahrenholz, D. W. (1981). Recruitment and exploitation of Gulf menhaden, *Brevoortia patronus*. *Fishery Bulletin*, *79*(2), 325–335.

Ahrenholz, D. W. (1991). Population biology and life history of the North American menhadens, *Brevoortia* spp. *Marine Fisheries Review*, *53*(4), 3–19.

Aires-da-Silva, A., Lennert-cody, C., Maunder, M., & Román-Verdesoto, M. (2013). *Document SAC-05-11a: Stock status of the silky shark in the eastern Pacific Ocean*. La Jolla, California, USA.

Ayón, P., Swartzman, G., Bertrand, A., Gutiérrez, M., & Bertrand, S. (2008). Zooplankton and forage fish species off Peru: Large-scale bottom-up forcing and local-scale depletion. *Progress in Oceanography*, *79*(2–4), 208–214. http://doi.org/10.1016/j.pocean.2008.10.023

Bacheler, N. M., Bailey, K. M., Ciannelli, L., Bartolino, V., & Chan, K. S. (2009). Density-dependent, landscape, and climate effects on spawning distribution of walleye pollock *Theragra chalcogramma*. *Marine Ecology Progress Series*, *391*, 1–12. http://doi.org/10.3354/meps08259

Bacheler, N. M., Buckel, J. A., Paramore, L. M., & Rochet, M.-J. (2012). Density-dependent habitat use and growth of an estuarine fish. *Canadian Journal of Fisheries and Aquatic Sciences*, *69*(11), 1734–1747. http://doi.org/10.1139/f2012-098

Barry, K. P., Condrey, R. E., Driggers, W. B., & Jones, C. M. (2008). Feeding ecology and growth of neonate and juvenile blacktip sharks *Carcharhinus limbatus* in the Timbalier-Terrebone Bay complex, LA, U.S.A. *Journal of Fish Biology*, *73*(3), 650–

662. http://doi.org/10.1111/j.1095-8649.2008.01963.x

Bass, R. J., & Avault, J. W. (1975). Food habits, length-weight relationship, condition factor, and growth of juvenile Red Drum, *Sciaenops ocellata*, in Louisiana. *Transactions of the American Fisheries Society*, *104*(1), 35–45. http://doi.org/10.1577/1548-8659(1975)104<35:FHLRCF>2.0.CO;2

Bates, D., Mächler, M., Bolker, B., & Walker, S. (2015). Fitting Linear Mixed-Effects Models Using lme4. *Journal of Statistical Software*, *67*(1), 51. http://doi.org/10.18637/jss.v067.i01

Baudron, A. R., Needle, C. L., & Marshall, C. T. (2011). Implications of a warming North Sea for the growth of haddock Melanogrammus aeglefinus. *Journal of Fish Biology*, *78*(7), 1874–1889. http://doi.org/10.1111/j.1095-8649.2011.02940.x

Beckman, D., & Wilson, C. (1995). Seasonal timing of opaque zone formation in fish otoliths. In D. Secor, J. Dean, & S. E. Campana (Eds.), *Recent Developments in Fish Otolith Research* (pp. 27–44). Columbia, OH: Belle W. Baruch.

Bjornsson, B. (2001). Optimal temperature for growth and feed conversion of immature cod (*Gadus morhua L.*). *ICES Journal of Marine Science*, *58*(1), 29–38. http://doi.org/10.1006/jmsc.2000.0986

Black, B. A. (2009). Climate-driven synchrony across tree, bivalve, and rockfish growth-increment chronologies of the northeast Pacific. *Marine Ecology Progress Series*, *378*(Campana 2001), 37–46. http://doi.org/10.3354/meps07854

Botsford, L. W., Lawrence, C. A., Dever, E. P., Hastings, A., & Largier, J. (2003). Wind strength and biological productivity in upwelling systems: An idealized study. *Fisheries Oceanography*, *12*(4–5), 245–259. http://doi.org/10.1046/j.1365-

2419.2003.00265.x

Botsford, L. W., Lawrence, C. A., Dever, E. P., Hastings, A., & Largier, J. (2006). Effects of variable winds on biological productivity on continental shelves in coastal upwelling systems. *Deep-Sea Research Part II: Topical Studies in Oceanography*, *53*(25–26), 3116–3140. http://doi.org/10.1016/j.dsr2.2006.07.011

Brosset, P., Ménard, F., Fromentin, J., Bonhommeau, S., Ulses, C., Bourdeix, J., … Saraux, C. (2015). Influence of environmental variability and age on the body condition of small pelagic fish in the Gulf of Lions. *Marine Ecology Progress Series*, *529*(JUNE), 219–231. http://doi.org/10.3354/meps11275

Brunel, T., & Dickey-Collas, M. (2010). Effects of temperature and population density on von Bertalanffy growth parameters in Atlantic herring: A macro-ecological analysis. *Marine Ecology Progress Series*, *405*(APRIL), 15–28. http://doi.org/10.3354/meps08491

Burnham, K. P., & Anderson, D. R. (2004). *Model Selection and Multimodel Inference*. (K. P. Burnham & D. R. Anderson, Eds.)*Ecological Modelling* (2nd Editio, Vol. 172). New York, NY: Springer New York. http://doi.org/10.1007/b97636

Cahuin, S. M., Cubillos, L. A., Ñiquen, M., & Escribano, R. (2009). Climatic regimes and the recruitment rate of anchoveta, Engraulis ringens, off Peru. *Estuarine, Coastal and Shelf Science*, *84*(4), 591–597. http://doi.org/10.1016/j.ecss.2009.07.027

Campana, S. (2001). Accuracy, precision and quality control in age determination, including a review of the use and abuse of age validation methods. *Journal of Fish Biology*, *59*(2), 197–242. http://doi.org/10.1006/jfbi.2001.1668

Campana, S. E. (1996). Year-class strength and growth rate in young Atlantic cod Gadus morhua. *Marine Ecology Progress Series*, *135*(1–3), 21–26. http://doi.org/10.3354/meps135021

CCAR, of Colorado, U., & Boulder. (2013). Reconstructed Sea Level Version 1. Ver. 1. PO.DAAC, CA, USA. http://doi.org/http://dx.doi.org/10.5067/RECSL-000V1

Chakraborty, S., & Lohrenz, S. E. (2015). Phytoplankton community structure in the river-influenced continental margin of the northern Gulf of Mexico. *Marine Ecology Progress Series*, *521*, 31–47. http://doi.org/10.3354/meps11107

Charrad, M., Ghazzali, N., Boiteau, V., & Niknafs, A. (2014). NbClust : an R package for determining the relevant number of clusters in a data set. *Journal of Statistical Software*, *61*(6), 1–36. http://doi.org/10.18637/jss.v061.i06

Chen, W., Govoni, J. J., & Warlen, S. M. (1992). Comparison of feeding and growth of larval round herring *Etrumeus teres* and gulf menhaden *Brevoortia patronus*. *Fishery Bulletin*, *90*(1), 183–189.

Chen, Y., Ye, Y., & Dennis, D. (2009). How reliable are the abundance indices derived from commercial catch–effort standardization? *Canadian Journal of Fisheries and Aquatic Sciences*, *66*(7), 1169–1178. http://doi.org/10.1139/F09-070

Christmas, J., & Waller, R. (1975). Location and time of menhaden spawning In the Gulf of Mexico. *Gulf Coast Research Laboratory. Ocean Springs, Mississippi.*, 20.

Ciannelli, L., Bailey, K., & Olsen, E. M. (2015). Evolutionary and ecological constraints of fish spawning habitats. *ICES Journal of Marine Science*, *72*(2), 285–296. http://doi.org/10.1093/icesjms/fsu145

Ciannelli, L., Bartolino, V., & Chan, K.-S. (2012). Non-additive and non-stationary

properties in the spatial distribution of a large marine fish population. *Proceedings of the Royal Society B: Biological Sciences*, *279*(1743), 3635–3642. http://doi.org/10.1098/rspb.2012.0849

Craig, J. K., & Crowder, L. B. (2005). Hypoxia-induced habitat shifts and energetic consequences in Atlantic croaker and brown shrimp on the Gulf of Mexico shelf. *Marine Ecology Progress Series*, *294*, 79–94. http://doi.org/10.3354/meps294079

Cubillos, L. A., Arcos, D. F., Bucarey, D. A., & Canales, M. T. (2001). Seasonal growth of small pelagic fish off Talcahuano, Chile (37°S, 73°W): a consequence of their reproductive strategy to seasonal upwelling? *Aquatic Living Resources*, *14*, 115–124. http://doi.org/10.1016/S0990-7440(01)01112-3

D'Alessandro, E. K., Sponaugle, S., & Cowen, R. K. (2013). Selective mortality during the larval and juvenile stages of snappers (Lutjanidae) and great barracuda Sphyraena barracuda. *Marine Ecology Progress Series*, *474*(McCormick 1998), 227–242. http://doi.org/10.3354/meps10114

Dahlberg, M. D. (1969). Fat cycles and condition factors of two species of Menhaden, *Brevoortia* (Clupeidae), and natural hybrids from the Indian River of Florida. *American Midland Naturalist*, *82*(1), 117. http://doi.org/10.2307/2423822

de Mutsert, K., Steenbeek, J., Lewis, K., Buszowski, J., Cowan, J. H., & Christensen, V. (2016). Exploring effects of hypoxia on fish and fisheries in the northern Gulf of Mexico using a dynamic spatially explicit ecosystem model. *Ecological Modelling*, *331*, 142–150. http://doi.org/10.1016/j.ecolmodel.2015.10.013

Deegan, L. A. (1986). Changes in body composition and morphology of young-of-the-year Gulf Menhaden, *Brevoortia patronus* Goode, in Fourleague Bay, Louisiana.

Journal of Fish Biology, *29*(4), 403–415.

Deegan, L. A. (1990). Effects of estuarine environmental conditions on population dynamics of young-of-the-year Gulf Menhaden. *Marine Ecology Progress Series*, *68*(1–2), 195–205. http://doi.org/10.3354/meps068195

Del Castillo, C. E., Coble, P. G., Conmy, R. N., Müller-Karger, F. E., Vanderbloemen, L., & Vargo, G. A. (2001). Multispectral in situ measurements of organic matter and chlorophyll fluorescence in seawater: Documenting the intrusion of the Mississippi River plume in the West Florida Shelf. *Limnology and Oceanography*, *46*(7), 1836–1843. http://doi.org/10.4319/lo.2001.46.7.1836

Denwood, M. J. (2016). runjags : An R Package Providing Interface Utilities, Model Templates, Parallel Computing Methods and Additional Distributions for MCMC Models in JAGS. *Journal of Statistical Software*, *71*(9), 1–25. http://doi.org/10.18637/jss.v071.i09

Domingues, R., Goni, G., Bringas, F., Muhling, B., Lindo-Atichati, D., & Walter, J. (2016). Variability of preferred environmental conditions for Atlantic bluefin tuna (Thunnus thynnus) larvae in the Gulf of Mexico during 1993-2011. *Fisheries Oceanography*, *25*(3), 320–336. http://doi.org/10.1111/fog.12152

Drinkwater, K. F. (2005). The response of Atlantic cod (Gadus morhua) to future climate change. *ICES Journal of Marine Science*, *62*(7), 1327–1337. http://doi.org/10.1016/j.icesjms.2005.05.015

Dycus, J. C., Wisniewski, J. M., & Peterson, J. T. (2015). The effects of flow and stream characteristics on the variation in freshwater mussel growth in a Southeast US river basin. *Freshwater Biology*, *60*(2), 395–409. http://doi.org/10.1111/fwb.12504

Eldridge, P. M., & Roelke, D. L. (2010). Origins and scales of hypoxia on the Louisiana shelf: Importance of seasonal plankton dynamics and river nutrients and discharge. *Ecological Modelling*, *221*(7), 1028–1042. http://doi.org/10.1016/j.ecolmodel.2009.04.054

Enfield, D. B. (1996). Relationships of inter-american rainfall to tropical Atlantic and Pacific SST variability. *Geophysical Research Letters*, *23*(23), 3305. http://doi.org/10.1029/96GL03231

Essington, T. E., Kitchell, J. F., & Walters, C. J. (2001). The von Bertalanffy growth function, bioenergetics, and the consumption rates of fish. *Canadian Journal of Fisheries and Aquatic Sciences*, *58*(11), 2129–2138. http://doi.org/10.1139/f01-151

Feng, J., Stige, L. C., Durant, J. M., Hessen, D. O., Zhu, L., Hjermann, D. O., … Stenseth, N. C. (2014). Large-scale season-dependent effects of temperature and zooplankton on phytoplankton in the North Atlantic. *Marine Ecology Progress Series*, *502*(April), 25–37. http://doi.org/10.3354/meps10724

Fore, P. (1970). Oceanic distribution of eggs and larvae of the Gulf Menhaden. *US Fish and Wildlife Service Circular*, *341*, 1–24.

Fossen, I., Albert, O. T., & Nilssen, E. M. (1999). Back-calculated individual growth of long rough dab (Hippoglossoides platessoides) in the Barents Sea. *ICES Journal of Marine Science*, (May 1994), 689–696. http://doi.org/10.1006/jmsc.1999.0486

Garrido, S., Ben-Hamadou, R., Santos, A. M. P., Ferreira, S., Teodósio, M. A., Cotano, U., … Ré, P. (2015). Born small, die young: Intrinsic, size-selective mortality in marine larval fish. *Scientific Reports*, *5*, 17065. http://doi.org/10.1038/srep17065

Gershunov, A., & Barnett, T. P. (1998). ENSO influence on intraseasonal extreme

rainfall and temperature frequencies in the contiguous United States: Observations and model results. *Journal of Climate, 11*(7), 1575–1586. http://doi.org/10.1175/1520-0442(1998)011<1575:EIOIER>2.0.CO;2

Goolsby, D. A., Battaglin, W. A., Aulenbach, B. T., & Hooper, R. P. (2001). Nitrogen input to the Gulf of Mexico. *Journal of Environment Quality*, *30*(2), 329–336. http://doi.org/10.2134/jeq2001.302329x

Govoni, J. J. (1993). Flux of larval fishes across frontal boundaries: examples from the Mississippi River plume front and the western Gulf Stream front in winter. *Bulletin of Marine Science*, *53*(2), 538–566.

Govoni, J. J. (1997). The association of the population recruitment of Gulf Menhaden, *Brevoortia patronus*, with Mississippi River discharge. *Journal of Marine Systems*, *12*(1–4), 101–108. http://doi.org/10.1016/S0924-7963(96)00091-7

Govoni, J. J., & Grimes, C. B. (1992). The surface accumulation of larval fishes by hydrodynamic convergence within the Mississippi River plume front. *Continental Shelf Research*, *12*(11), 1265–1276. http://doi.org/10.1016/0278-4343(92)90063-P

Govoni, J. J., Hoss, D. E., & Colby, D. R. (1989). The spatial distribution of larval fishes about the Mississippi River plume. *Limnology and Oceanography*, *34*(1), 178–187. http://doi.org/10.4319/lo.1989.34.1.0178

Grimes, C. B. (2001). Fishery production and the Mississippi River discharge. *Fisheries*, *26*(July 2014), 17–26. http://doi.org/10.1577/1548-8446(2001)026<0017:FPATMR>2.0.CO;2

Grimes, C. B., & Finucane, J. H. (1991). Spatial distribution and abundance of larval and juvenile fish, chlorophyll and macrozooplankton around the Mississippi River

discharge plume, and the role of the plume in fish recruitment. *Marine Ecology Progress Series*, *75*(2–3), 109–119. http://doi.org/10.3354/meps075109

Hamlington, B. D., Leben, R. R., & Kim, K. Y. (2012). Improving sea level reconstructions using non-sea level measurements. *Journal of Geophysical Research: Oceans*, *117*(10), 1–14. http://doi.org/10.1029/2012JC008277

Hamlington, B. D., Leben, R. R., Strassburg, M. W., & Kim, K.-Y. (2014). Cyclostationary empirical orthogonal function sea-level reconstruction. *Geoscience Data Journal*, *1*(1), 13–19. http://doi.org/10.1002/gdj3.6

Hartigan, J. A., & Wong, M. A. (1979). Algorithm AS 136: A K-Means Clustering Algorithm. *Journal of the Royal Statistical Society. Series C (Applied Statistics)*, *28*(1), 100–108. http://doi.org/10.2307/2346830

Hastie, T., & Tibshirani, R. (1986). Generalized Additive Models. *Statistical Science*, *1*(3), 297–318. http://doi.org/10.1214/ss/1177013609

Hastie, T., & Tibshirani, R. (1993). Varying-coefficient models. *Journal of the Royal Statistical Society. Series B (Methodological)*, *55*(4), 757–796.

He, J. X., Bence, J. R., Roseman, E. F., Fielder, D. G., & Ebener, M. P. (2015). Using time-varying asymptotic length and body condition of top piscivores to indicate ecosystem regime shift in the main basin of Lake Huron: a Bayesian hierarchical modeling approach. *Canadian Journal of Fisheries and Aquatic Sciences*, *1103*(December 2015), cjfas-2015-0235. http://doi.org/10.1139/cjfas-2015-0235

Hitchcock, G. L., Wiseman, W. J., Boicourt, W. C., Mariano, A. J., Walker, N., Nelsen, T. A., & Ryan, E. (1997). Property fields in an effluent plume of the Mississippi River. *Journal of Marine Systems*, *12*(1–4), 109–126. http://doi.org/10.1016/S0924-

7963(96)00092-9

Hollowed, A. B., Hare, S. R., & Wooster, W. S. (2001). Pacific Basin climate variability and patterns of Northeast Pacific marine fish production. *Progress in Oceanography*, *49*(1–4), 257–282. http://doi.org/10.1016/S0079-6611(01)00026-X

Holsman, K. K., Ianelli, J. N., & Aydin, K. (2016). *Multi-species Stock Assessment for walleye pollock , Pacific cod , and arrowtooth flounder in the Eastern Bering Sea*.

Houde, E. D. (1989). Comparative growth, mortality, and energetics of marine fish larvae: temperature and implied latitudinal effects. *Fishery Bulletin*, *87*(3), 471–495.

Houde, E. D. (2008). Emerging from Hjort's shadow. *Journal of Northwest Atlantic Fishery Science*, *41*, 53–70. http://doi.org/10.2960/J.v41.m634

Houde, E. D., Annis, E. R., Harding, L. W., Mallonee, M. E., & Wilberg, M. J. (2016). Factors affecting the abundance of age-0 Atlantic menhaden (*Brevoortia tyrannus*) in Chesapeake Bay. *ICES Journal of Marine Science: Journal Du Conseil*, *73*(9), 2238–2251. http://doi.org/10.1093/icesjms/fsw063

Houde, E. D., & Zastrow, C. E. (1993). Ecosystem- and taxon-especific dynamic and energetics properties of larval fish assemblages. *Bulletin of Marine Science*, *53*(2), 290–335.

Huang, W.-J., Cai, W.-J., Castelao, R. M., Wang, Y., & Lohrenz, S. E. (2013). Effects of a wind-driven cross-shelf large river plume on biological production and CO 2 uptake on the Gulf of Mexico during spring. *Limnology and Oceanography*, *58*(5), 1727–1735. http://doi.org/10.4319/lo.2013.58.5.1727

Humphrey, J., Wilberg, M. J., Houde, E. D., & Fabrizio, M. C. (2014). Effects of temperature on age-0 Atlantic Menhaden growth in Chesapeake Bay. *Transactions*

of the American Fisheries Society, *143*(5), 1255–1265. http://doi.org/10.1080/00028487.2014.931299

Johnson, D. W., Grorud-Colvert, K., Sponaugle, S., & Semmens, B. X. (2014). Phenotypic variation and selective mortality as major drivers of recruitment variability in fishes. *Ecology Letters*, *17*(6), 743–755. http://doi.org/10.1111/ele.12273

Karnauskas, M., Schirripa, M. J., Craig, J. K., Cook, G. S., Kelble, C. R., Agar, J. J., … Wang, C. (2015). Evidence of climate-driven ecosystem reorganization in the Gulf of Mexico. *Global Change Biology*, *21*(7), 2554–2568. http://doi.org/10.1111/gcb.12894

Kimura, D. K. (2008). Extending the von Bertalanffy growth model using explanatory variables. *Canadian Journal of Fisheries and Aquatic Sciences*, *65*(9), 1879–1891. http://doi.org/10.1139/F08-091

Kristensen, K., Nielsen, A., Berg, C. W., Skaug, H., & Bell, B. (2015). TMB: Automatic Differentiation and Laplace Approximation. *arXiv*, *70*(5), 1–21. http://doi.org/10.18637/jss.v070.i05

Krohn, M., Reidy, S., & Kerr, S. (1997). Bioenergetic analysis of the effects of temperature and prey availability on growth and condition of northern cod (Gadus morhua). *Canadian Journal of Fisheries and Aquatic Sciences*, *54*(S1), 113–121. http://doi.org/10.1139/cjfas-54-S1-113

Langseth, B. J., Purcell, K. M., Craig, J. K., Schueller, A. M., Smith, J. W., Shertzer, K. W., … Fennel, K. (2014). Effect of changes in dissolved oxygen concentrations on the spatial dynamics of the Gulf Menhaden fishery in the northern Gulf of Mexico.

Marine and Coastal Fisheries, *6*(1), 223–234. http://doi.org/10.1080/19425120.2014.949017

Lau, N.-C., & Nath, M. J. (2001). Impact of ENSO on SST variability in the North Pacific and North Atlantic: Seasonal dependence and role of extratropical sea–air coupling. *Journal of Climate*, *14*(13), 2846–2866. http://doi.org/10.1175/1520-0442(2001)014<2846:IOEOSV>2.0.CO;2

LeCren, E. D. (1951). The length-weight relationship and seasonal cycle in gonad weight and condition in the Perch (*Perca fluviatilis*). *Journal of Animal Ecology*, *20*(2), 201–219.

Lester, N. P., Shuter, B. J., & Abrams, P. A. (2004). Interpreting the von Bertalanffy model of somatic growth in fishes: the cost of reproduction. *Proceedings of the Royal Society B*, *271*(1548), 1625–1631. http://doi.org/10.1098/rspb.2004.2778

Lewis, R., & Roithmayr, C. (1980). Spawning and sexual maturity of Gulf Menhaden, *Brevoortia patronus*. *Fishery Bulletin*, *78*(4), 947–951.

Lohrenz, S. E., Fahnenstiel, G. L., Redalje, D. G., Lang, G. A., Chen, X. G., & Dagg, M. J. (1997). Variations in primary production of northern Gulf of Mexico continental shelf waters linked to nutrient inputs from the Mississippi River. *Marine Ecology Progress Series*, *155*, 45–54. http://doi.org/10.3354/meps155045

Lohrenz, S. E., Fahnenstiel, G. L., Redalje, D. G., Lang, G. A., Dagg, M. J., Whitledge, T. E., & Dortch, Q. (1999). Nutrients, irradiance, and mixing as factors regulation primary production in coastal waters impacted by the Mississippi River plume. *Continental Shelf Research*, *19*, 1113–1141.

Lohrenz, S. E., Redalje, D. G., Cai, W.-J., Acker, J., & Dagg, M. (2008). A retrospective

analysis of nutrients and phytoplankton productivity in the Mississippi River plume. *Continental Shelf Research*, *28*(12), 1466–1475. http://doi.org/10.1016/j.csr.2007.06.019

Lorenzen, K. (2016). Toward a new paradigm for growth modeling in fisheries stock assessments: Embracing plasticity and its consequences. *Fisheries Research*, *180*, 4–22. http://doi.org/10.1016/j.fishres.2016.01.006

Marra, G., & Wood, S. N. (2011). Practical variable selection for generalized additive models. *Computational Statistics and Data Analysis*, *55*(7), 2372–2387. http://doi.org/10.1016/j.csda.2011.02.004

Millar, R. B. (1992). Modelling environmental effects on growth of cod: fitting to growth increment data versus fitting to size-at-age data. *ICES Journal of Marine Science*, *49*(3), 289–295. http://doi.org/10.1093/icesjms/49.3.289

Minami, M., Lennert-Cody, C. E., Gao, W., & Román-Verdesoto, M. (2007). Modeling shark bycatch: The zero-inflated negative binomial regression model with smoothing. *Fisheries Research*, *84*(2), 210–221. http://doi.org/10.1016/j.fishres.2006.10.019

Morey, S. L. (2003). Export pathways for river discharged fresh water in the northern Gulf of Mexico. *Journal of Geophysical Research*, *108*(C10), 1–15. http://doi.org/10.1029/2002JC001674

Morey, S. L., Zavala-Hidalgo, J., & O'Brien, J. J. (2005). The seasonal variability of continental shelf circulation in the northern and western Gulf of Mexico from a high-resolution numerical model (pp. 203–218). http://doi.org/10.1029/161GM16

Morrongiello, J. R., & Thresher, R. E. (2014). A statistical framework to explore

ontogenetic growth variation among individuals and populations: a marine fish example. *Ecological Monographs*, *85*(1), 93–115. http://doi.org/10.1890/13-2355.1

Morrongiello, J. R., Thresher, R. E., & Smith, D. C. (2012). Aquatic biochronologies and climate change. *Nature Climate Change*, *2*(12), 849–857. http://doi.org/10.1038/nclimate1616

Murase, H., Nagashima, H., Yonezaki, S., Matsukura, R., & Kitakado, T. (2009). Application of a generalized additive model (GAM) to reveal relationships between environmental factors and distributions of pelagic fish and krill: A case study in Sendai Bay, Japan. *ICES Journal of Marine Science*, *66*(6), 1417–1424. http://doi.org/10.1093/icesjms/fsp105

Olsen, Z., Fulford, R., Dillon, K., & Graham, W. (2014). Trophic role of Gulf Menhaden *Brevoortia patronus* examined with carbon and nitrogen stable isotope analysis. *Marine Ecology Progress Series*, *497*, 215–227. http://doi.org/10.3354/meps10519

Pauly, D., & Tsukayama, I. (1987). *The Peruvian Anchoveta and Its Upwelling Ecosystem : Three Decades of Change*. *ICLARM Studies and Reviews*. Manila: International Center for Living Aquatic Resources Management (ICLARM). http://doi.org/10.1577/1548-8659-117.3.317

Pepin, P., Robert, D., Bouchard, C., Dower, J. F., Falardeau, M., Fortier, L., … Sponaugle, S. (2015). Once upon a larva: revisiting the relationship between feeding success and growth in fish larvae. *ICES Journal of Marine Science*, *72*(2), 359–373. http://doi.org/10.1093/icesjms/fsu201

Pillar, S. C. (1984). A comparison of the performance of four zooplankton samplers. *S. Afr. J. Mar. Sci.*, *2*(May), 1–18. http://doi.org/10.2989/02577618409504354

Pilling, G. M., Kirkwood, G. P., & Walker, S. G. (2002). An improved method for estimating individual growth variability in fish, and the correlation between von Bertalanffy growth parameters. *Fisheries Bethesda*, *432*(3), 424–432. http://doi.org/10.1139/f02-022

Pilling, G. M., Millner, R. S., Easey, M. W., Maxwell, D. L., & Tidd, A. N. (2007). Phenology and North Sea cod Gadus morhua L.: has climate change affected otolith annulus formation and growth? *Journal of Fish Biology*, *70*(2), 584–599. http://doi.org/10.1111/j.1095-8649.2007.01331.x

Pristas, P., Levi, E. J., & Dryfoos, R. (1976). Analysis of returns of tagged gulf menhaden. *Fishery Bulletin*, *74*(1), 112–117.

Rabalais, N. N., Turner, R. E., & Wiseman, W. J. (2001). Hypoxia in the Gulf of Mexico. *Journal of Environmental Quality*, *30*(2), 320–329. http://doi.org/10.2134/jeq2001.302320x

Rabalais, N. N., Turner, R. E., & Wiseman, W. J. (2002). Gulf of Mexico Hypoxia, A.K.A. "The Dead Zone." *Annual Review of Ecology and Systematics*, *33*(1), 235–263. http://doi.org/10.1146/annurev.ecolsys.33.010802.150513

R Core Team. (2015). R: A Language and Environment for Statistical Computing. Vienna, Austria. Retrieved from http://www.r-project.org/

R Core Team. (2016). R: A Language and Environment for Statistical Computing. Vienna, Austria. Retrieved from https://www.r-project.org/

Rester, J. (2012). Environmental and biological atlas of the Gulf of Mexico 2010. *Gulf States Marine Fisheries Commission. Ocean Springs, MS*, (206), 84.

Rice, J. A., Miller, T. J., Rose, K. A., Crowder, L. B., Marschall, E. A., Trebitz, A. S., &

DeAngelis, D. L. (1993). Growth rate variation and larval survival: inferences from an individual-based size-dependent predation model. *Canadian Journal of Fisheries and Aquatic Sciences*, *50*(1), 133–142. http://doi.org/10.1139/f93-015

Richardson, D. E., Vanwye, J. D., Exum, A. M., Cowen, R. K., & Crawford, D. L. (2007). High-throughput species identification: From DNA isolation to bioinformatics: Technical article. *Molecular Ecology Notes*, *7*(2), 199–207. http://doi.org/10.1111/j.1471-8286.2006.01620.x

Robinson, K. L., Ruzicka, J. J., Hernandez, F. J., Graham, W. M., Decker, M. B., Brodeur, R. D., & Sutor, M. (2015). Evaluating energy flows through jellyfish and gulf menhaden (Brevoortia patronus) and the effects of fishing on the northern Gulf of Mexico ecosystem. *ICES Journal of Marine Science*, *72*(8), 2301–2312. http://doi.org/10.1093/icesjms/fsv088

Rodionov, S. N. (2004). A sequential algorithm for testing climate regime shifts. *Geophysical Research Letters*, *31*(9), 2–5. http://doi.org/10.1029/2004GL019448

Rojbek, M. C., Tomkiewicz, J., Jacobsen, C., & Stottrup, J. G. (2014). Forage fish quality: seasonal lipid dynamics of herring (*Clupea harengus* L.) and sprat (*Sprattus sprattus* L.) in the Baltic Sea. *ICES Journal of Marine Science*, *71*(1), 56–71. http://doi.org/10.1093/icesjms/fst106

Ropelewski, C. F., & Halpert, M. S. (1986). North american precipitation and temperature patterns associated with the El Nino/Southern Oscillation (ENSO). *Monthly Weather Review*. http://doi.org/10.1175/1520-0493(1986)114<2352:napatp>2.0.co;2

Sagarese, S. R., Nuttall, M. A., Geers, T. M., Lauretta, M. V., Walter III, J. F., & Serafy,

J. E. (2016). Quantifying the trophic importance of Gulf Menhaden within the Northern Gulf of Mexico Ecosystem. *Marine and Coastal Fisheries, 8*(1), 23–45. http://doi.org/10.1080/19425120.2015.1091412

Sanchez-Rubio, G., & Perry, H. (2015). Climate-related meteorological and hydrological regimes and their influence on recruitment of Gulf Menhaden (*Brevoortia patronus*) in the northern Gulf of Mexico. *Fishery Bulletin, 113*(4), 391–406. http://doi.org/10.7755/FB.113.4.3

Sanchez-Rubio, G., Perry, H. M., Biesiot, P. M., Johnson, D. R., & Lipcius, R. N. (2011). Oceanic-atmospheric modes of variability and their influence on riverine input to coastal Louisiana and Mississippi. *Journal of Hydrology*, *396*(1–2), 72–81. http://doi.org/10.1016/j.jhydrol.2010.10.034

Scharf, F. S., & Schlight, K. K. (2000). Feeding habits of Red Drum (*Sciaenops ocellatus*) in Galveston Bay, Texas: Seasonal diet variation and predator-prey size relationships. *Estuaries, 23*(1), 128–139. http://doi.org/10.2307/1353230

Schiller, R. V., & Kourafalou, V. H. (2014). Loop Current Impact on the Transport of Mississippi River Waters, 1287–1306. http://doi.org/10.2112/JCOASTRES-D-13-00025.1

Schiller, R. V., Kourafalou, V. H., Hogan, P., & Walker, N. D. (2011). The dynamics of the Mississippi River plume: Impact of topography, wind and offshore forcing on the fate of plume waters. *Journal of Geophysical Research: Oceans*, *116*(6), 1–22. http://doi.org/10.1029/2010JC006883

Schueller, A. M., Williams, E. H., & Cheshire, R. T. (2014). A proposed, tested, and applied adjustment to account for bias in growth parameter estimates due to

selectivity. *Fisheries Research, 158*, 26–39. http://doi.org/10.1016/j.fishres.2013.10.023

SEDAR. (2013). *SEDAR 32A - Gulf of Mexico menhaden Stock Assessment Report.* North Charleston, SC, USA.

Shaw, R. F., Cowan, J. H., & Tillman, T. L. (1985). Distribution and Density of *Brevoortia patronus* (Gulf Menhaden) Eggs and Larvae in the Continental Shelf Waters of Western Louisiana. *Bulletin of Marine Science, 36*(I), 96–103.

Shaw, R. F., & Drullinger, D. L. (1990). Early-life-history profiles, seasonal abundance, and distribution of four species of clupeid larvae from the Northern Gulf of Mexico, 1982 and 1983. *NOAA Technical Report NMFS 88*, (April).

Shaw, R. F., Wiseman, W. J., Turner, R. E., Rouse, L. J., Condrey, R. E., & Kelly, F. J. (1985). Transport of Larval Gulf Menhaden *Brevoortia patronus* in Continental Shelf Waters of Western Louisiana: A Hypothesis. *Transactions of the American Fisheries Society*, *114*(4), 452–460. http://doi.org/10.1577/1548-8659(1985)114<452:TOLGMB>2.0.CO;2

Shelton, A. O., & Mangel, M. (2012). Estimating von Bertalanffy parameters with individual and environmental variations in growth. *Journal of Biological Dynamics*, *6*(sup2), 3–30. http://doi.org/10.1080/17513758.2012.697195

Siddon, E. C., Kristiansen, T., Mueter, F. J., Holsman, K. K., Heintz, R. A., & Farley, E. V. (2013). Spatial match-mismatch between juvenile fish and prey provides a mechanism for recruitment variability across contrasting climate conditions in the eastern Bering Sea. *PLoS ONE*, *8*(12), e84526. http://doi.org/10.1371/journal.pone.0084526

Simpson, C. A., Wilberg, M. J., Bi, H., Schueller, A. M., Nesslage, G. M., & Walsh, H. J. (2016). Trends in relative abundance and early life survival of Atlantic menhaden during 1977–2013 from long-term ichthyoplankton programs. *Transactions of the American Fisheries Society*, *145*(5), 1139–1151. http://doi.org/10.1080/00028487.2016.1201004

Sirois, P., & Dodson, J. J. (2000). Critical periods and growth-dependent survival of larvae of an estuarine fish, the rainbow smelt Osmerus mordax. *Marine Ecology Progress Series*, *203*(October), 233–245. http://doi.org/10.3354/meps203233

Sogard, S. M. (1997). Size-selective mortality in the juvenile stage of teleost fishes: A review. *Bulletin of Marine Science*, *60*(3), 1129–1157.

Sogard, S. M., Hoss, D. E., & Govoni, J. J. (1988). Density and depth distribution of larval gulf menhaden, *Brevoortia patronus*, Atlantic croaker, Micropogonias undulatus, and spot, Leiostomus xanthurus, in the northern Gulf of Mexico. *Fishery Bulletin*, *85*(3), 601–609.

Stocks, J., Stewart, J., Gray, C. a., & West, R. J. (2011). Using otolith increment widths to infer spatial, temporal and gender variation in the growth of sand whiting Sillago ciliata. *Fisheries Management and Ecology*, *18*(Campana 2005), 121–131. http://doi.org/10.1111/j.1365-2400.2010.00761.x

Stoecker, D. K., & Govoni, J. J. (1984). Food selection by young larval gulf menhaden (*Brevoortia patronus*). *Marine Biology*, *80*(3), 299–306. http://doi.org/10.1007/BF00392825

Su, N. J., Sun, C. L., Punt, A. E., Yeh, S. Z., & Dinardo, G. (2011). Modelling the impacts of environmental variation on the distribution of blue marlin, *Makaira*

nigricans, in the Pacific Ocean. *ICES Journal of Marine Science*, *68*(6), 1072–1080. http://doi.org/10.1093/icesjms/fsr028

Sutton, S. G., Bult, T. P., & Haedrich, R. L. (2000). Relationships among fat weight, body weight, water weight, and condition factors in wild Atlantic salmon parr. *Transactions of the American Fisheries Society*, *129*(2), 527–538. http://doi.org/10.1577/1548-8659(2000)129<0527:RAFWBW>2.0.CO;2

Szuwalski, C. S., Vert-Pre, K. A., Punt, A. E., Branch, T. A., & Hilborn, R. (2015). Examining common assumptions about recruitment: A meta-analysis of recruitment dynamics for worldwide marine fisheries. *Fish and Fisheries*, *16*(4), 633–648. http://doi.org/10.1111/faf.12083

Takahashi, M., Checkley, D. M., Litz, M. N. C., Brodeur, R. D., & Peterson, W. T. (2012). Responses in growth rate of larval northern anchovy (*Engraulis mordax*) to anomalous upwelling in the northern California Current. *Fisheries Oceanography*, *21*(6), 393–404. http://doi.org/10.1111/j.1365-2419.2012.00633.x

Takasuka, A., Aoki, I., & Mitani, I. (2004). Three synergistic growth-related mechanisms in the short-term survival of larval Japanese anchovy Engraulis japonicus in Sagami Bay. *Marine Ecology Progress Series*, *270*, 217–228. http://doi.org/10.3354/meps270217

Takasuka, A., Oozeki, Y., & Aoki, I. (2007). Optimal growth temperature hypothesis: Why do anchovy flourish and sardine collapse or vice versa under the same ocean regime? *Canadian Journal of Fisheries and Aquatic Sciences*, *64*(5), 768–776. http://doi.org/10.1139/f07-052

Teletchea, F. (2009). Molecular identification methods of fish species: Reassessment and

possible applications. *Reviews in Fish Biology and Fisheries*, *19*(3), 265–293. http://doi.org/10.1007/s11160-009-9107-4

Thorson, J. T., Monnahan, C. C., & Cope, J. M. (2015). The potential impact of time-variation in vital rates on fisheries management targets for marine fishes. *Fisheries Research*, *169*, 8–17. http://doi.org/10.1016/j.fishres.2015.04.007

Thresher, R. E., Koslow, J. A., Morison, A. K., & Smith, D. C. (2007). Depth-mediated reversal of the effects of climate change on long-term growth rates of exploited marine fish. *Proceedings of the National Academy of Sciences of the United States of America*, *104*(18), 7461–7465. http://doi.org/10.1073/pnas.0610546104

Tommasi, D., Nye, J., Stock, C., Hare, J. A., Alexander, M., Drew, K., & Tierney, K. (2015). Effect of environmental conditions on juvenile recruitment of alewife (*Alosa pseudoharengus*) and blueback herring (*Alosa aestivalis*) in fresh water: a coastwide perspective. *Canadian Journal of Fisheries and Aquatic Sciences*, *72*(7), 1037–1047. http://doi.org/10.1139/cjfas-2014-0259

Tsoukali, S., Visser, A., & MacKenzie, B. (2016). Functional responses of North Atlantic fish eggs to increasing temperature. *Marine Ecology Progress Series*, *555*, 151–165. http://doi.org/10.3354/meps11758

Van Beveren, E., Bonhommeau, S., Fromentin, J.-M., Bigot, J.-L., Bourdeix, J.-H., Brosset, P., … Saraux, C. (2014). Rapid changes in growth, condition, size and age of small pelagic fish in the Mediterranean. *Marine Biology*, *161*(8), 1809–1822. http://doi.org/10.1007/s00227-014-2463-1

Vaughan, D. S., Govoni, J. J., & Shertzer, K. W. (2011). Relationship between Gulf Menhaden recruitment and Mississippi River flow: Model development and

potential application for management. *Marine and Coastal Fisheries*, *3*(1), 344–352. http://doi.org/10.1080/19425120.2011.620908

Vaughan, D. S., Levi, E. J., & Smith, J. W. (1996). Population characteristics of Gulf Menhaden, *Brevoortia patronus*. *NOAA Technical Report NMFS*, *125*(February), 1–17.

Vaughan, D. S., Shertzer, K. W., & Smith, J. W. (2007). Gulf menhaden (*Brevoortia patronus*) in the U.S. Gulf of Mexico: Fishery characteristics and biological reference points for management. *Fisheries Research*, *83*(2–3), 263–275. http://doi.org/10.1016/j.fishres.2006.10.002

Vincenzi, S., Crivelli, A. J., Munch, S., Skaug, H. J., & Mangel, M. (2016). Trade-offs between accuracy and interpretability in von Bertalanffy random-effects models of growth. *Ecological Applications*, *26*(5), 1535–1552. http://doi.org/10.1890/15-1177

von Bertalanffy, L. (1957). Quantitative Laws in Metabolism and Growth. *The Quarterly Review of Biology*, *32*(3), 217–231. http://doi.org/10.1086/401873

Walker, N. D. (1996). Satellite assessment of Mississippi River plume variability: Causes and predictability. *Remote Sensing of Environment*, *58*(1), 21–35. http://doi.org/10.1016/0034-4257(95)00259-6

Walker, N. D., Wiseman, W. J., Rouse, L. J., & Babin, A. (2005). Effects of river discharge, wind stress, and slope eddies on circulation and the satellite-observed structure of the Mississippi River plume. *Journal of Coastal Research*, *216*(1971), 1228–1244. http://doi.org/10.2112/04-0347.1

Walker, N., & Hammack, A. B. (2000). Impacts of Winter Storms on Circulation and Sediment Transport: Atchafalaya-Vermilion Bay Region, Louisiana, U.S.A. *Journal*

of Coastal Research, *16*(4), 996–1010.

Ward, P. J., Beets, W., Bouwer, L. M., Aerts, J. C. J. H., & Renssen, H. (2010). Sensitivity of river discharge to ENSO. *Geophysical Research Letters*, *37*(12), 1–6. http://doi.org/10.1029/2010GL043215

Weisberg, S., Spangler, G., & Richmond, L. S. (2010). Mixed effects models for fish growth. *Canadian Journal of Fisheries and Aquatic Sciences*, *67*(2), 269–277. http://doi.org/10.1139/F09-181

Whitten, A. R., Klaer, N. L., Tuck, G. N., & Day, R. W. (2013). Accounting for cohort-specific variable growth in fisheries stock assessments: A case study from south-eastern Australia. *Fisheries Research*, *142*, 27–36. http://doi.org/10.1016/j.fishres.2012.06.021

Winton, M. V., Wuenschel, M. J., & McBride, R. S. (2014). Investigating spatial variation and temperature effects on maturity of female winter flounder (Pseudopleuronectes americanus) using generalized additive models. *Canadian Journal of Fisheries and Aquatic Sciences*, *71*(April), 1279–1290. http://doi.org/10.1139/cjfas-2013-0617

Wood, S. N. (2006). *Generalized Additive Models: an introduction with R* (1st ed.). Boca Raton: Chapman and Hall/CRC. http://doi.org/10.1111/j.1467-842X.2007.00490.x.

Wood, S. N. (2008). Fast stable direct fitting and smoothness selection for generalized additive models. *Journal of the Royal Statistical Society. Series B: Statistical Methodology*, *70*(3), 495–518. http://doi.org/10.1111/j.1467-9868.2007.00646.x

Wood, S. N. (2011). Fast stable restricted maximum likelihood and marginal likelihood estimation of semiparametric generalized linear models. *Journal of the Royal*

Statistical Society: Series B (Statistical Methodology), *73*(1), 3–36. http://doi.org/10.1111/j.1467-9868.2010.00749.x

Xu, Y., Chai, F., Rose, K. A., Ñiquen, M., & Chavez, F. P. (2013). Environmental influences on the interannual variation and spatial distribution of Peruvian anchovy (*Engraulis ringens*) population dynamics from 1991 to 2007: A three-dimensional modeling study. *Ecological Modelling*, *264*, 64–82. http://doi.org/10.1016/j.ecolmodel.2013.01.009

Zhang, H., Mason, D. M., Stow, C. A., Adamack, A. T., Brandt, S. B., Zhang, X., … Ludsin, S. A. (2014). Effects of hypoxia on habitat quality of pelagic planktivorous fishes in the northern Gulf of Mexico. *Marine Ecology Progress Series*, *505*, 209–226. http://doi.org/10.3354/meps10768

Zhao, Y., & Quigg, A. (2014). Nutrient limitation in Northern Gulf of Mexico (NGOM): Phytoplankton communities and photosynthesis respond to nutrient pulse. *PLoS ONE*, *9*(2), e88732. http://doi.org/10.1371/journal.pone.0088732